

THE UNIVERSITY OF CALGARY

OXIDATION AND REDUCTION PROCESSES OF LEAD
IN pH 9 TO 14 SOLUTIONS

by

WALYAMBILLAH WAUDO

A THESIS

SUBMITTED TO THE FACULTY OF GRADUATE STUDIES
IN PARTIAL FULFILLMENT OF THE REQUIREMENTS FOR THE
DEGREE OF MASTER OF SCIENCE

DEPARTMENT OF CHEMISTRY

CALGARY, ALBERTA

JULY, 1988

© WALYAMBILLAH WAUDO 1988

Permission has been granted to the National Library of Canada to microfilm this thesis and to lend or sell copies of the film.

The author (copyright owner) has reserved other publication rights, and neither the thesis nor extensive extracts from it may be printed or otherwise reproduced without his/her written permission.

L'autorisation a été accordée à la Bibliothèque nationale du Canada de microfilmer cette thèse et de prêter ou de vendre des exemplaires du film.

L'auteur (titulaire du droit d'auteur) se réserve les autres droits de publication; ni la thèse ni de longs extraits de celle-ci ne doivent être imprimés ou autrement reproduits sans son autorisation écrite.

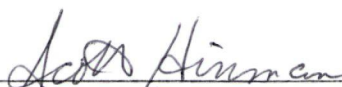
ISBN 0-315-46678-2

THE UNIVERSITY OF CALGARY
FACULTY OF GRADUATE STUDIES


The undersigned certify that they have read, and recommend to the Faculty of Graduate Studies for acceptance, a thesis entitled "Oxidation and Reduction processes of Lead in pH 9 to 14 Solutions" submitted by Walyambillah Waudo in partial fulfillment of the requirements for the degree of Master of Science.



Dr. V.I. Birss, Supervisor
Department of Chemistry



Dr. A.S. Hinman
Department of Chemistry



Dr. R.A. Kydd
Department of Chemistry



Dr. W.J.D. Shaw
Dept. of Mechanical Engineering

ABSTRACT

The oxidation and reduction processes which take place at Pb electrodes in aqueous alkaline solutions have been studied by cyclic voltammetry and potential step techniques in this work. The initial stages of lead oxidation in a range of alkaline solutions of varying pH and ion content have been found to show strong similarities. In both carbonate and borate buffered solutions ($\text{pH} > 9$), and in more alkaline solutions, Pb oxidation commences at a potential of ca. 140 mV vs. RHE. In pH 14 solutions, $\text{Pb}(\text{OH})_2$ is soluble, hence producing $\text{Pb}(\text{OH})_3^-$ and only a small amount of a stable surface film. At lower pH's, $\text{Pb}(\text{OH})_2$ is not predicted to be soluble, and in borate-buffered solutions, a stable, reducible $\text{Pb}(\text{OH})_2$ film appears to form. In carbonate-buffered solutions, unusual electrochemical behaviour was observed.

It is suggested that, in these carbonate-containing solutions, some $\text{Pb}(\text{OH})_2$ is transformed to an adherent Pb/oxide/carbonate phase, which is difficult to remove electrochemically in a normal cathodic sweep. The film can be reduced at very negative potentials. Also, the surface film which is formed by potential holding at the positive potentials, can be reduced. A model for the early stages of lead oxidation in carbonate solutions is presented.

Scanning Electron Microscopy has been utilized to study the effect of various electrode pretreatments on the cycling

behaviour of lead in carbonate solutions. It has also been used to analyse anodic deposits formed during electrochemical experimentation. It was found that two types of electrochemical response occur depending on the condition of the surface of the lead electrode. The results are correlated with photomicrographs.

Other surface analytical techniques such as Auger Electron Spectroscopy have also been utilized to examine the anodic films formed on a lead electrode in carbonate-containing solutions.

ACKNOWLEDGEMENTS

It is a pleasant duty to express my gratitude to my supervisor, Dr. Viola Birss, for the many valuable comments and encouragement during the preparation of this work.

I gratefully acknowledge the help of Mr. D. Tilleman at the University of Calgary with the SEM experiments and Dr. D. Llyod at Alcan International Ltd, Kingston Laboratory, for the AES analyses.

Special thanks to my colleagues in the laboratory, who have been a joy to work with and for their stimulating discussions and help during the course of this work.

Finally, financial support from the Canadian International Development Agency General Training Fund Scholarship from Kenya and the Department of Chemistry is also acknowledged.

DEDICATION

To my wife Anne and children Nanyokya, Njeri and Simema
whose love and encouragement are inexpressibly precious.

TABLE OF CONTENTS

	Page
ABSTRACT	iii
ACKNOWLEDGEMENTS	v
DEDICATION	vi
TABLE OF CONTENTS	vii
LIST OF TABLES	x
LIST OF FIGURES	xi
CHAPTER 1 Introduction	1
1.0 The electrochemistry of lead in aqueous solutions	1
1.1 The electrochemical behaviour of lead in acidic media	1
1.2 The electrochemical behaviour of lead in alkaline solutions	4
1.2.1 The lead-carbonate system	9
1.3 Aim of thesis	14
CHAPTER 2 Experimental	17
2.1 Electrochemical experiments	17
2.1.1 Electrodes	19
2.1.1.1 Working electrodes	19
2.1.1.2 Reference and counter	

	page
electrodes	21
2.1.2 Cells and solutions	22
2.1.3 Determination of the electrode	
surface area	25
2.2 Surface analytical techniques	27
2.2.1 Scanning Electron Microscopy	27
2.2.2 Auger Electron Spectroscopy	28
2.3 Atomic Absorption Spectroscopy	29
2.4 Other techniques used	29
CHAPTER 3 General electrochemical behaviour of lead	
in 1 M NaOH solutions	31
3.1 Introduction	31
3.2 Sweep rate studies in the region	
of A'	37
3.3 Peaks A_0/C_0	42
3.4 Summary of lead oxidation in	
1 M NaOH	46
CHAPTER 4 SEM study of electrode surface preparation ..	48
4.1 Introduction	48
4.2 Electrode surface preparation	
studies	50
CHAPTER 5 Electrochemistry of Pb in carbonate	
solutions (pH 9.6)	57
5.1 Introduction	57
5.2 Detailed study of processes in	

	page
peaks A' and A ₁	67
5.2.1 General observations	67
5.2.2 Effect of time of potential holding in A' region	78
5.2.2.1 Potentiostatic transients at the Pb in carbonate solutions	87
5.2.3 Effect of cathodic sweep rate on Ca to Cd	92
5.2.4 Effect of negative potential limit	98
CHAPTER 6 Surface analysis of Pb electrode after electrochemical experimentation	103
6.1 SEM results	103
6.2 Scanning Auger Microscopy results	110
CHAPTER 7 Model for the early stages of anodic oxidation of Pb in carbonate/bicarbonate solutions	115
CHAPTER 8 Conclusions	126
8.1 Initial stages of lead oxidation in alkaline solutions	126
8.2 Potential holding effect	128
8.3 Electrode surface preparation	129
8.4 Future work	130
REFERENCES	132

List of Tables

page

Table I	Equilibrium reactions for Pb/carbonate/ water system	11
Table II	Potentials and charge densities in region of peaks A'/C'	41
Table III	Dependence of anodic and cathodic charge densities on E_+ for Pb electrode in 0.05 M NaHCO_3	70

LIST OF FIGURES

	Page
Fig. 2.1 The three electrode circuitry for the electrochemical experiments	18
Fig. 2.2 (a) The electrochemical cell	23
Fig. 2.2 (b) The reference electrode compartment	24
Fig. 3.1 Cyclic voltammogram of Pb chip electrode (0.015 cm ²) in 1 M NaOH at $s = 20$ mV/s	32
Fig. 3.2 i/t response to a potential step into the region of A' (from 0 to 210 mV vs. RHE)	35
Fig. 3.3 Cyclic voltammetric response of Pb chip electrode (0.02 cm ²) at high sweep rates in 1 M NaOH. $s = 2$ V/s (—), 5 V/s (.....), and 10 V/s (- - -)	38
Fig. 3.4 Ratio of anodic to cathodic charge densities passed in the region of A'/C'	39
Fig. 3.5 Cyclic voltammograms of Pb chip electrode (0.02 cm ²) at high sweep rates after several hours of electrochemical experimentation in 1 M NaOH. $s = 10$ V/s (—), 20 V/s (.....), and 30 V/s (- - -)	43
Fig. 3.6 Relationship between anodic peak current density of A ₀ and potential sweep rate in 1 M NaOH	44

Fig. 4.1	SEM view of a mechanically polished Pb surface (down to 600 grit emery paper)	51
Fig. 4.2	Mechanically polished Pb surface (emery paper, 600 grit size) showing embedded silicon carbide particles	51
Fig. 4.3	Pb surface mechanically polished with emery paper (600 grit), various grades of diamond paste (down to 0.1 μm) followed with ultrasonic washing	53
Fig. 4.4	A freshly sheared Pb electrode and tissue polished. (No mechanical polishing)	55
Fig. 5.1	Cyclic voltammogram of Pb chip electrode (0.02 cm^2) in 0.05 M NaHCO_3 (pH 9.6) at $s = 50$ mV/s.	59
Fig. 5.2	Cyclic voltammogram of Pb chip electrode (0.02 cm^2) in 0.025 M Sodium borate at $s = 20$ mV/s.	61
Fig. 5.3	Dependence of the peak current density of A' on sweep rate in pH 9.6 bicarbonate (a) and borate solutions (b).	68
Fig. 5.4	Series of cyclic voltammograms obtained for a Pb chip electrode (0.02 cm^2) with progressively increasing positive potential limit in 0.05 M NaHCO_3 . $s = 100$ mV/s	69
Fig. 5.5	Cyclic voltammograms obtained for Pb electrode	

in 0.05 M NaHCO₃ after various times of continuous potential cycling. Initial response (——), after 20 hours of continuous cycling (.....). $s = 50$ mV/s.74

Fig. 5.6 Cyclic voltammograms obtained with Pb electrode in 0.05 M NaHCO₃. Steady-state response (-----) and after holding at $E_- = -0.9$ V (——) $s = 50$ mV/s.76

Fig. 5.7(a) Cyclic voltammetric response for Pb chip electrode in 0.05 M NaHCO₃ with potential holding for 30 secs at $E_+ = 300$ mV. $s = 300$ mV/s80

Fig. 5.7(b) Cyclic voltammetric response for Pb chip electrode in 0.05 M NaHCO₃ with potential holding for 30 secs at $E_+ = 250$ mV. $s = 100$ mV/s.81

Fig. 5.8 Plot of total cathodic charge, Q_c , vs. $t^{1/2}$ for Pb electrode obtained in 0.05 M NaHCO₃ with potential holding at $E_+ = 300$ mV.84

Fig. 5.9 Cyclic voltammetric response for Pb in 0.05 M NaHCO₃ obtained with the perturbation programme depicted in the figure. The potential scan direction is reversed at different E_- . At C_b (.....); C_c (-----); C_d (——).86

Fig. 5.10 Current-time transient in 0.05 M NaHCO₃

	recorded at $E_+ = 350$ mV.	88
Fig. 5.11	i/t response to potential step from -900 mV to 350 mV in 0.05 M NaHCO ₃ with and without stirring. a- without stirring b - with stirring	91
Fig. 5.12	Cyclic voltammetric response for Pb electrode in 0.05 M NaHCO ₃ after potential holding at E_+ for 30 secs; various cathodic sweep rates. $s_c = 50, 100, 200$ and 300 mV/s.	93
Fig. 5.13(a)	Dependence of i_p on s for peaks C_a , C_b and C_c in 0.05 M NaHCO ₃	96
Fig. 5.13(b)	Dependence of i_p on $s^{1/2}$ for peak C_d in 0.05 M NaHCO ₃	97
Fig. 5.14	The effect of negative potential limit on CV response of Pb in 0.05 M NaHCO ₃ solution. $E_- = -0.9$ V (—), -1.2 V (- - -)	99
Fig. 5.15	Cyclic voltammogram of Pb electrode obtained in 0.05 M NaHCO ₃ when the negative potential limit was extended to -2.0 V. $s = 50$ mV/s.	101
Fig. 6.1	SEM view of electrode surface following (a) continuous potential cycling between -0.9 V and 0.3 V in 0.05 M NaHCO ₃ ; (b) as in (a), but followed by holding at	

	page
-2.0 V for 5 min.	105
Fig. 6.2 A high magnification SEM view of Fig. 6.1, region "a".	107
Fig. 6.3 SEM view of a sheared Pb electrode surface polished with tissue, after anodic scan to potential positive of peak A ₁ , in carbonate solutions (pH 9.6).	108
Fig. 6.4 SEM view of Pb electrode surface after one anodic scan beyond peak A ₁ in 1 M NaOH.	109
Fig. 6.5 SEM view of Pb electrode surface after continuous cycling between -0.9 V and 0.35 V in 0.05 M NaHCO ₃ solutions.	112
Fig. 6.6 SEM view of Pb electrode surface after potential holding in the region of peak A' in 0.05 M NaHCO ₃	112
Fig. 6.7 SEM view of Pb electrode surface after potential scan is extended to -2.0 V in 0.05 M NaHCO ₃	113
Fig. 7.1 Schematic representation of lead electrode surface in carbonate solutions during potential sweep experiments.	117
Fig. 7.2 Cyclic voltammetric response of a fresh Pb electrode in 0.05 M NaHCO ₃ when the positive potential limit is only +300 mV. s = 50 mV/s.	119

Fig. 7.3 Schematic representation of surface processes at a lead electrode in carbonate solutions during potential holding experiments.	122
--	-----

CHAPTER 1

INTRODUCTION

1.0 The electrochemistry of lead in aqueous solutions

Lead has been used extensively since ancient times to make statues, waterproof linings, sheaths for power and communications cables, containers, etc. (1-3). This is because of its good corrosion resistance when exposed to the atmosphere and to a variety of different electrolytes in aqueous solutions. The majority of the corrosion products are relatively insoluble lead salts that deposit on the lead surface as impervious films which tend to inhibit further attack. The formation of such insoluble protective films is responsible for the high resistance of lead to corrosion by acids such as sulfuric and phosphoric acids (1). For example, during the installation of an underground cable sheathed in lead, it can complex with sulphate ions in the soil, forming lead sulphate which is insoluble, hence providing a good protective film towards corrosion (1). In contrast, iron corrodes under the same conditions because the iron sulphate formed is soluble and does not form a protective surface film (1,3)

1.1 The electrochemical behaviour of lead in acidic media

The processes of oxidation and reduction occurring at lead electrodes in acidic environments have been a subject

of considerable study (4-8). This is primarily a result of the major role these reactions have played in the development of energy storage devices, e.g. lead-acid batteries (9).

In the lead-acid battery, Pb forms the anode while PbO₂ serves as the cathode. Many studies of this cell in sulphuric acid have helped elucidate some of the reactions that take place at lead electrodes in acidic media. When lead is placed in sulphuric acid, it is oxidized to Pb²⁺ ions, which then react with sulfate ions to form PbSO₄ (10).



Lead sulphate is very insoluble and therefore it forms a film at the electrode surface which passivates the lead from further reaction.

However, detailed investigation of the electrochemical processes involving lead oxidation in sulphuric acids have shown that the anodic oxidation products formed on the lead surface depend on the potential of the metal surface (8,10). It has been shown (7) that under potentiostatic conditions at potentials below that for PbO₂ formation, a layer of PbO film is formed at the electrode surface. At high potentials, PbO₂ forms on the outer electrode surface as a protective surface film. The rate of formation of the oxidation products has been found to be dependent also on the acid concentration and the temperature (11,12). It has

also been observed that as the acid concentration decreases and the temperature increases, an increase in the rate of corrosion of lead is observed (7,11). The cycle life of the lead-acid battery, for instance, depends on the concentration of the sulphuric acid solution (13).

Increasing the concentration of acid from 4.5 M to 5.7 M, for example, enhances the battery output, while the cycle life of the electrodes decreases. This has resulted in several studies (13-15) concerning the mechanism of formation of a passivating PbSO_4 film on the electrode surface. Two different mechanisms (14,15) have been offered to explain this film formation reaction, a solid-state mechanism and a dissolution-precipitation process.

Investigations of the behaviour of Pb in other acidic media such as perchloric acid (16) and phosphoric acid (17) have also been carried out, although to a relatively lesser extent than in sulphuric acid. The effect of phosphoric acid on the positive electrode (PbO_2) of the acid battery has also been investigated (17). Using cyclic voltammetry, it was proposed (17) that the phosphate ion is reversibly adsorbed on the PbO_2 surface during the charging process and that this modifies PbO_2 crystal growth on the grid, producing a PbO_2 structure which is comparatively difficult to reduce to PbSO_4 . It has been suggested that the adsorption of the phosphate ions on the PbO_2 inhibits the three-dimensional growth of the PbO_2 crystals in favour of

two-dimensional growth, resulting in a film which is not easily reduced. These effects occur with additions of H_3PO_4 as low as 0.2 wt% and involve the formation of $\text{Pb}_3(\text{PO}_4)_2$ as an intermediate in the oxidation of Pb to PbO_2 .

The electrochemical reactions occurring at the PbO_2 electrode in perchloric acid have also been investigated (16). It is expected that PbO_2 will dissolve in perchloric acid during anodic polarization. Because of the high solubility of PbO_2 in perchloric acid, it has been possible to obtain information about the mechanism of the electrolytic dissolution and deposition of PbO_2 from electrolytes containing Pb(II) ions.

1.2 Electrochemical behaviour of lead in alkaline solutions

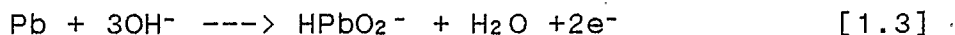
The electrochemical characteristics of lead in alkaline solutions have been relatively less investigated than those in acidic media, partly because of the complex mixture of dissolution and film formation reactions which are expected to occur in basic solutions (18). Lead generally passivates in these alkaline media, forming a protective film, but at sufficiently high current densities or potentials, PbO and ultimately PbO_2 are formed so that Pb dissolution is largely, but not completely, inhibited.

Although lead finds extensive use in energy storage devices (e.g. the lead-acid battery), no reports exist for its use in alkaline storage devices. Alkaline batteries

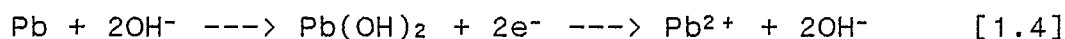
more commonly utilize electrodes such as nickel oxide and iron in electrolytes such as potassium hydroxide (9,19).

Some of the early work reported on the electrochemical behaviour of lead in alkaline solutions appears in the paper of Elbs and Forsell (20). It was shown in that paper that under galvanostatic conditions in alkaline solutions, lead can dissolve to form Pb^{2+} at low applied current densities. At higher current densities, a PbO_2 film is expected to form at the electrode surface, with the subsequent evolution of oxygen. The evolution of oxygen was also attributed (20) to the decomposition of PbO_2 into PbO and oxygen.

Further work by Glasstone (21) postulated that oxygen evolution at the lead anode takes place through the intermediate formation of unstable oxides. This occurs at high current densities ($> 25 \text{ mA/cm}^2$), where Pb_3O_4 and/or Pb_2O_3 were proposed to form as intermediates before the eventual evolution of oxygen. At low current densities, i.e. $< 25 \text{ mA/cm}^2$, dissolution of lead as biplumbite is thought to occur according to the following reaction [1.3].



Also, a certain amount of lead is thought to dissolve as bivalent plumbous ions (21).

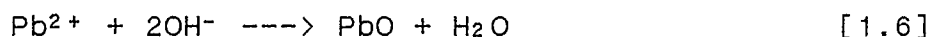


Jones et al (22) showed that Pb treated in 1N KOH dissolved first to plumbite (PbO_2^{2-}), and was then passivated by a film of PbO_2 . An electron diffraction

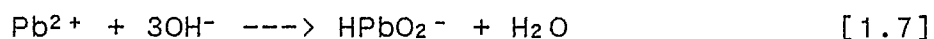
examination of the film formed after repeated charging and self-discharging showed it to consist of a mixture of Pb_3O_4 and Pb_2O_3 , the results being consistent with the lead intermediates suggested by Glasstone (21).

Other work which appears in the literature in this area includes that of Popova and co-workers (23). It has been shown from their galvanostatic and potentiostatic results that the anodic oxidation of lead results in the formation of PbO , PbO_2 and the evolution of oxygen. A soluble species, biplumbite ($HPbO_2^-$) ions was also suggested as resulting from the reaction between OH^- ions and PbO .

The work of Abdul Azim et al (24), also involving galvanostatic and potentiostatic methods in solutions ranging from 0.1 N to 6 N NaOH, has also confirmed the formation of the lead oxide species (i.e. PbO , Pb_3O_4 , PbO_2) proposed by others (21,22). The following reactions were suggested as being the possible routes to PbO formation in the alkaline solutions. It was proposed that under these conditions, PbO film growth occurs via a dissolution-precipitation process.



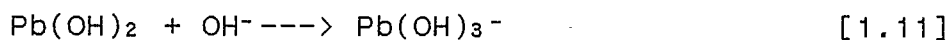
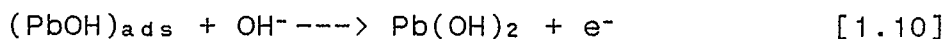
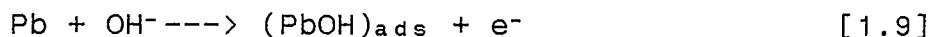
or





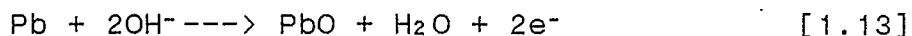
It was further suggested that at low OH^- concentrations (e.g. 0.1 N NaOH), reaction pathway [1.5] and [1.6] plays a significant role in the formation of PbO . As the concentration of OH^- increases (> 1 N NaOH), reaction [1.7] becomes the rate determining step.

A more recent study carried out by Ptitsyn et al (25), using potentiostatic and potentiometric methods, has shown that the oxidation of lead in alkaline solutions involves first the formation of Pb(OH)_2 , which subsequently dissolves as Pb(OH)_3^- , with the latter dissolution step being rate determining. Even more recently (26), it has been suggested on the basis of results obtained with cyclic voltammetry as well as steady-state and transient potentiostatic techniques, that the first stage in the anodic oxidation of lead in 1M NaOH solutions involves the formation of a surface intermediate, PbOH , followed by the deposition of a thin Pb(OH)_2 film on the Pb electrode surface, as shown in reactions [1.9] and [1.10]. The Pb(OH)_2 film then dissolves to form a soluble species, Pb(OH)_3^- (reaction [1.11]), as was also suggested by Ptitsyn et al (25).



At higher potentials, it was suggested (27) that a PbO film forms, both by the dehydration of Pb(OH)_2 and also via

a nucleation and growth process at the free Pb surface, according to reactions [1.12] and [1.13], respectively. PbO is also thought to be somewhat soluble (reaction [1.14]).



These suggested reactions pathways and products are supported by thermodynamic calculations (26-28) which indicate that Pb(OH)₂ is predicted to form at a potential more negative than that for PbO formation.

The electrochemistry of lead in alkaline solutions other than simple alkali metal solutions has also been investigated in the past (29-33). The work of Abdul Azim et al (29) describes the electrochemical behaviour of lead in a variety of alkaline media containing a number of different anions. It was shown by potentiostatic and galvanostatic experiments that lead passivates by the initial formation of a film of the corresponding salt of the anion, i.e., in the case of solutions containing sulfate or carbonate ions, the surface film formed would be PbSO₄ or PbCO₃, respectively. This is followed by the formation of a PbO film at the metal surface within the pores of the salt layer. The PbO can then be further oxidized to PbO₂ and eventually lead to the evolution of oxygen.

More recently, using photoelectrochemical methods, it has been suggested (30) that in borate-buffered alkaline

solutions, the initial stage of Pb oxidation involves the formation of a lead borate surface film, followed by PbO deposition at higher potentials. This is in agreement with the suggestions of Abdul Azim et al (29) to some extent, although no attempt was made in either of these studies to identify the initial surface products with the use any surface analytical techniques.

Cyclic voltammetry (CV) has also been used recently (31) to investigate the anodic oxidation of Pb electrodes in carbonate solutions (pH 10 to 12). The CV result shows a small anodic peak preceding a main peak. This small peak has been attributed to the formation of a lead hydroxy-carbonate surface compound (31). It has been suggested that within the potential range of the small peak, some Pb dissolution may also occur, possibly via a surface intermediate, while at higher anodic potentials, further surface film formation occurs and the rate of dissolution diminishes.

1.2.1 The lead-carbonate system

Only a few papers have been published regarding the effect of carbonate ions on the electrochemical reactions of Pb (29,31,33,34). It has been shown that the presence of carbonate ions accelerates the passivation of Pb electrode during anodization in alkaline solutions (33). Carbonate may be introduced to aqueous solutions by contact with

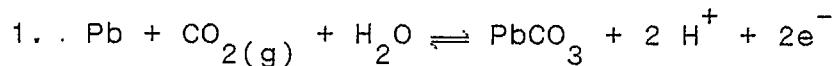
atmospheric air, as carbon dioxide can dissolve into solution as carbonate ions. It is also known that in the presence of air and water vapour, Pb forms a thin surface film of oxycarbonate, which protects the underlying metal surface (35). This film can easily be observed to form when freshly cut metal loses its bright lustre with time in air.

The attack of lead by oxygenated water can produce soluble lead hydroxy compounds, which can result in lead poisoning by consumption of water carried in lead pipes (2,35). However, if the water contains small amounts of carbonate, the attack on the pipes is lessened due to a decrease in the soluble lead concentration, resulting from PbCO_3 precipitation. The knowledge of the effect of carbonate species on Pb oxidation is therefore important from numerous practical standpoints.

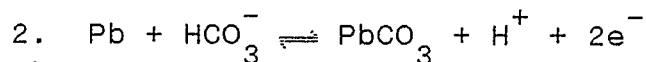
It is desirable to define the chemical species that may arise as a result of the oxidation of Pb in aqueous alkaline carbonate-containing solutions. Table 1 summarizes the chemical species which are thermodynamically predicted to form when Pb is in contact with aqueous carbonate and bicarbonate solutions (36).

In the presence of dissolved carbonate ions, lead can also form several basic hydroxycarbonates (35,37,38), in addition to lead carbonate, PbCO_3 . Lead plumbonacrite, $\text{Pb}_{10}\text{O}(\text{OH})_6(\text{CO}_3)_6$ and hydrocerrusite, $\text{Pb}_3(\text{OH})_2(\text{CO}_3)_2$, are among the well characterized hydroxycarbonates (37).

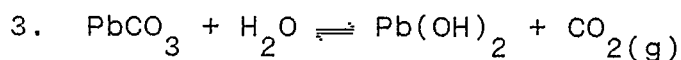
Table I. Equilibrium reactions for Pb/carbonate/water system.



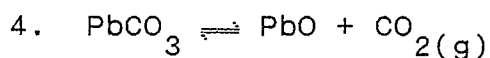
$$E = 0.031 - 0.0591 \text{ pH} - 0.0295 \log p_{\text{CO}_2}$$



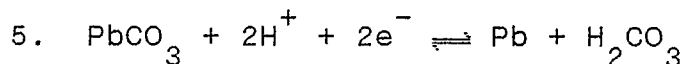
$$E = -0.200 - 0.0295 \text{ pH} - 0.0295 \log a_{\text{HCO}_3^-}$$



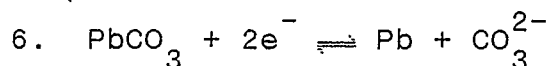
$$\log p_{\text{CO}_2} = -7.15$$



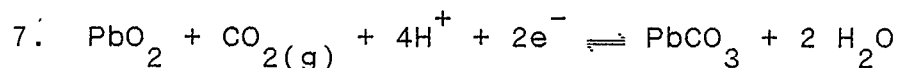
$$\log p_{\text{CO}_2} = -7.36$$



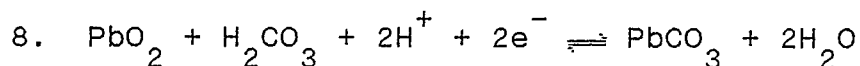
$$E = 0.012 - 0.0591 \text{ pH} - 0.0295 \log a_{\text{H}_2\text{CO}_3}$$



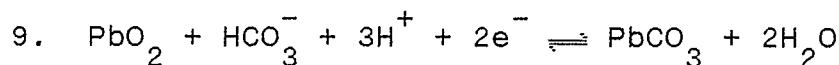
$$E = -0.506 - 0.0295 \log a_{\text{CO}_3^{2-}}$$



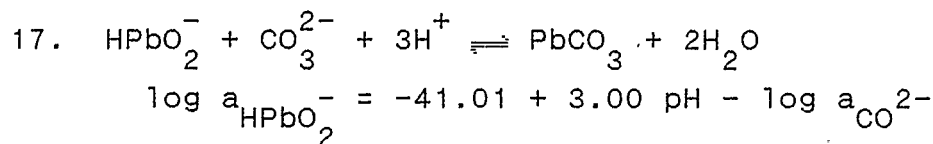
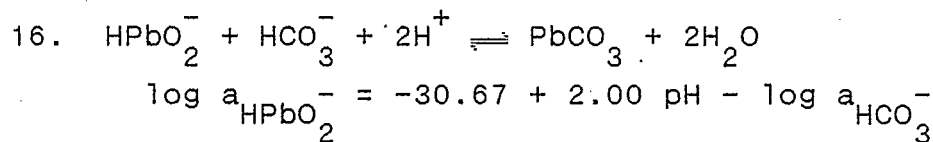
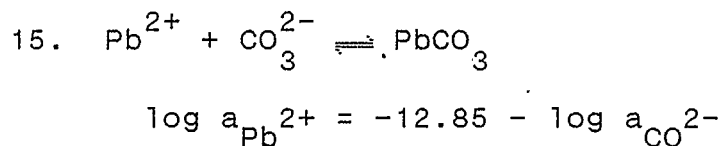
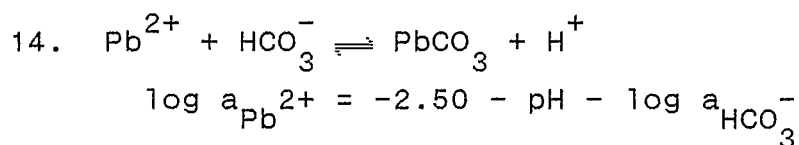
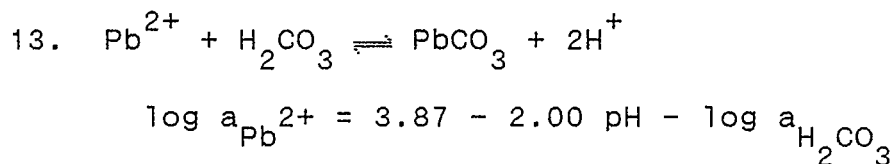
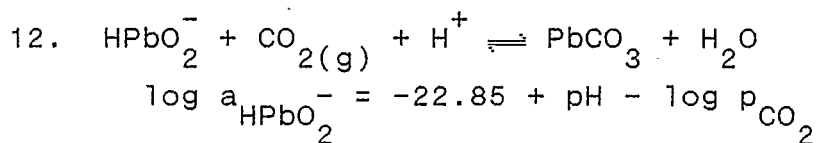
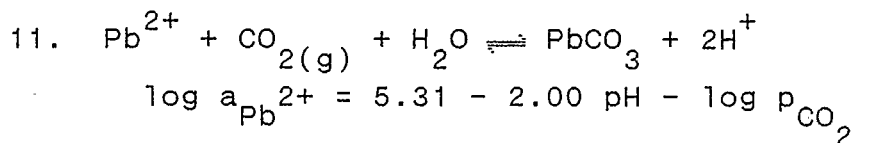
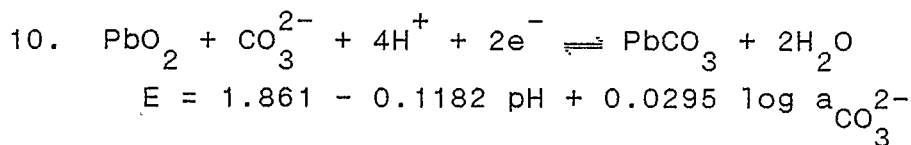
$$E = 1.324 - 0.0591 \text{ pH} + 0.0295 \log p_{\text{CO}_2}$$



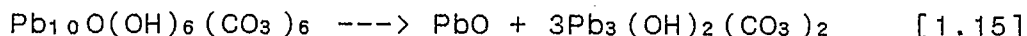
$$E = 1.367 - 0.0591 \text{ pH} + 0.0295 \log a_{\text{H}_2\text{CO}_3}$$



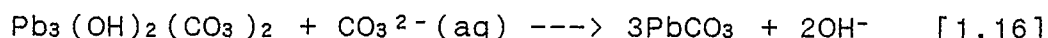
$$E = 1.555 - 0.0886 \text{ pH} + 0.0295 \log a_{\text{HCO}_3^-}$$



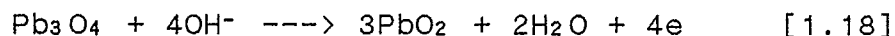
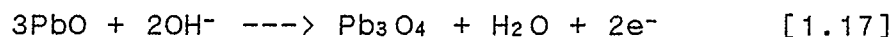
Plumbonacrite has been (39) reported to be metastable and hence can decompose to the more stable hydrocerrusite form, according to the following reaction



It has been shown experimentally that (38), at room temperature, lead carbonate can be transformed to hydrocerrusite and vice versa, according to the following reaction :



Using galvanostatic techniques, Khairy et al (33) have studied the anodic oxidation of lead in 0.05 M carbonate solutions. During the anodic polarization of the lead at constant-current, the potential rises rapidly to a steady-state value which is close to the potential of the Pb/PbCO₃ couple at -0.46 V vs. NHE. Upon further oxidation, PbCO₃ transforms into PbO on the electrode surface. It was then further suggested that this surface PbO reacts with hydroxyl ions to form higher lead oxides, according to the following reactions:



Abdul Azim et al (29) have also shown that the anodic polarization curves for pure Pb in carbonate and borate solutions display well-defined arrests corresponding to the formation of the Pb carbonate and Pb borate. It was also concluded that since the product of current and the time

required for passivation was constant, the process leading to passivation was diffusion controlled.

The most recent study concerning the electrochemistry of lead in alkaline carbonate solutions is that of Shoesmith et al (31). Using voltammetric and potentiostatic methodologies, as well as X-ray diffraction, two forms of hydroxycarbonates, i.e plumbonacrite and hydrocerussite were suggested to be the primary species forming on the lead electrode surface in 1 M K_2CO_3 .

1.3 Aim of thesis

Lead and its oxides are low-cost materials with interesting chemical and electrochemical properties. In most applications, they are used as inert electrodes in electrolysis and electrosynthesis (10) or as porous electrodes in batteries. The electrocatalytic activity of electrodeposited lead dioxide for anodic oxygen evolution reactions has also been studied (10,40). The importance of the role that lead has played in the storage battery industry cannot be overemphasized.

Interest in the behaviour of lead in alkaline carbonate- containing solutions is growing due to the possible future use of lead to precipitate $^{14}CO_3$, which is a radioactive contaminant produced in heavy-water moderator systems (41). Lead may also be used as a storage material for nuclear waste in deep underground vaults in the future

(42). This will prevent the nuclear waste from reaching the groundwater, consequently inhibiting the release of radionuclides.

It is therefore important to study the chemical and electrochemical processes which are likely to occur when lead is exposed to solutions similar to groundwater. In underground water, there exists a variety of ions (e.g. Cl^- , SO_4^{2-} , HCO_3^- , CO_3^{2-} , etc.) and generally the water is somewhat alkaline (pH ca. 8 - 10).

The present study was initiated in order to understand the effects of carbonate and bicarbonate ions on the electrochemical reactions of Pb in alkaline solutions, particularly as extensive prior research had been carried out (28) concerning the electrochemistry in simple alkaline solutions. It was anticipated that the presence of $\text{HCO}_3^-/\text{CO}_3^{2-}$ ions would lead to the formation of new surface compounds and that these might alter the mechanism and extent of film growth, the rate of Pb dissolution, etc. As it is recognized that the study of the electrochemical behaviour of lead in groundwater would be rather complex because of the numerous reactions that could occur between Pb, Pb^{2+} and the many anions present (Cl^- , SO_4^{2-} , HCO_3^- , CO_3^{2-} , etc), the study was simplified in that only CO_3^{2-} , HCO_3^- and later Cl^- ions, were added to alkaline aqueous solutions.

Using cyclic voltammetry and potential step techniques,

the electrochemical oxidation and reduction processes that occur at a Pb electrode in aqueous carbonate solutions have been studied in comparison with the behaviour of Pb observed in borate buffered solutions, as well as in simple hydroxide solutions. The results have aided in the formulation of a model for the mechanism of lead oxidation in these carbonate/bicarbonate solutions.

CHAPTER 2

EXPERIMENTAL

2.1 Electrochemical experiments

During the course of this study of the electrochemical behaviour of lead in aqueous alkaline solutions, cyclic voltammetry (CV) and potential step techniques have been the principal electrochemical methodologies used.

In a CV experiment, the potential of a working electrode (WE) is varied linearly with time vs. a reference electrode (RE) from an initial potential E_i to a final potential E_f where the direction of the scan is reversed and the potential is swept back to E_i . The resulting current is recorded as a function of the applied potential. In potential step experiments, the potential of the working electrode is changed instantaneously, and the resulting current or charge response is recorded versus time. These are useful for a detailed investigation of the electrode kinetics.

The CV and chronoamperometric experiments were carried out using standard three electrode circuitry (Fig. 2.1) (43). An EG & G PARC 173 Potentiostat coupled to an EG & G PARC 175 function generator was used to control the WE potential with respect to the RE. The current (I) vs potential (E) profiles were plotted on the HP 7045 X/Y recorder at slow potential sweep rates (s), while all the

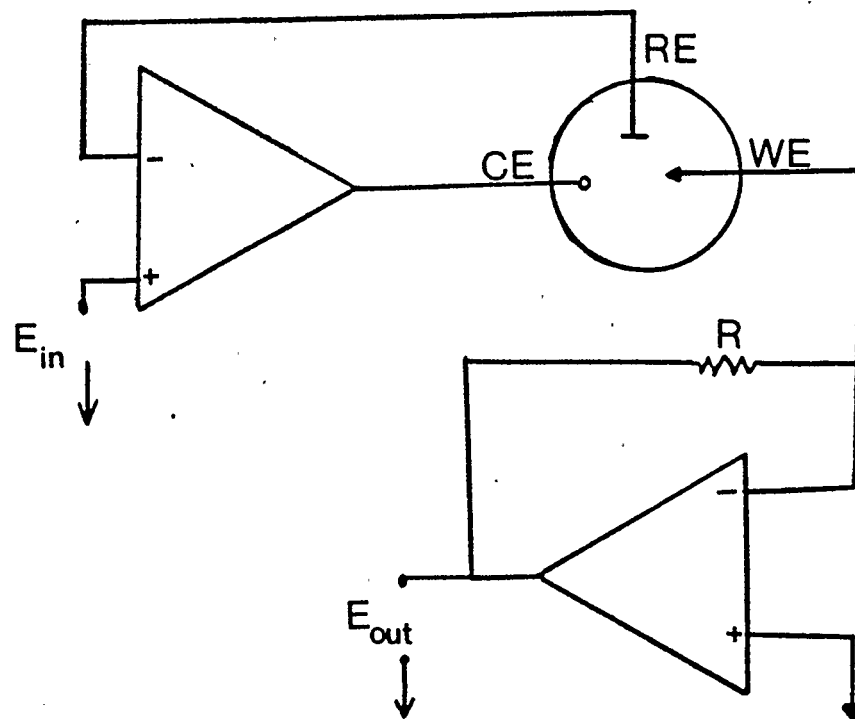


Fig. 2.1 The three electrode circuitry for the electrochemical experiments

CE - counter electrode; WE - working electrode

RE - reference electrode

I/t data, and I/E curves at sweep rates greater than 300 mV/sec, were monitored on a Nicolet 3091 digital oscilloscope, and then transferred to the X/Y recorder.

2.1.1 Electrodes

A three electrode cell arrangement as shown in Fig. 2.2 was utilized during this study. The three electrodes consisted of a reversible hydrogen electrode (RHE) or a saturated calomel electrode (SCE) as the RE, a large area Pt gauze as a counter electrode (CE) and a WE made of a high purity Pb chip or disc. The details of WE construction are given below.

2.1.1.1 Working electrodes

The working electrodes were constructed from 8 mm diameter lead rods of 99.999% purity, obtained from Johnson and Matthey. There were several different types of electrode designs which were used during the course of this work.

Type 1

Pb chip electrodes having a geometrical area of ca. 1.5 to 3.0 mm² were obtained by shearing from a Pb rod. These were then sealed into a close-fitting pyrex tube with epoxy resin. A silver wire, which was press-fitted against the back of the Pb chip, maintained the electrical contact with the potentiostat. The back and the edges were covered with

the epoxy, such that only a flat surface was exposed. The surface of the electrode was then mechanically polished in stages with various grades of emery paper (250 to 600 grit). This was then followed with further polishing with 0.1 μm alumina paste (Gamal grade B polishing compound, Fisher Scientific Co.) on a polishing cloth. After a smooth electrode surface was obtained, the electrode was washed well with a stream of distilled water, ultrasonically cleaned in acetone and then finally rinsed again with distilled water. This was done in an attempt to remove any particles which may have become attached/embedded into the surface during the polishing procedure.

Type 2

A small Pb chip (ca. 0.015 cm^2) was cut from a Pb rod using a stainless steel knife edge, exposing a smooth, bright and shiny surface. It was then mounted in a pyrex tube and was allowed to set with epoxy resin for 24 hours.

Since it became clear over the course of this work that soft metals like Pb can change their surface structure during electrode preparation, mechanical polishing was avoided in this particular case. Instead the lead surface was polished by light abrasion with a soft material like tissue paper, as was also done with Pb in prior studies in other solutions (17,44).

Type 3

Using a stainless steel knife edge, a small Pb chip of geometrical area ca. 0.015 cm^2 to 0.03 cm^2 was cut from a Pb rod. This was then held with an alligator clip, leaving the smooth and shiny cross-section of the chip exposed. The sides of the Pb electrode and the alligator clip were carefully wrapped with teflon tape. This Pb electrode surface was treated reproducibly by light polishing with tissue paper, as described above for Type 2. The electrode was then ultrasonically cleaned in acetone, and then finally rinsed well with a jet of distilled water to remove any adherents. After drying at room temperature, the electrode was transferred to the electrolytic cell. This type of electrode was used for SEM experiments and other surface analyses since electrodes stuck in epoxy wouldn't be transferred to SEM without ruining the WE.

2.1.1.2 Reference and counter electrodes

The reference electrode used in this study was either a platinized Pt/hydrogen reversible electrode (RHE) or a saturated calomel electrode. The RHE was mounted in a separate compartment through which a stream of hydrogen gas was continuously bubbled. The compartments were separated by a loosely fitting stopcock allowing also for electrical contact to be maintained between the two compartments. The CE, a large area platinum gauze, was placed in the third

compartment.

All potentials in this work are given with respect to the RHE.

2.1.2 Cells and solutions

The experiments were carried out utilizing a three-compartment electrochemical cell, with each electrode placed in a separate compartment. The electrolytic contact between WE and the RE compartments was maintained via a luggin capillary. The luggin capillary was finely drawn out at the tip to minimize shielding of the working electrode surface. The tip of the capillary was positioned within a few millimeters of the working electrode surface, further minimizing the IR drop. The CE was connected to the main cell by means of a glass stopcock.

The bulk of this study was carried out in alkaline carbonate/bicarbonate solutions. All solutions were prepared from 'Analar' grade chemicals supplied by Fisher Scientific. Buffered carbonate solutions were prepared by dissolving exact amounts of sodium bicarbonate and NaOH into triply distilled water according to some prescribed procedure (45). Unbuffered alkaline solutions and buffered solutions with addition of the appropriate amounts of NaOH and sodium borate were made up similarly. The solution pH was checked with a Fisher Accumet pH meter (model 825P). Several runs were also carried in carbonate-free NaOH but no differences

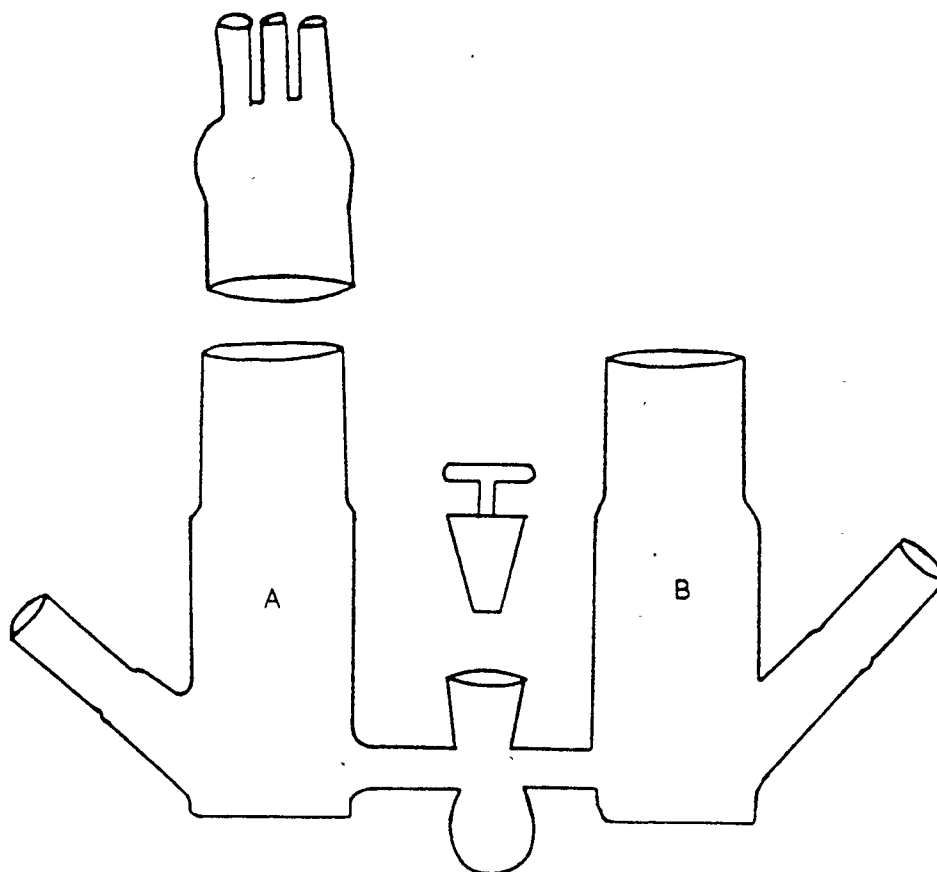


Fig. 2.2 (a) The electrochemical cell

A- counter electrode compartment

B- working electrode compartment

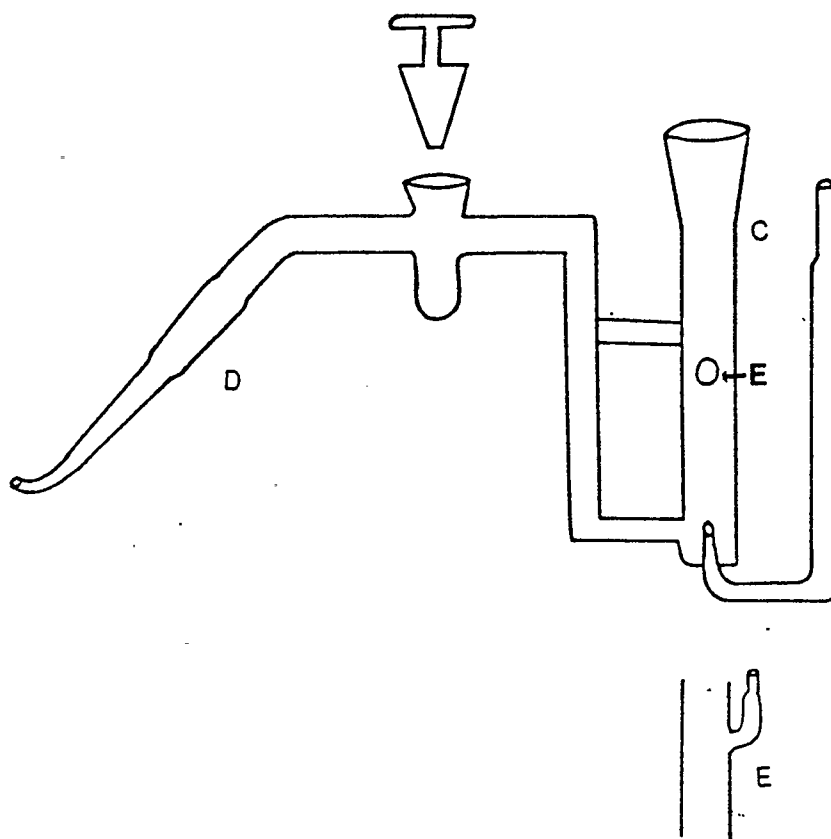


Fig. 2.2 (b) The reference electrode compartment

C- reference electrode compartment

D- luggin capillary

E- side view of hydrogen outlet

were seen in these results vs. those obtained in regular NaOH solutions.

Since oxygen in the electrolytic solution can react with Pb to produce an oxide, solutions were deoxygenated by bubbling pure argon gas through the cell prior to and during the electrochemical experiments. At least ten minutes of argon bubbling was found to be satisfactory for the complete removal of dissolved oxygen, before introducing the WE into the cell.

All experiments in this study were conducted at room temperature, i.e. $23^{\circ}\text{C} \pm 2$.

2.1.3 Determination of the electrode surface area

Before any meaningful attempt can be made to quantitatively analyse the growth of very thin films on an electrode surface, it is essential to know the true area of the metal surface. In most cases, the true area of a solid electrode surface appreciably exceeds the corresponding apparent geometrical area because of a certain degree of 'roughness' (46). The roughness factor, i.e. the ratio of the true area to the apparent geometric area, will depend on the preparation of the metallic surface and the history of the electrode.

In the present work, the true surface area of the WE could be obtained from double layer capacitance measurements in 0.1 N Na_2SO_4 solutions (47). This was done in order to

compare the initial surface areas of different electrodes. The double layer capacitance was measured at high sweep rates (e.g. 1 to 5 V/s) over a narrow range of potential (e.g. -1.2 V to -1.25 V vs. SCE) in which no faradaic processes were expected to occur. The resulting charging current, I_c , was monitored on a Nicolet 3091 digital oscilloscope.

The double layer capacitance, C_{d1} , can be calculated from the following relationship,

$$C_{d1} = I_c / s \quad [2.1]$$

where I_c is the charging current of the double layer. Using a double layer capacitance, C_0 , of Pb of a known surface area in 0.1 N Na_2SO_4 , i.e. $20 \mu\text{F}/\text{cm}^2$ (47), the true electrode surface area, A_0 , was calculated according to equation [2.2]

$$A_0 = C_{d1} / C_0 \quad [2.2]$$

The measured roughness factor, γ , was calculated using the following equation,

$$\gamma = A_0 / A_{app} \quad [2.3]$$

where A_{app} is the apparent geometrical area of the electrode. This generally varied from 1.1 to 2 for an

electrode surface that had just been sheared from a Pb rod and polished with tissue paper.

However, because Pb is roughened by repeated oxidation/reduction cycles in alkaline solutions, resulting in some change in A_0 with time of experimentation, all of the current and charge densities are given with respect to the apparent electrode surface area in this work.

2.2 Surface analytical techniques

2.2.1 Scanning Electron Microscopy

Scanning electron microscopy (SEM) was used to examine the Pb electrode surface at various stages of this study. One set of experiments involved the investigation of different surface preparation methods on the microstructure of the Pb surface and its degree of roughness.

Pb electrodes of appropriate dimensions were sheared from the pure Pb rod, using a sharp stainless steel knife. The electrodes were held with an alligator clip (Section 2.1.1.1). Before each experiment, the electrodes were pretreated with two different polishing procedures which were characterized by the materials used.

In the first case, the electrode surface was polished in succession with various grades of emery paper (250 to 600 grit). After an apparent smooth surface was obtained, the electrode was then thoroughly washed with distilled water, ultrasonically cleaned in acetone and then finally rinsed

with distilled water. It was then dried with filter paper before being transferred to the electrolytic cell. In the second type of preparation, the electrodes were polished only with a soft material such as tissue paper, before use and thoroughly rinsed with distilled water and then placed in the cell.

After electrochemical study, the electrode was removed from the solution, rinsed thoroughly with distilled water and dried with filter paper. The alligator clip was released and the Pb chip was then mounted on a graphite carbon stub using some high purity silver paint, before being transferred to the SEM for analysis.

All the scanning electron micrographs were recorded on a Cambridge S-150 model which was equipped with an EDAX 711 Energy Dispersive X-ray Analyzer.

2.2.2 Auger Electron Spectroscopy (AES)

Electrodes prepared as described in Section (2.1.1.1) were studied electrochemically and then analyzed by AES. This technique yields some information about the elemental composition of the anodic film formed on the electrode surface. With the use of Ar ion sputtering, the surface material can be analyzed as a function of depth from the surface. Samples were sent to Alcan International Ltd. and AES analyses were done with a PHI 600 SAM model equipped with Ar atom sputtering capability.

2.3 Atomic absorption spectroscopy

Atomic Absorption Spectroscopy (AAS) was utilized to analyze the carbonate-containing cell solutions for the presence of dissolved Pb species. After an electrochemical experiment, the cell solution was transferred to a volumetric flask and acidified with the addition of nitric acid in order to release Pb from $\text{Pb}(\text{OH})_3^-$ or Pb/carbonate complexes. The AAS signals were compared to those of a set of Pb standards.

A freshly prepared solution of sodium bicarbonate, which had not been exposed to the Pb metal during the electrochemical measurements was also analyzed, after acidification, for comparison with the test solution. All these analyses were done utilizing an IL VIDEO II AA/AE Spectrophotometer.

2.4 Other techniques used

The Houston Instruments Digitizing Pad, connected to an IBM-PC was used to measure the graphical areas of the CVs. The charge densities passed during CV experiments were calculated using areas measured in this way. The following equation was used to calculate the charge density,

q ($\mu\text{C}/\text{cm}^2$),

$$q = A_c V_x i_y / A_{app} s \quad [2.4]$$

where A_c is the measured area on the CV curve, V_x and i_y are the X and Y recorder voltage and current scales (per cm) respectively, s is the potential scan rate and A_{app} is the apparent electrode area.

CHAPTER 3

GENERAL ELECTROCHEMICAL BEHAVIOUR OF LEAD

IN 1M NaOH SOLUTIONS

3.1 Introduction

There has been a significant amount of research carried out previously with Pb in alkaline solutions, using relatively large area Pb disc electrodes (e.g. 0.385 cm^2) (26-28). During the course of the present study, additional experiments have been carried out in pH 14 solutions, but primarily with the use of small area Pb electrodes. The small electrode area was chosen in order to maintain low cell currents. As a result, diminished IR drop and distributed potential effects are expected (48), as compared to the prior work with large area Pb electrodes.

The initial experiments were conducted purposely to become familiarized with the general electrochemical behaviour of lead in aqueous alkaline solutions. Also, it was essential to determine the potential at which various lead oxide films formed at these small area Pb electrodes, as this is relevant to the subsequent study of Pb in less alkaline solutions containing a number of different ions (e.g. carbonate and borate).

Fig. 3.1 shows a typical CV obtained with a mechanically polished Pb chip electrode (ca. 0.015 cm^2) in 1M NaOH at a sweep rate of 20 mV/sec. When the potential is extended

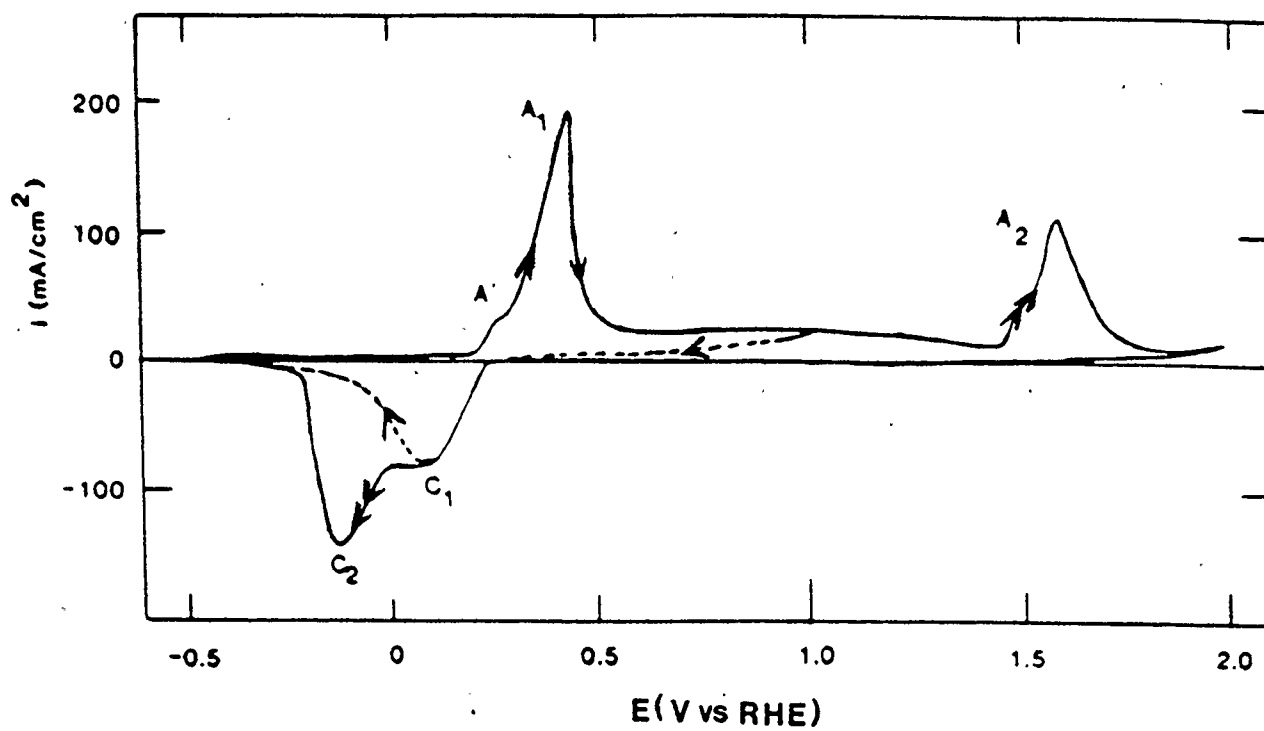
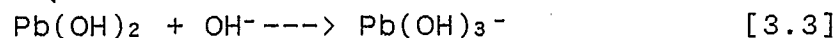
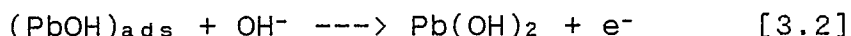
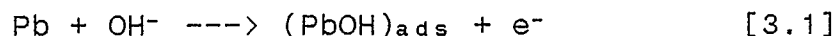


Fig. 3.1 Cyclic voltammogram of Pb chip electrode
(0.015 cm²) in 1 M NaOH at $\nu = 20$ mV/s

positively towards the oxygen evolution reaction (OER) at ca. 2.0 V, and then negatively towards the potential range of hydrogen evolution (HER), two main anodic peaks (A₁ and A₂) and corresponding cathodic peaks (C₁ and C₂) are observed. A shoulder (A') is also seen on the cathodic side of peak A₁. This CV is generally similar to that reported previously at large area Pb electrodes, although the peaks are now substantially sharper and occupy a smaller range of potential in this work as compared to the prior research. It was also noted that the shoulder A' is now more clearly seen, in contrast to the previous work where it tended to be obscured.

In the earlier work at the large area Pb electrodes (28), in pH 14 solutions it was proposed that the shoulder, A', is related to Pb(OH)₂ film formation and its subsequent dissolution, as shown by reactions [3.1 to 3.3].



Although PbO is the equilibrium lead oxide phase at pH 14 (18), a recent thermodynamic calculation has shown (26,27) that Pb(OH)₂ is expected to form at ca. 115 mV vs. RHE, while PbO is not predicted to form until ca. 255 mV (18,28). At a higher current scale sensitivity than in Fig. 3.1, the potential at the foot of shoulder A' is seen to be at ca. 150 mV, which is only a small overpotential relative to the theoretical value for Pb(OH)₂ formation.

A Tafel study carried out previously (26) with a Pb disc electrode (ca. 0.385 cm²) in the range of potential of A', showed that reaction [3.3] was the likely rate determining step of reaction sequence [3.1] to [3.3], consistent with the results reported by Ptitsyn et al (25). It should be noted that when a positive going potential sweep was reversed in the region of A', very little cathodic current was seen at sweep rates less than ca. 200 mV/s (26). As a result, the charge densities passed during the oxidation process (q_a) significantly exceed those passed in the cathodic sweep (q_c), indicative of an anodic dissolution process. This evidence for the dissolution of the product formed in the anodic reaction (i.e. Pb(OH)₂) by reaction [3.3]) under the conditions of these experiments has been confirmed with ring-disc electrode experiments (27,28).

Transient potentiostatic experiments in which the potential was stepped from an initial value of 0 V (vs. RHE) to a potential in the range of A' and then back to 0 V revealed (26) an exponential decrease of the current with time (Fig. 3.2). This type of I/t response is typical of the formation of a surface film, e.g. Pb(OH)₂, on an electrode surface by a random deposition mechanism (e.g. reactions [3.1] and [3.2]). The current decreases to zero with time due to the continuously decreasing free electrode area as film material is deposited on the electrode surface (49). The steady-state current observed at longer times was

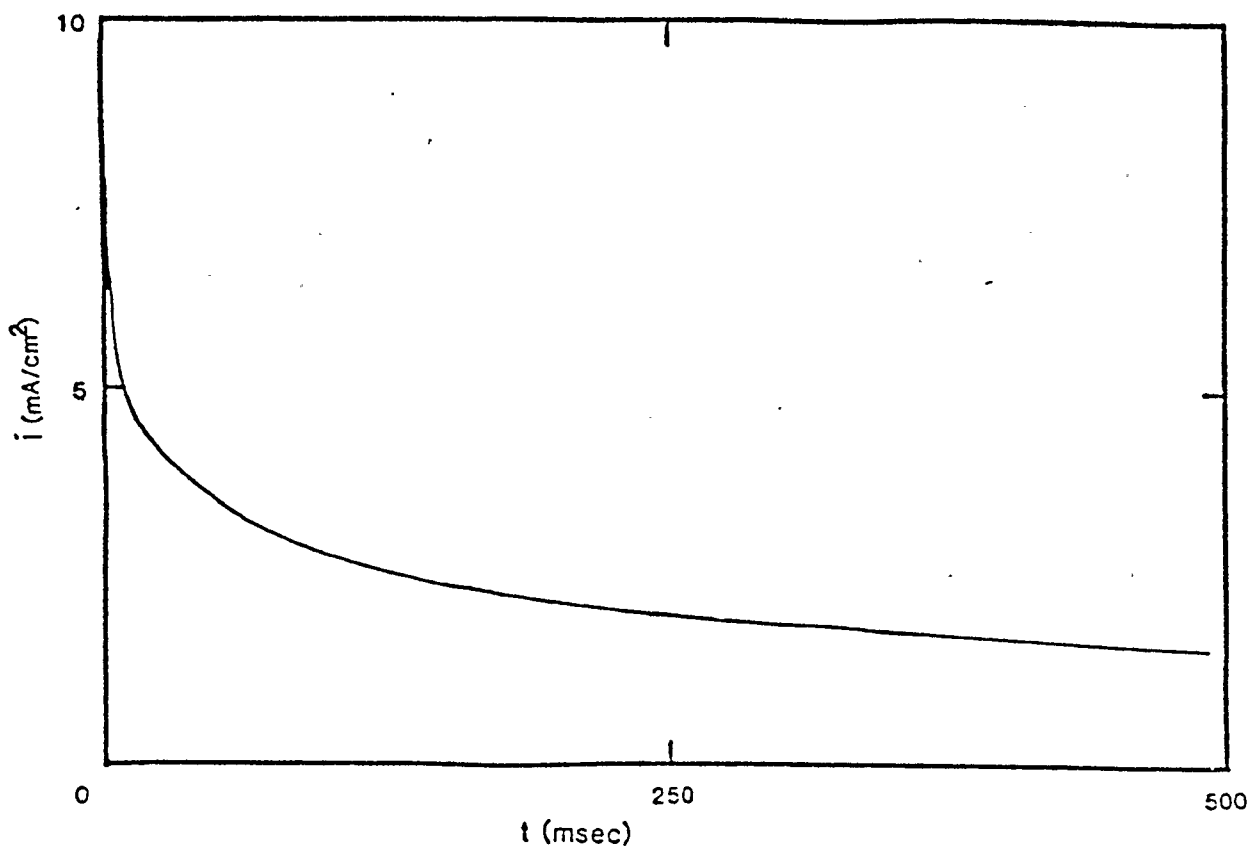
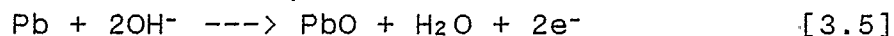


Fig. 3.2 i/t response to a potential step into the region of A' (from 0 to 210 mV vs. RHE)

found (26) to increase with electrode rotation rate, consistent with the influence of reaction [3.3] on the overall mechanism.

The potential obtained by extrapolating the current to the foot of peak A₁ in Fig. 3.1 is ca. 220 mV. Since this potential is quite close to the calculated potential for PbO formation (255 mV), and as Peak A₁ is one of the most dominant features of the CV response of Pb in pH 14 solutions, i.e. indicative of the formation of a thermodynamically stable product, it has been suggested that peak A₁ depicts the formation of a PbO surface film. This was also the assignment made at large area Pb electrodes in 1 M NaOH solutions (26-28). It has been shown that PbO forms both by Pb(OH)₂ dehydration (reaction [3.4]) and via a nucleation and growth mechanism (reaction [3.5]) under diffusion control (27) in Peak A₁, and is reduced in Peak C₁. Some dissolution of PbO is also thought to occur (reaction [3.6]).



Peak A₂ (Fig. 3.1) is considered to represent the formation of a PbO₂ surface film, which can subsequently be reduced in the potential range of Peak C₂. The deposition and removal of PbO₂ was not studied in detail in this work.

3.2 Sweep rate studies in the region of A'

Further work has been undertaken in the course of this study with the use of high potential sweep rates and small area Pb electrodes to confirm some of the earlier results in pH 14 solutions (25-28). The first series of experiments involved the use of high potential sweep rates as a test of the previously suggested (26) reaction mechanism (reactions [3.1 to 3.3]) in pH 14 solutions. Fig. 3.3 shows the CV response in the region of A' at sweep rates of 2 to 10 V/s at a Pb chip electrode (surface area ca. 0.02 cm²). At these high sweep rates, the potential at the positive end of the scan, E₊, was incremented somewhat with increasing sweep rate in order to reach all of A' in each scan. In contrast to the large q_a/q_c ratios observed at low sweep rates (26), it can be seen that as the sweep rate is increased, the anodic (q_a') and cathodic (q_c') charge densities become similar in value (Fig. 3.4).

For the formation of a monolayer of Pb(OH)₂ having the density of the bulk material, the charge density (q) can be given by the following equation (50)

$$q = (pL/M)^{2/3} zF/L \quad [3.7]$$

where F is the Faraday constant, L is Avogadro's number, M is the molecular weight of Pb(OH)₂, p is the density of Pb(OH)₂ (7.59 g cm⁻³) and z is the number of electrons passed (= 2) per molecule of Pb(OH)₂. Solving equation

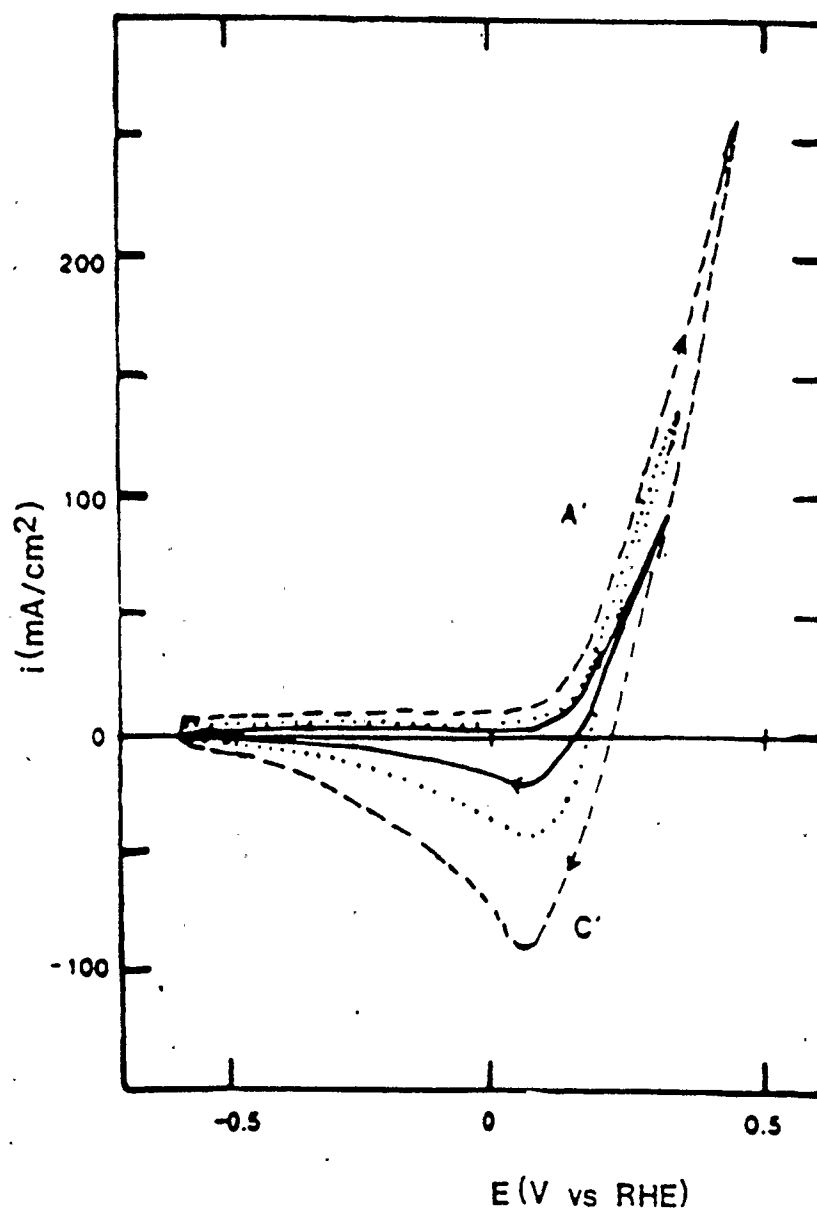


Fig. 3.3 Cyclic voltammetric response of Pb chip electrode (0.02 cm²) at high sweep rates in 1 M NaOH. $s = 2$ V/s (—), 5 V/s (.....), and 10 V/s (---)

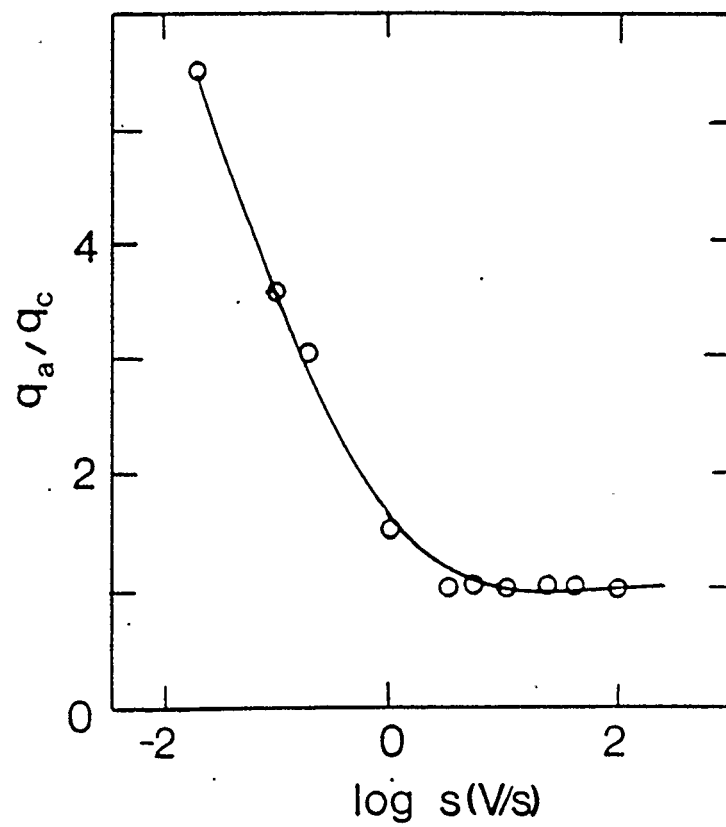


Fig. 3.4 Ratio of anodic to cathodic charge densities passed in the region of A'/C'

[3.7] yields a charge density of about 230 $\mu\text{C}/\text{cm}^2$ per monolayer of $\text{Pb}(\text{OH})_2$. The charge density passed in A'/C' in Fig. 3.3 is ca. $2.3 \pm 0.2 \text{ mC}/\text{cm}^2$ at high sweep rates, i.e. a charge density equivalent to ca. 10 monolayers of $\text{Pb}(\text{OH})_2$, assuming a roughness factor, γ , of unity. Alternatively, the high charge density passed in A'/C' could mean that the lead electrode surface had been roughened tenfold. Such extensive electrode roughening should have led to a 10-fold increase in the peak currents, but this was not observed in these experiments. Therefore, it is more likely that the charge equivalent of ten monolayers of $\text{Pb}(\text{OH})_2$ is deposited in A'.

The similarity of the anodic and cathodic charge densities of A'/C' at high sweep rates (Fig. 3.4) indicates that insufficient time is available for any dissolution of $\text{Pb}(\text{OH})_2$ (reaction [3.3]) to occur, so that only the formation and reduction of $\text{Pb}(\text{OH})_2$ nuclei is monitored in A'/C'. Table II summarizes the principal observations about peaks A'/C', including the charge densities in A'/C' and the potential at the foot of A', as a function of sweep rate. This table shows that the charge ratio, q_a/q_c , is close to unity for high sweep rates ($> 2 \text{ V}/\text{sec}$), indicative of the lack of time for dissolution to take place. The appearance of a cathodic peak and subsequent increase in cathodic charge is also clear evidence that there is more material build-up on the electrode when there is insufficient time

Table II Potentials and charge densities in region of peaks A'/C'

Solution/pH	s	E+	E _{foot} *	q _a '	q _c	q _a '/q _c '
<u> </u>	<u>V/s</u>	<u>(mV vs. RHE)</u>		<u>(mC/cm²)</u>		<u> </u>
1 M NaOH	0.02	175	140	2.4	0.4	5.5
pH 14	0.10	175	140	1.3	0.4	3.3
	2.0	300	150	2.2	1.7	1.3
	10.0	400	150	2.4	2.4	1.0
Na borate	0.05	450	150	4.7	4.2	1.1
pH 9.6						
Na carbonate	0.10	350	130	4.6	0.40	11.5

* at foot of A'

for the soluble species to be transported away from the electrode surface. This also supports the suggested reaction mechanism (reaction 3.1 to 3.3).

3.3 Peaks A₀/C₀

After several hours of experimentation with a Pb chip electrode in the same 1 M NaOH solution, a new phenomenon was seen to develop in the potential range just negative of A'. Fig. 3.5 shows that at high sweep rates, a matching pair of small peaks (A₀/C₀) are seen, centred at a potential of ca. 0 V vs. RHE, i.e. at an underpotential of ca. 100 mV relative to the calculated potential for Pb(OH)₂ formation (115 mV vs. RHE). An analysis of the relationship between the peak current densities of Peaks A₀ and C₀ as a function of potential sweep rate reveals a linear dependence between these parameters (Fig. 3.6). The charge density contained in the peaks in Fig. 3.5 is ca. 40 $\mu\text{C}/\text{cm}^2$, if the apparent electrode area is assumed. If the electrode area is higher by a factor of 2 or 3, the charge density would be still smaller than this.

It should be noted that the formation of a monolayer of Pb(OH)₂ might be anticipated to occur at an underpotential. Also, a linear i_p/s relationship would be consistent with monolayer formation and removal. However, a single monolayer of Pb(OH)₂, having the same density as the bulk

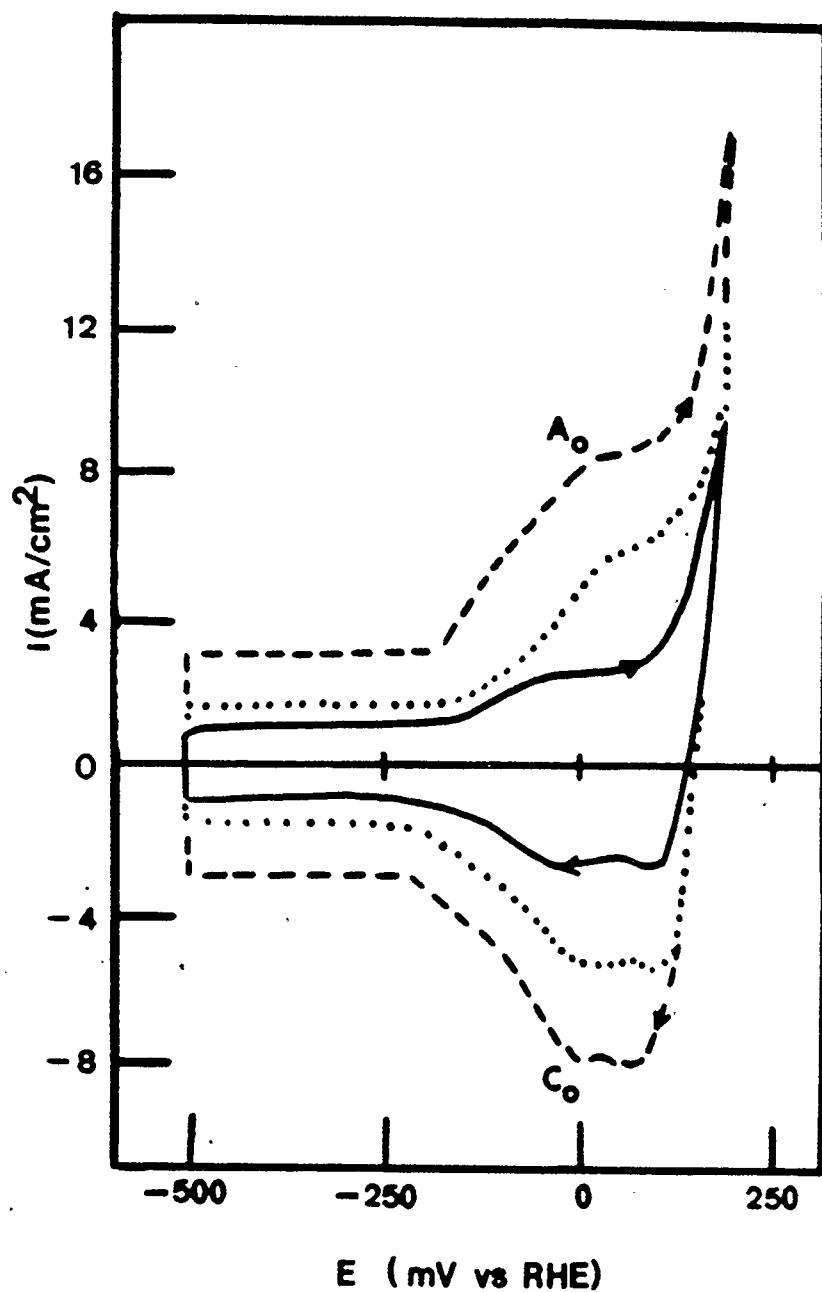


Fig. 3.5 Cyclic voltammograms of Pb chip electrode (0.02 cm²) at high sweep rates after several hours of electrochemical experimentation in 1 M NaOH. $s = 10$ V/s (—), 20 V/s (.....), and 30 V/s (- - -)

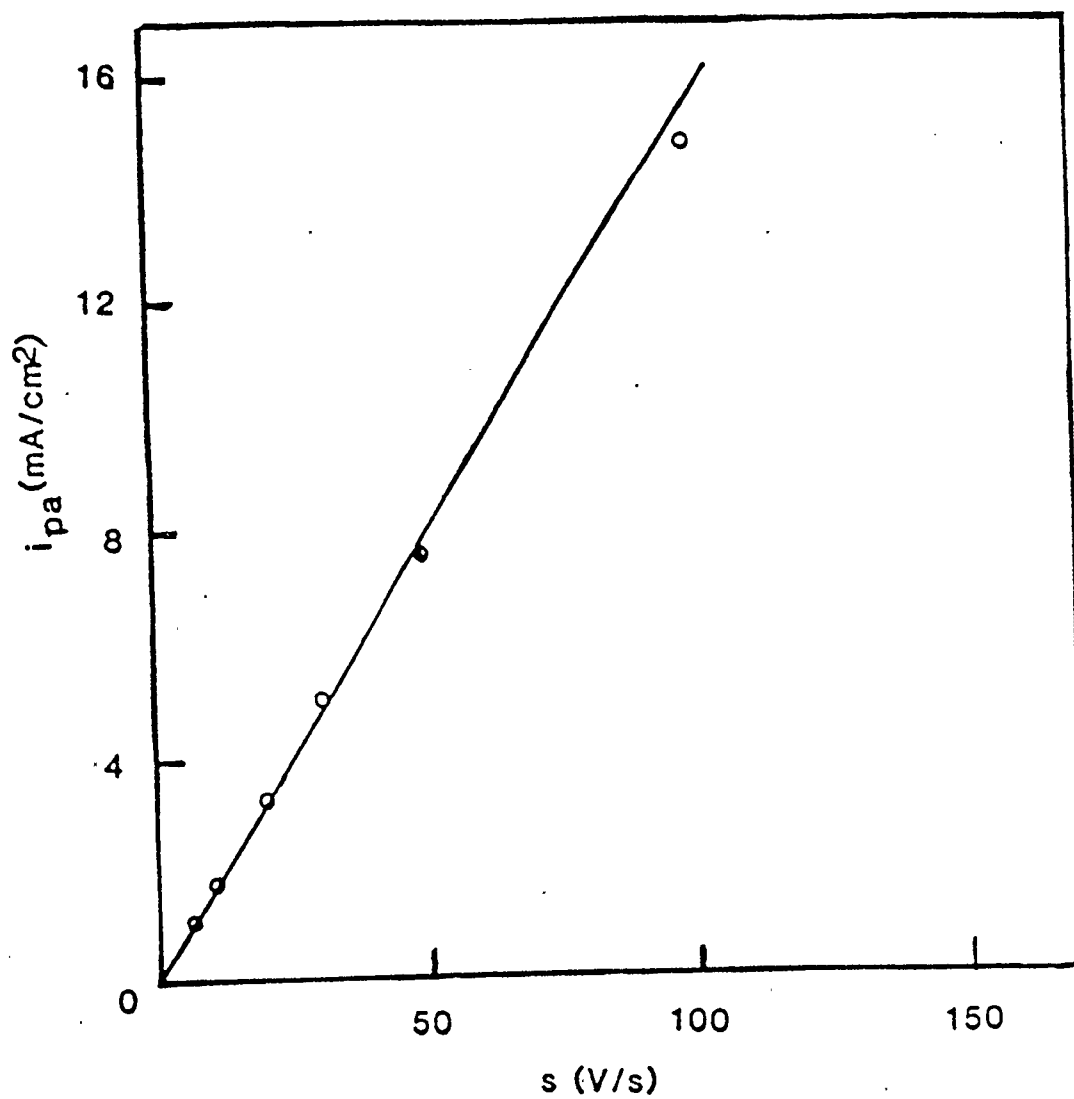


Fig. 3.6 Relationship between anodic peak current density of A_0 and potential sweep rate in 1 M NaOH

material, would be expected to involve a charge density of ca. $230 \mu\text{C}/\text{cm}^2$ (50,51). As the charges are significantly less than this, Peaks A_0/C_0 may represent the formation of a two-dimensional layer of $\text{Pb}(\text{OH})_2$ on only part of the electrode surface, or the deposition of a very open $\text{Pb}(\text{OH})_2$ structure over the entire electrode surface. Alternatively, Peaks A_0/C_0 may reflect the adsorption of OH^- on the Pb surface, as suggested in reaction [3.1], followed by a partial charge transfer reaction (52). This latter process is also likely to be seen at an underpotential, and would be expected to involve a lower charge density than that for the formation of a monolayer of $\text{Pb}(\text{OH})_2$ film. These two possibilities cannot be distinguished from the data presented here, as was also the case in attempting to identify the process occurring in the pre-peak observed at Ag electrodes in chloride-containing solutions [53].

The fact that peaks A_0/C_0 are only seen after some time of experimentation, during which many sweeps of potential are made to positive potentials, was originally thought to indicate that the Pb electrode had become activated, perhaps by an etching process, with time of potential cycling in these alkaline solutions. However, the development of Peaks A_0/C_0 with time may also be related to the gradual deposition of high energy Pb nuclei on the Pb electrode surface by the reduction of $\text{Pb}(\text{OH})_3^-$ at negative potentials. It is reasonable to suggest that Pb sites of this kind would

be more active towards either two-dimensional film formation and/or anion adsorption, as they would be likely to have a different surface energy from the original Pb electrode surface (53).

The suggestion that newly deposited Pb nuclei are responsible for the gradual appearance of Peaks A_0/C_0 , rather than being related to the development of active sites by surface etching, is supported by the following observation. A fresh Pb electrode, placed into a solution which had been studied previously, and therefore would be expected to contain dissolved Pb, probably in the form of $Pb(OH)_3^-$, rapidly developed Peaks A_0/C_0 . In contrast, a fresh Pb electrode in a fresh 1 M NaOH solution required several hours of continuous potential cycling before Peaks A_0/C_0 appeared. As the rate of Pb surface etching should depend only on the time spent in the solution (and the potential), this result rules out an etching process as the cause for the development of A_0/C_0 .

3.4 Summary of lead oxidation in 1 M NaOH

The anodic oxidation processes which take place at the Pb electrode in 1M NaOH have been shown by CV experiments to involve the formation of several lead oxide phases. The main anodic peaks A_1 and A_2 correspond to the formation of PbO and PbO_2 films, respectively, while the shoulder (A') is related to the formation of $Pb(OH)_2$, which subsequently

dissolves to Pb(OH)_3^- .

The CV experiments conducted at high sweep rates in the region of A' show that the anodic charge densities are now similar to the cathodic charge densities, i.e. $q_{A'} = q_{C'}$. It was observed earlier (26) that at lower s (< 200 mV/s), no cathodic peak corresponding to A' was seen. However, at high sweep rates, insufficient time is available for Pb(OH)_2 dissolution and therefore Pb(OH)_2 reduces in C'.

It has also been shown that after several hours of experimentation, two corresponding peaks A_0 and C_0 emerge at an underpotential of ca. 100 mV relative to the potential of Pb(OH)_2 formation. This observation has been explained as resulting from the deposition of high energy Pb nuclei on the electrode surface during the reduction process at very negative potentials.

The use of a small area Pb electrode results in improved peak resolution in the cyclic voltammograms, although the same processes as seen previously with the use of large area electrodes occur at similar potentials. The appearance of the shoulder (A') is more salient with small area electrodes than it was at large area electrodes.

CHAPTER 4

SEM STUDY OF ELECTRODE SURFACE PREPARATION

4.1 Introduction

Early on in the research, an investigation of the effects of various Pb electrode surface preparation methods on the electrochemical behaviour of lead in aqueous solutions (particularly carbonate solutions, see Chapter 5) was undertaken. It has been pointed out by others (54-56) how crucial the surface morphology can be in terms of the electrochemical reactivity of solid electrodes, especially when dealing with soft metals such as Pb. These soft metals have been known to significantly change their surface structure during electrode preparation and hence their electrochemical response is also likely to be variable.

In the previous work of the behaviour of lead in 1 M NaOH (26-28), mechanical polishing using various grades of emery paper was used to prepare the electrode surface. As will be shown below, this polishing procedure has deleterious effects on the electrode surface. In the work at pH 14, very thick oxide films can be formed and therefore a variable state of the surface may not have a major influence on the electrochemical response, although the nucleation mechanism and kinetics of PbO formation at these Pb electrodes would have been expected to be surface dependent.

In the present work in carbonate and borate buffered solutions, comparatively thin films are being formed and studied and therefore, the state of the electrode surface is expected to be critical to the mechanism and kinetics of the surface film formation. It is important to produce a surface which is reproducible and smooth, especially when dealing with the formation and reduction of very thin films. A roughened surface tends to produce irreproducible results and is likely to obscure surface structural features which may result from the oxidation and reduction processes. This would make it difficult to evaluate and compare results obtained from different electrode surfaces, as well as to interpret SEM observations.

It was also realized in the initial stages of this study that there are two general types of electrochemical response of Pb in the carbonate-containing solutions (Type I and II), (see Section 5.2.1). As it was considered likely that the type of electrochemical response was dependent on the electrode pretreatment, a detailed investigation of electrode surface preparation was commenced.

During the course of this study, SEM has been used to investigate the nature of the electrode surface prepared by various techniques. It has also been used to investigate the structural features on the electrode surface after controlled electrochemical experimentation in alkaline carbonate solutions.

4.2 Electrode surface preparation studies

There were several methods used to prepare the electrode surface for the SEM investigations. These included various mechanical polishing techniques, chemical polishing, and sample fracturing methodologies. The mechanical polishing techniques included the use of various grades of emery paper (down to 600 grit) and the use of diamond paste and also alumina paste (down to $1.0\ \mu\text{m}$). During chemical polishing, the electrode was dipped into a solution of glacial acetic acid and hydrogen peroxide in methanol for about 1 min (30,56). Although the electrode surface appeared mirror-like after this treatment, its electrochemical response was found to be very irreproducible. Fracturing methods involved the use of a stainless steel knife to cut off a piece of Pb from the Pb rod.

Fig. 4.1 shows a typical SEM photomicrograph of a freshly sheared Pb electrode which was then subjected to mechanical polishing with various grades of emery paper. This electrode was never exposed to aqueous solutions or any electrochemical experimentation. It can be seen from Fig. 4.1 that this type of mechanical polishing of Pb leaves a microscopically very rough and heterogeneous surface. The surface is covered by many small crystals of $\text{ca. } 1 \pm 0.5\ \mu\text{m}$ in diameter. These crystallites were initially thought to be from the emery paper itself. However, an examination of the emery paper by SEM showed silicon carbide crystals of

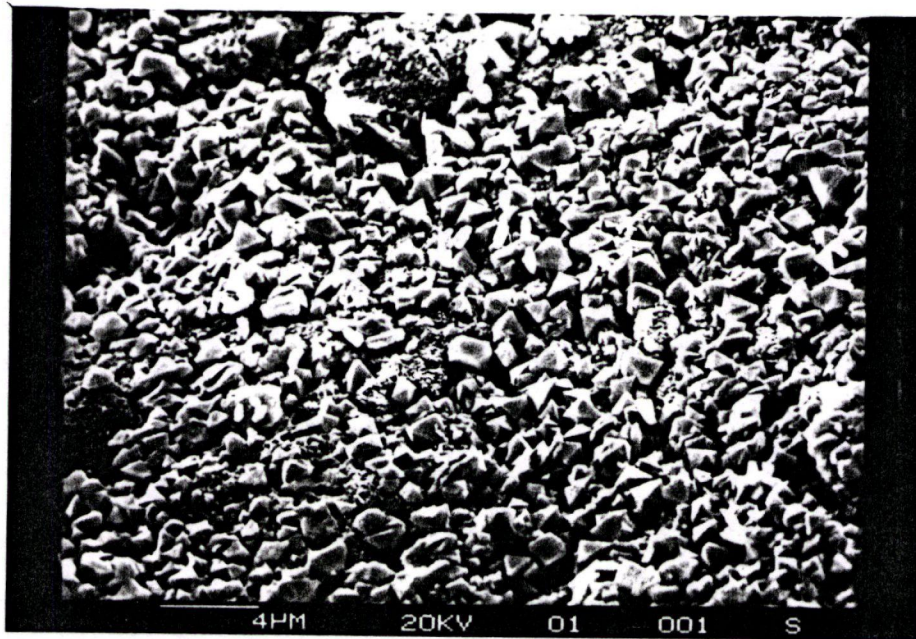


Fig. 4.1 SEM view of a mechanically polished Pb surface

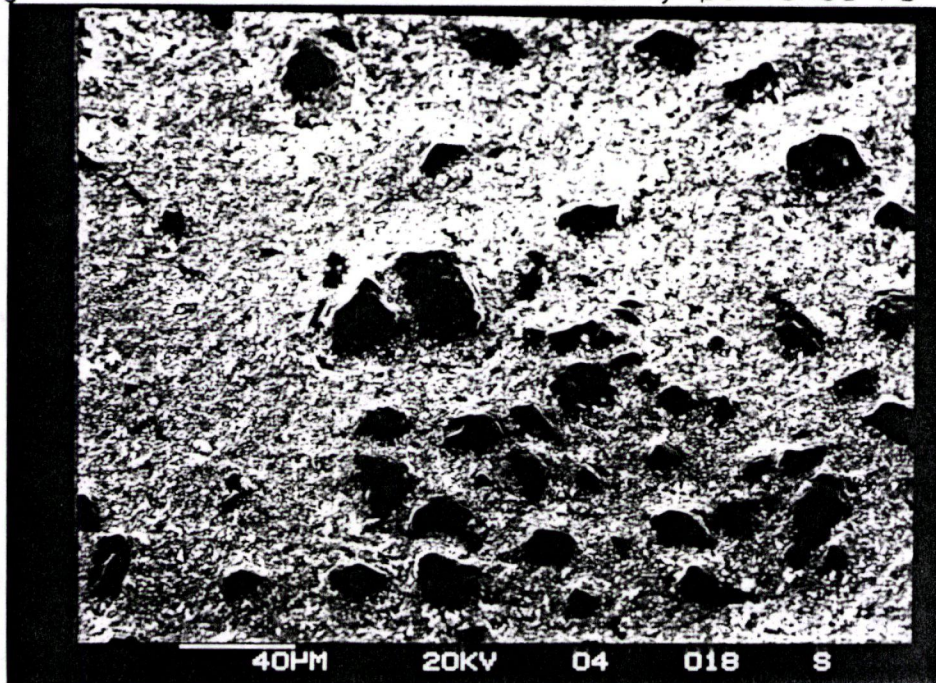


Fig. 4.2 Mechanically polished Pb surface (emery paper, 600 grit size) showing embedded silicon carbide particles

diameter ca. 20 μm , consistent with the grit size of the paper, this being about tenfold the crystal size in Fig. 4.1. This implies that the emery paper polishing of the Pb electrode surface causes loose Pb crystallites to be produced on the surface. The electrochemical response of such a mechanically polished Pb electrode showed a considerable increase in the total charge passed during a CV experiment relative to a smooth fractured electrode (see below), consistent with the large area of the surface in Fig. 4.1.

At lower SEM magnification, it was shown that emery paper polishing, even if followed with ultrasonic cleaning, does indeed leave emery paper particles embedded in the Pb surface. Fig. 4.2 shows an emery paper mechanically polished Pb surface with several large particles embedded in the surface. These particles were analysed by EDAX and were found to contain silicon. The presence of silicon, indicative of silicon carbide, confirms the dangers of the use of emery paper mechanical polishing methods for the surface preparation of soft metals such as Pb.

A scanning electron micrograph obtained after the mechanical polishing of Pb with 0.1 μm diamond paste is shown in Fig. 4.3. In this case, the electrode was first polished successively with various grades of emery paper (250 to 600 grit size), ultrasonically washed in acetone and then polished with 0.1 μm diamond paste. The Pb was then thoroughly rinsed with distilled water. Although Fig. 4.3

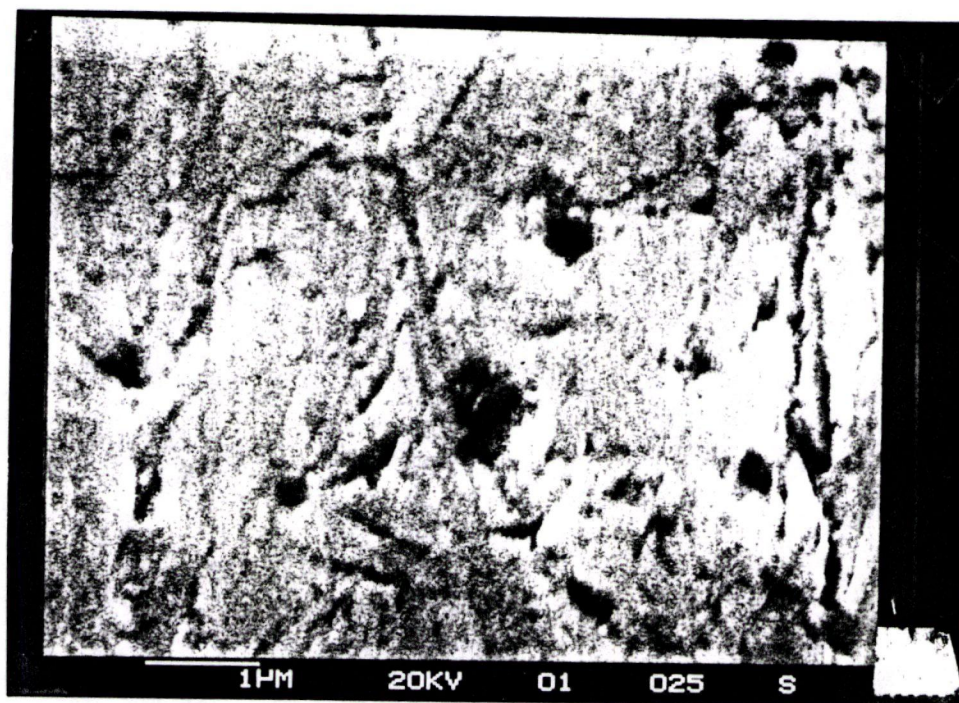


Fig. 4.3 Pb surface mechanically polished with emery paper (600 grit), various grades of diamond paste (down to $0.1\ \mu\text{m}$) followed with ultrasonic washing

shows a rather smooth microstructure, the overall surface has many visible (to the eye) pits, perhaps resulting from the initial abrasive action of the emery paper. With alumina paste polished surfaces, small particles of alumina could be seen embedded in the surface. This was positively confirmed by the XRD.

Since mechanical polishing appears to result in a microscopically roughened surface, with polishing material embedded within it, other approaches were undertaken to prepare smooth and reproducible electrode surfaces for the electrochemical experiments.

Chemical polishing procedures were also attempted. However, this resulted in irreproducible electrochemical response, and hence was not pursued further.

A third approach involved the use of a stainless steel knife edge to cut off (shear) a small Pb chip from the Pb rod. Immediately prior to any subsequent experiments, the lead surface was polished with a soft material such as tissue paper or cloth to obtain a shiny and smooth surface. This approach has also been used previously (17,44) in the preparation of Pb electrode surfaces, prior to electrochemical studies in various other solutions. This method was found to be the best in achieving a smooth and most reproducible lead surface, as well as reproducible electrochemistry.

Fig. 4.4 shows a SEM micrograph of a Pb surface which

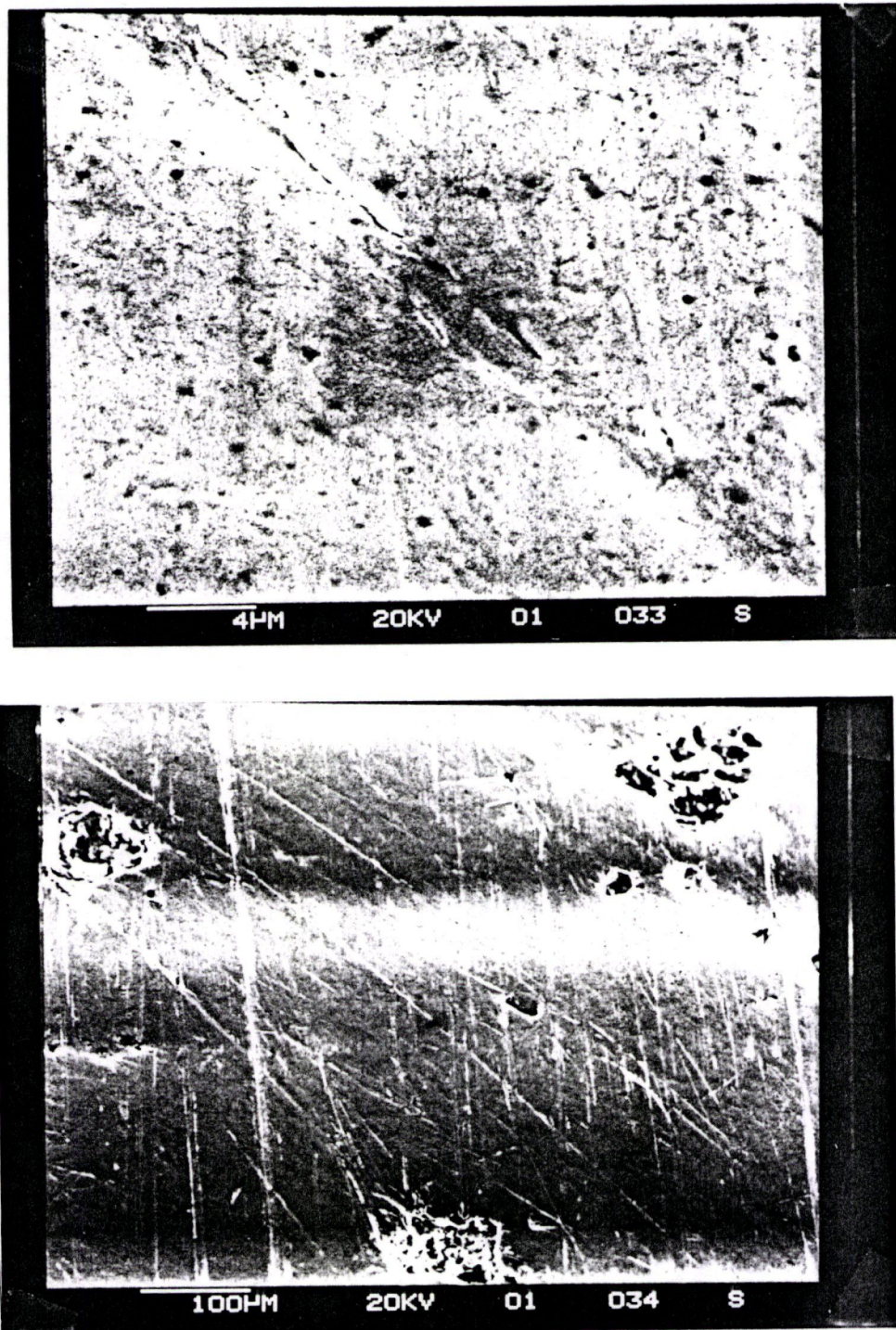


Fig. 4.4 A freshly sheared Pb electrode and tissue polished. (No mechanical polishing)

had been prepared by shearing it from the Pb rod with a stainless steel knife edge. This type of procedure produces a smooth, rather featureless electrode surface, particularly as compared to that seen in Fig. 4.1. There appear to be occasional irregular pits within the surface, perhaps resulting from the shearing process. It is also possible that these pits are an inherent property of the Pb rod. In any case, this method of Pb electrode preparation was clearly superior, and therefore the bulk of the electrochemical experiments carried out in this work utilized electrodes which had been prepared in this way.

Another possible approach to Pb electrode surface preparation would be to mechanically polish the electrode surface at very low temperatures, e.g. in a liquid nitrogen environment. This would harden the metal and minimize the embedding of polishing compounds into the surface. However, this method was not attempted in this work.

CHAPTER 5

ELECTROCHEMISTRY OF Pb IN CARBONATE SOLUTIONS (pH 9.6)

5.1 Introduction

After familiarization with the electrochemistry of Pb in pH 14 solutions, subsequent experiments were conducted in less alkaline solutions. The objective of this research was to investigate the oxidation and reduction processes which occur at a Pb electrode in solutions containing different anions, e.g. CO_3^{2-} and $\text{B}_4\text{O}_7^{2-}$. The electrochemical behaviour of Pb in these solutions is compared with the behaviour in pH 14 solutions.

The main focus has been on carbonate solutions, partly due to the need to use lead to precipitate $^{14}\text{CO}_3$ species present in heavy-water moderator systems (41) and also as it has been suggested that lead could serve as a storage material for nuclear waste in underground vaults (42). Therefore, it is of interest to study Pb electrochemistry in carbonate-containing solutions in order to gain a good understanding of the chemical and electrochemical processes which can occur at the electrode surface.

It will be shown below that Pb behaviour in carbonate solutions involves a number of complex reactions, including the formation of a number of Pb/oxy/carbonate compounds. Borate- buffered solutions (containing no carbonate ions)

have also been studied in order to aid in the understanding of the electrochemical processes in carbonate solutions. The use of borate ion allows for pH control, but in the absence of carbonate, thus aiding in distinguishing Pb oxide/hydroxide reactions from those involving carbonate ions.

Fig. 5.1 shows the cyclic voltammogram (CV) obtained with a polished Pb chip electrode (ca. 0.02 cm^2) in a buffered 0.05M NaHCO_3 solution (pH 9.6) over the potential range of -0.9 to 1.0 V at a sweep rate of 50 mV/sec . This potential range was initially chosen as it was very similar to the potential range studied in pH 14 solutions, i.e. over which the processes involving Pb(OH)_2 and PbO formation and reduction occurred. In typical electrochemical experiments in pH 14 solutions (e.g. Fig. 3.1) the potential limits -1.0 to 2.0 V vs. RHE were found to be appropriate for the study of the oxidation/reduction processes that occur at the lead electrode surface. When studying more closely the initial stages of the lead oxidation processes associated with only peaks A' and A_1 , $E_+ = 1.0 \text{ V}$ was found to be sufficient. An E_- of ca. -1.0 V was chosen to avoid extensive evolution of hydrogen and hence avoiding the build-up of OH^- at the electrode surface similar to the work at pH 14. This E_- also appeared to be adequately negative to complete the reduction process in peak C_1 .

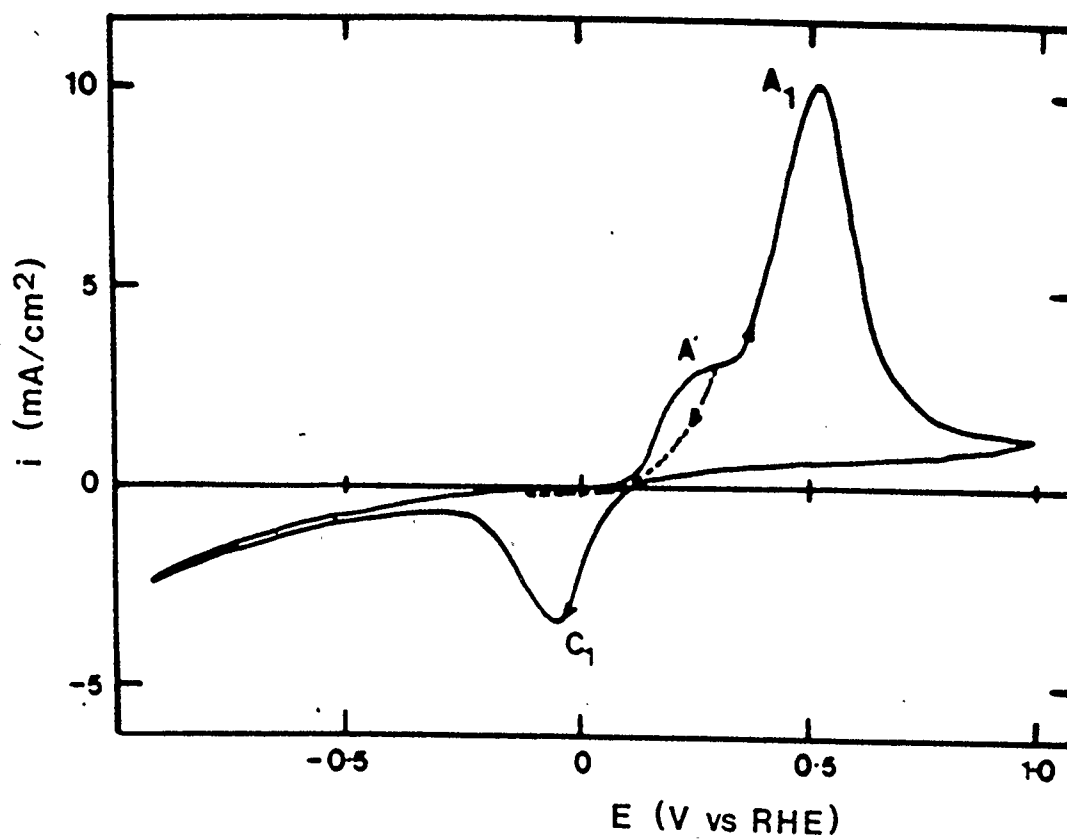


Fig. 5.1 Cyclic voltammogram of Pb chip electrode
(0.02 cm^2) in 0.05 M NaHCO_3 (pH 9.6) at
 $s = 50 \text{ mV/s}$.

In order to achieve reproducible CVs over this potential range, the Pb chip electrode potential was usually held at the negative limit of the sweep for at least 10 secs before initiating the next cycle of potential. Alternatively, repeated potential cycling also led to reproducible CVs, but having a diminished response i.e. lower currents and charges overall. During a typical anodic scan, after potential holding at E_- , two anodic peaks (A' and A_1) are observed, while only one cathodic peak (C_1) is seen when the potential scan is reversed (Fig. 5.1). The onset of the oxidation process in A' occurs at ca. 140 ± 10 mV vs. RHE. This is also similar to the potential observed at the foot of A' in pH 14 solutions. The potential at the foot of peak A_1 , obtained by extrapolation to zero current, is about 220 mV, a value which is close to the calculated thermodynamic potential (18,28) of 255 mV for the formation of PbO . A plateau current is observed positive of the main anodic peak (A_1) before the subsequent evolution of oxygen at about 2.2 V. Sometimes in these carbonate solutions, anodic peak A_2 was also observed.

The cyclic voltammetric response obtained with lead in borate buffered solutions (pH 9.6) is shown in Fig. 5.2. In this experiment, the positive limit has been extended to only ca. 1.0 V. During the anodic going scan, two anodic peaks A' and A_1 are seen while only one major cathodic peak

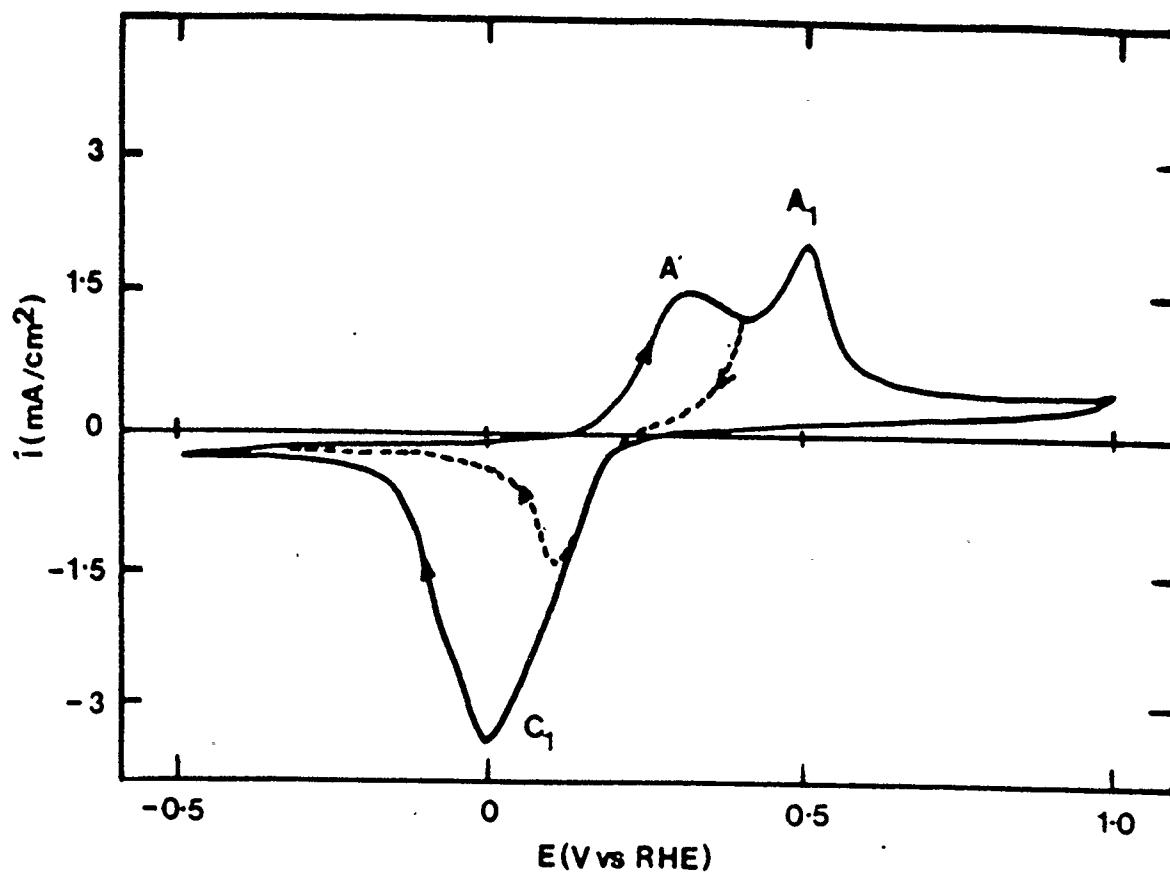


Fig. 5.2 Cyclic voltammogram of Pb chip electrode
(0.02 cm²) in 0.025 M Sodium borate at
 $s = 20$ mV/s.

C_i was observed when the potential scan was reversed. These observations in carbonate and borate buffered solutions (pH 9.6) can be compared to those in 1M NaOH solutions (Fig. 3.1). It can be seen that the general appearance of the CVs in these pH 9.6 solutions is quite similar to that at pH 14, although A' now appears as a distinct peak rather than as a shoulder and peak A_i is significantly smaller at pH 9.6 than at pH 14. This may indicate that the extent of PbO formation (A_i) is diminished at lower OH⁻ concentrations. Importantly, the principal peaks are all seen at virtually the same potentials (vs. RHE) in all of these solutions.

The overall similarity of the CVs of Pb in the carbonate and borate solutions is very marked, lending support to a common sequence of reactions and products. One noticeable difference in Figs. 5.1 and 5.2, however, is that the anodic charge is substantially greater than the cathodic charge in carbonate solutions, while in the borate media, these charges are very similar. Figs. 5.1 and 5.2 display this more clearly when the potential is reversed just positive of peak A'. In the carbonate solution, almost no cathodic charge is observed under the conditions of this experiment, while in borate solutions, the charges are very similar. It will be shown below that this difference in the anodic and cathodic charges in the carbonate solutions is not the result of Pb dissolution in the anodic scan but rather the

result of the incomplete removal of the oxidation products from the electrode surface during each cathodic sweep.

It can be seen that the onset of the initial oxidation process in A' is at ca. 140 mV in both the carbonate and borate solutions (Table II), i.e. very close to the potential at the foot of A' in pH 14 solutions. A' was also seen to commence at a similar potential (RHE) over the range of pH from ca. 10 to 14, and with either carbonate/bicarbonate or borate ions present. This is strong evidence for the formation of the same phase in A' in all of these solutions, i.e. at least in the early stages of A'. As this phase has been identified as Pb(OH)_2 in pH 14 solutions from thermodynamic calculations, it is therefore proposed that the first step of Pb oxidation in all of these solutions involves Pb(OH)_2 formation.

The charges passed in Peaks A'/C' in borate and carbonate solutions are given in Table II, for comparison with the pH 14 case. It can be seen that the charge densities are similar at pH 9.6 at low sweep rates to those in pH 14 solutions at high sweep rates. It should be noted that Pb(OH)_2 is not expected to be very soluble at pH 9.6 (18), consistent with the matching anodic and cathodic charge densities in borate solutions, Fig. 5.2.

The suggestion that the same species, i.e. Pb(OH)_2 , is formed initially in all of these solutions, is supported by

recent results reported for Zn electrodes (57). During the oxidation of Zn in various alkaline solutions, the potential at the onset of Zn oxidation was also found to be independent of the nature of the electrolyte used. It was therefore proposed that the initial stage of Zn oxidation must also involve Zn(OH)_2 formation. The electrochemical behaviour of iron in carbonate/bicarbonate solutions (58,59) has also been studied using cyclic voltammetry. In this work it is also argued that the initial stages of surface film formation on the iron electrode involve the formation of a monolayer of Fe(OH)_2 species.

Shoesmith et al (31) have also studied the oxidation of lead in carbonate solutions (1 M K_2CO_3 , pH 12). At this comparatively high pH, the CV response appears quite similar to that at pH 14 (Fig.3.1) including the presence of a small anodic shoulder (A') preceding the first anodic peak (A_1). It was suggested in their work that hydroxy-carbonate complexes of lead (e.g. plumbonacrite (PN), $\text{Pb}_{10}\text{O(OH)}_6(\text{CO}_3)_6$ and hydrocerussite (HC), $\text{Pb}_3(\text{OH})_2(\text{CO}_3)_2$, are formed in A', as determined by XRD analyses after long times of oxidation. However, the potential obtained by extrapolating to the foot of peak A' in their data also yields a potential of ca. 130 to 150 mV vs RHE, similar to that in carbonate free solutions (e.g. borate buffered solutions, Fig. 5.2 and in 1 M NaOH solutions (Fig. 3.1).

If a PN or HC phase is indeed the equilibrium phase formed in peak A' in pH 12 (1 M carbonate) solutions, it is possible that the initial step in the reaction is still the formation of Pb(OH)_2 , hence defining the thermodynamic conditions, and that Pb(OH)_2 subsequently transforms to the carbonate/Pb oxide phase after reaction with carbonate. This suggestion would be even more likely in the experiments of Shoesmith et al (31), where the hydroxycarbonate phases were observed after one hour of potential holding in the region of A'. Therefore, sufficient time would have been provided for these complexes to form. It is also feasible that the free energy of formation of the PN and/or HC phases is similar to that of Pb(OH)_2 in these carbonate-containing solutions, and that this is the cause of the similar potentials observed in their work as compared to those found in the course of this study.

In an earlier study (30) of the electrochemical behaviour of Pb in pH 9 solutions, but using 0.1 M sodium borate as the buffer, the foot of the first anodic peak was also observed at a potential of ca. 150 mV vs RHE. In that study (30), the first peak was attributed to the formation of a lead borate surface film, although no supporting evidence (e.g. surface analysis) was provided for this assignment. It seems more likely that this first peak also depicts Pb(OH)_2 formation. The second anodic peak (A_1),

seen at 246 mV vs. RHE, a similar potential to peak A_1 in Fig. 3.1, was considered (30) to represent PbO formation on the basis of photoelectrochemical measurements. This agrees with the assignment in all the solutions under study in this work.

In order to determine the nature of the reaction occurring in A' in borate solutions, a series of experiments were carried out to determine the pH dependence of peak A' in borate solutions. It was found that when the borate concentration was held constant, while the pH was varied from ca. 9.5 to 12, peaks A' and A_1 both shifted negatively in an identical manner with increasing pH. This indicates that the processes occurring in A' and A_1 both involve the same pH dependence, which would be more consistent with $Pb(OH)_2$ and PbO forming respectively.

On the basis of all the results obtained in borate and carbonate solutions as well as pH 14 solutions, it appears to be more likely that the first peak (A') reflects $Pb(OH)_2$ deposition, at least initially, rather than the formation of a lead borate film in borate solutions or the direct formation of a Pb /oxide/carbonate film in carbonate solutions. $Pb(OH)_2$ deposition appears to be followed by PbO formation in peak A_1 in all of these solutions. Since peak A_2 is usually not seen prior to oxygen evolution in the bicarbonate solutions, it appears that higher oxides (e.g.

PbO₂) are not readily formed in these solutions.

An analysis of the sweep rate dependence of peak A' in bicarbonate and borate solutions is shown in Fig. 5.3 (curves a and b, respectively). This type of analysis could not be done in pH 14 solutions, as A' did not appear as a peak in this solution, even at high sweep rates (Fig. 3.3). Fig. 5.3 demonstrates a linear relationship between $i_{p,A'}$, and $s^{1/2}$ in both 9.6 solutions, probably indicative of a diffusion controlled process. This i_p vs. $s^{1/2}$ relationship can also be observed when the solution resistance in the pores of a growing film controls the rate of film formation (60). Nevertheless, since the plots in Fig. 5.3 are almost parallel, there is some indication of a similar rate determining step and a common reaction product, Pb(OH)₂ in both of the solutions.

5.2 Detailed study of processes in peaks A' and A₁

5.2.1 General observations

A number of experiments were carried out in the carbonate solutions in order to establish the relationship between the magnitude and identity of the two anodic peaks (A' and A₁) and the corresponding cathodic peak, C₁. In the initial experiments, E₊ was progressively incremented during each successive cycle of potential. The resulting CVs are shown in Fig. 5.4. It is seen that the appearance of the

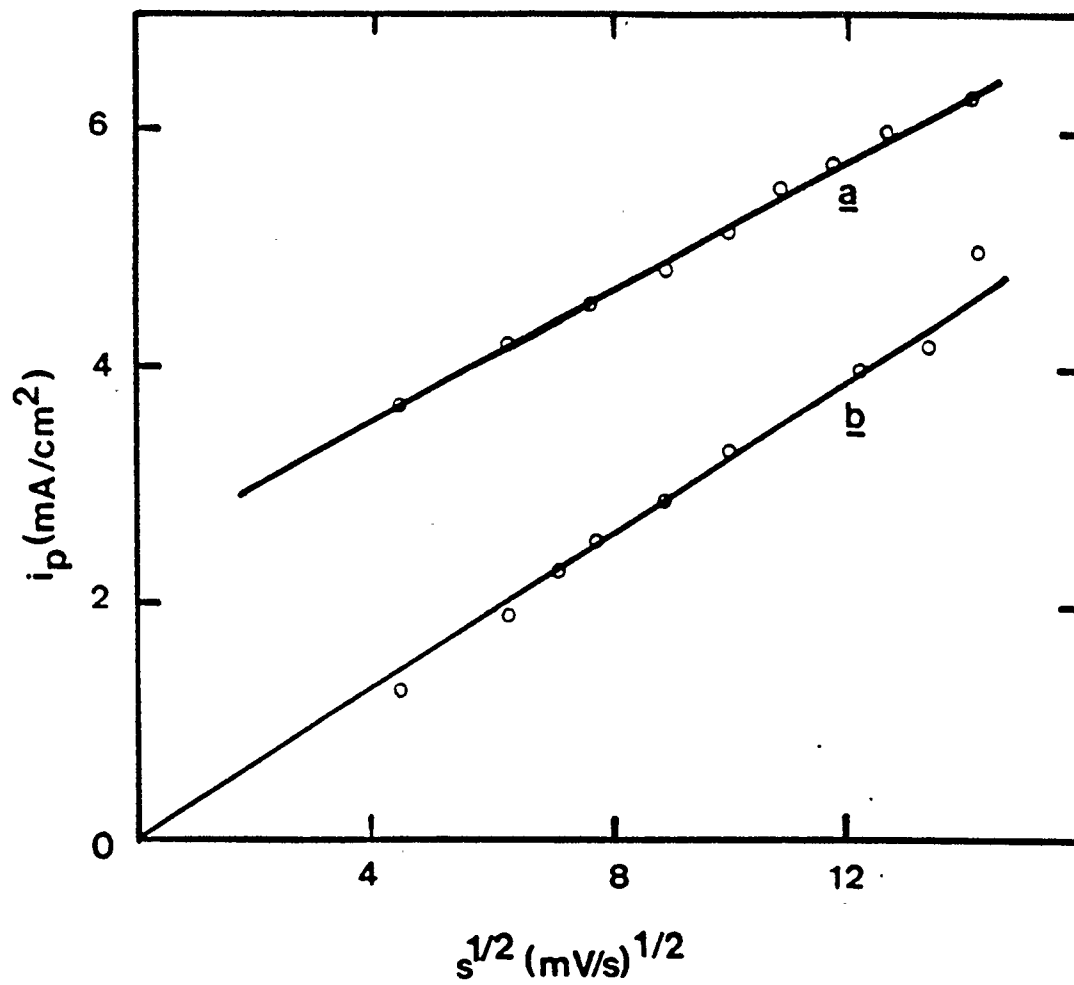


Fig. 5.3 Dependence of the peak current density of A' on sweep rate in pH 9.6 bicarbonate (a) and borate solutions (b).

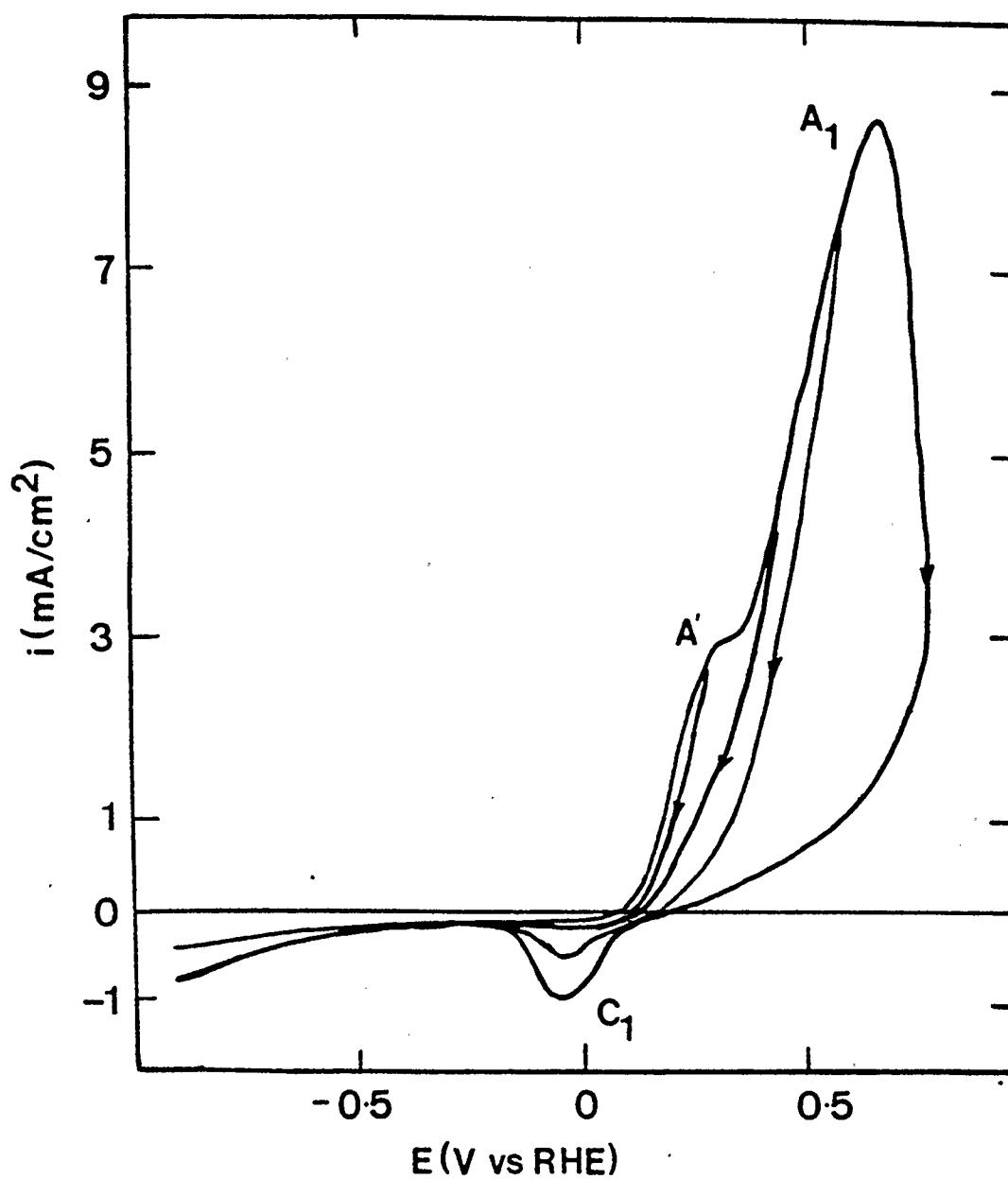


Fig. 5.4 Series of cyclic voltammograms obtained for a Pb chip electrode (0.02 cm²) with progressively increasing positive potential limit in 0.05 M NaHCO₃. $s = 100$ mV/s

Table III Dependence of anodic and cathodic charge densities on
E+ for Pb electrode in 0.05 M NaHCO₃

Potential, E+	Q _a	Q _c	Q _a /Q _c
(mV vs. RHE)	(mc/cm ²)		
300	4.1	1.1	3.6
350	6.3	1.7	3.7
400	9.4	2.1	4.5
500	17.4	2.5	6.9
600	29.3	3.4	8.6
800	38.6	4.5	8.7

reduction peak depends strongly on E_+ . For example, when E_+ was extended only into the region of A' , no corresponding cathodic peak was seen (Fig. 5.4). When the potential limit was extended into the major anodic peak (A_1) and then reversed, only a small cathodic peak (C_1) was observed. From these experiments, it can be argued that the cathodic peak (C_1) is associated primarily with the process taking place in peak A_1 rather than that in A' .

It is clear from the CVs in Fig. 5.4 and from Table III that under the conditions of these experiments, the charge densities passed during the anodic scan are much greater than those passed in the cathodic scan (i.e. $q_a \gg q_c$). This is particularly true in the region of A' , but also for scans into A_1 . This observation could have at least two interpretations:

(i) It is possible that the oxidation products formed in A' and A_1 dissolve, and that only a small fraction of these products remain on the electrode surface, to be reduced in C_1 . At pH 14, peak A' was found to correspond to the formation of a soluble species, i.e. $Pb(OH)_3^-$ and no matching cathodic peak to A' was observed in those solutions.

(ii) It is also possible that the product formed in the anodic sweep is difficult to reduce electrochemically, i.e. the reaction is not electrochemically reversible. This

interpretation of the high q_a/q_c ratio would require that the material which is not reduced is porous in nature, in order to allow further Pb oxidation in the next anodic scan.

A series of experiments were carried out in order to test these two hypotheses. These involved first a number of tests for Pb dissolution under typical experimental conditions. The potential of a Pb chip electrode in a fresh 0.05 M NaHCO_3 (pH 9.6) solution was scanned continuously between the potential limits of -0.9 V and 1 V for ca. 20 hours. The amount of Pb dissolved in solution during one complete cycle was calculated from the difference between the anodic and the cathodic charges passed, ΔQ . Using Faraday's law,

$$\Delta Q = mnF \quad [5.1]$$

where m is the total number of moles of Pb(II) species dissolved and $n = 2$ (assuming a soluble product such as $\text{Pb}(\text{OH})_3^-$), the expected quantity of lead in solution was about 2×10^{-8} M of Pb(II) per cycle. Therefore, for about one thousand cycles, the concentration of Pb(II) was expected to be ca. 10^{-5} M. This is well within the detection limit of the instrument, which is ca. 10^{-8} M. After removing the electrode from solution, the solution was acidified with the addition of nitric acid and was then

analyzed by atomic absorption spectroscopy (AAS) for the presence of lead. A freshly prepared sodium bicarbonate solution was also analyzed for comparison with the test solution. No lead was detected in either solution, as compared to a set of Pb standards.

Another important observation made during this experiment is that after 20 hours of potential cycling, the currents in the regions of A' and A₁ had diminished significantly (Fig. 5.5). If some Pb dissolution had been occurring in each anodic cycle, it is anticipated that the lead electrode surface would have become substantially roughened with time, thus leading to higher measured currents. This was not observed in this experiment.

In other experiments, it was seen that when the rate of solution agitation during potential cycling was increased, the currents for peaks A' and A₁ decreased, with the decrease of peak A' being more pronounced than that of peak A₁. This observation is contrary to what would be expected if dissolution were accompanying the oxidation process.

These tests for Pb dissolution, as well as the fact that Pb oxides and hydroxides are not expected to be very soluble at pH 9.6 (18), all indicate that the significantly lower cathodic charges observed as compared to the anodic charges (Table III) are more likely to be related to a difficulty in reducing the product formed in peaks A' and A₁, rather than

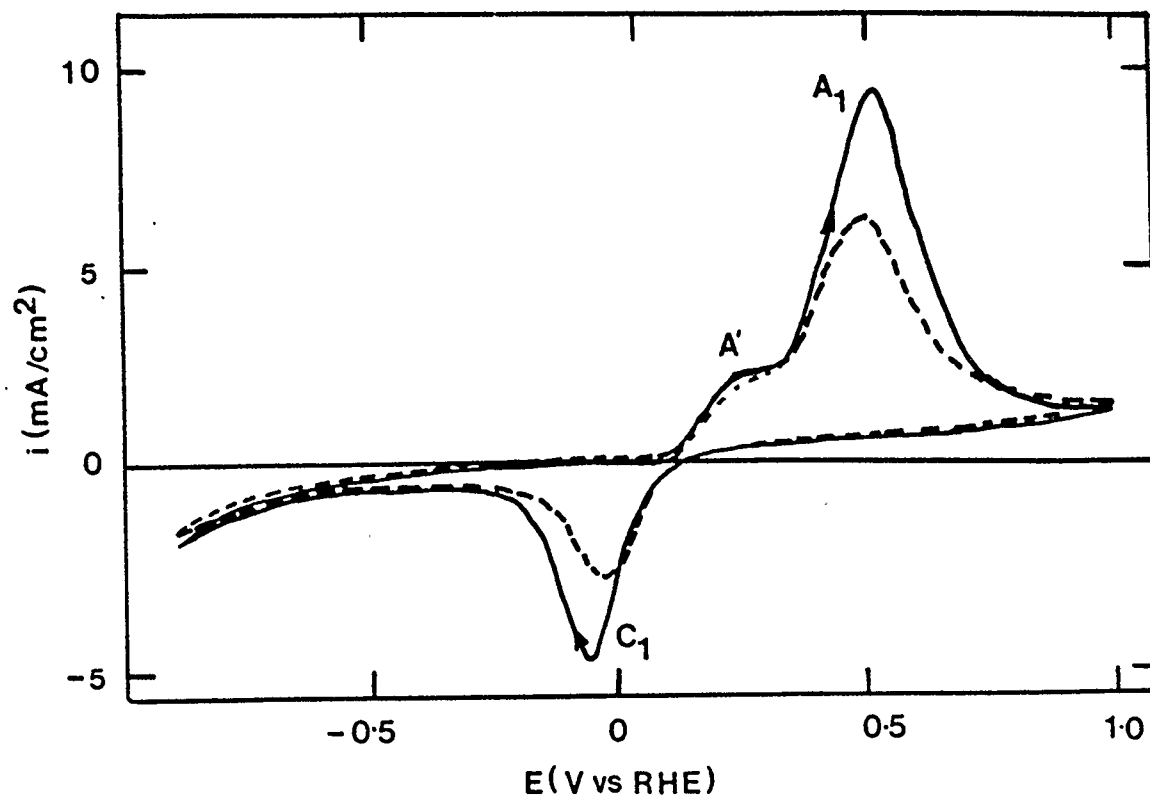


Fig. 5.5 Cyclic voltammograms obtained for Pb electrode in 0.05 M NaHCO₃ after various times of continuous potential cycling. Initial response (—), after 20 hours of continuous cycling (---).

to a dissolution process.

An experiment which supports this interpretation involved the holding of E- (e.g. at -0.9 V) for a few minutes following a regular CV experiment in which the potential had been cycled repeatedly until a steady-state current/potential (I/E) response was achieved. It was observed during the subsequent anodic scan (after holding at E-) that the anodic current was significantly increased while the cathodic current was virtually the same as in the initial CV (Fig. 5.6). By holding the potential at E-, it appears that enough time had been allowed for some surface material to be removed (reduced), so that a higher reaction rate could be achieved in the next oxidation cycle. However, it is also seen that as soon as the oxidation products are formed again in A' and A₁, it is again difficult to remove them in the next cathodic sweep. This results in anodic charges continuing to be significantly greater than the cathodic charges (i.e. $Q_a \gg Q_c$).

When the potential is continuously cycled again from E- ca. -1.0 V to potentials in the region of A' or A₁, reproducible CVs were obtained (Fig. 5.5). However, it can be seen in Fig. 5.5 that continuous cycling results in the diminishment of all the observed currents, with Q_a remaining much greater than Q_c . This decrease in the reactivity of the electrode surface with continuous cycling indicates that

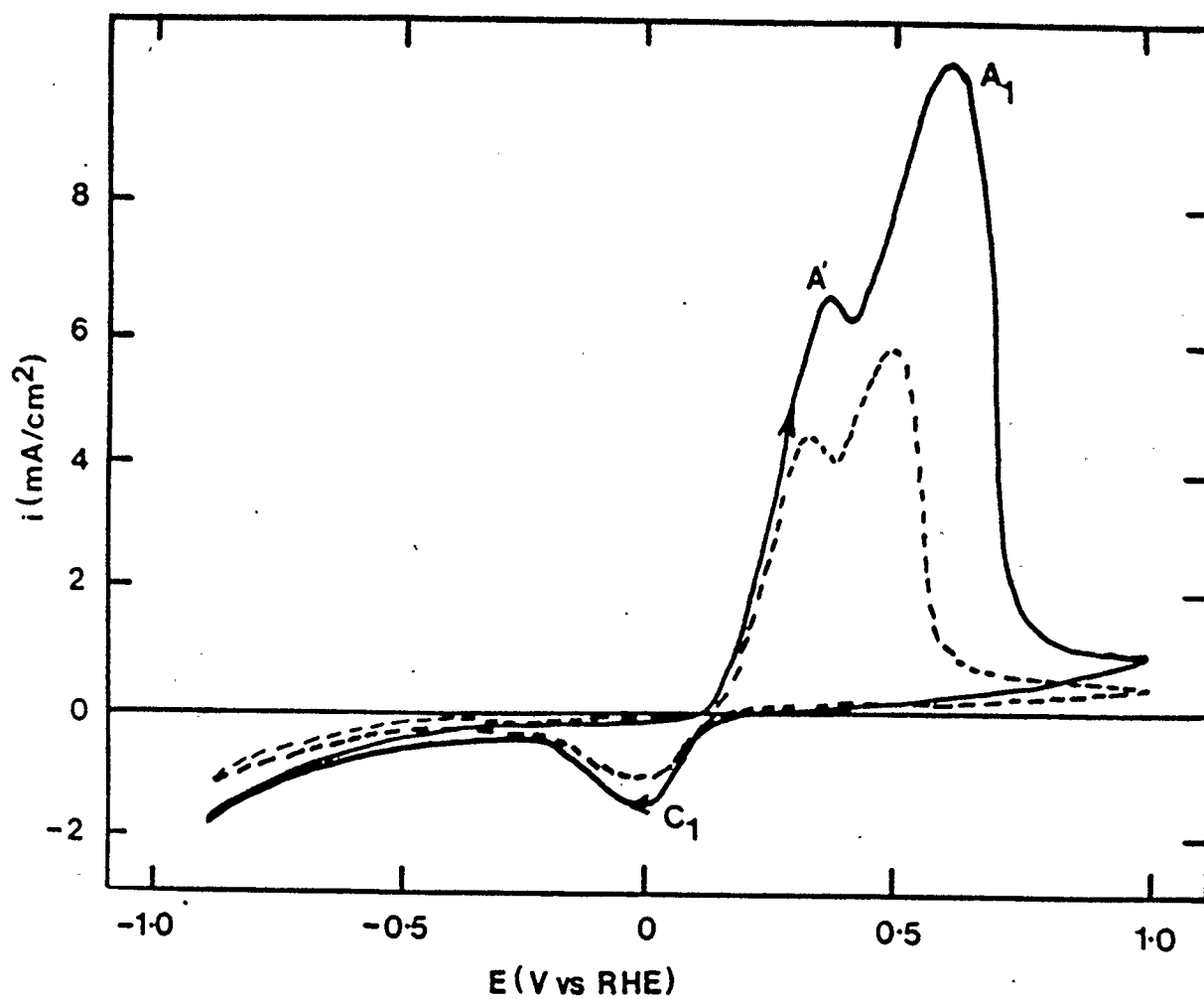


Fig. 5.6 Cyclic voltammograms obtained with Pb electrode in 0.05 M NaHCO_3 . Steady-state response (-----) and after holding at $E_- = -0.9$ V (—) $s = 50$ mV/s.

the oxidation process is somewhat inhibited by the build up of unreduced material on the electrode surface. It was also observed that even if a very slow cathodic sweep rate (e.g. 1 mV/sec) is applied after a fast anodic sweep to peaks A' or A₁, Q_a continues to be much greater than Q_c (i.e. Q_c is still very small). This shows that the time taken to reach E⁻ is not a critical factor in removing the surface film. Rather, it will be shown below that the magnitude of E⁻ is the most important factor in removing the adherent surface films from Pb electrodes in carbonate solutions.

Further support of the hypothesis that a tenacious surface film forms on the Pb electrode surface in a typical CV experiment in these carbonate solutions was obtained from a scanning electron microscopy (SEM) investigation. In this study, the lead electrode had been sheared from a lead rod, thus exposing a very shiny and smooth surface. The potential of this electrode was cycled several times between the potential limits of -0.9 V to 0.35 V and the electrode was then removed from the solution at the E⁻. The electrode surface when removed at E⁻ was found to be covered by a deposit of small crystallites randomly distributed on the surface. The film layer appears porous so that oxidation can still take place at the pore sites (Fig. 6.2, Chapter 6).

This supports the suggestion above that potential

scanning alone over a typical range of potentials does not remove the surface film which builds up on the electrode surface with time of cycling. This is unique to carbonate-containing solutions (pH 9.6). In borate solutions and pH 14 solutions (no carbonate), any film material formed can be readily reduced electrochemically. In order to understand the behaviour of Pb in carbonate-containing solutions further, a more detailed investigation of the electrochemistry of Pb in these carbonate solutions (Peaks A' and A₁) is presented below. The objectives are to determine the conditions under which the tenacious surface film forms and can be removed and to determine what the nature and identity of the film material is, particularly in comparison with the surface products formed at pH 14 and in borate-buffered solutions.

5.2.2 Effect of time of potential holding in A' region

Having seen that the oxidation product formed in A' is difficult to remove electrochemically, it was considered of interest to determine whether there is any influence on the reduction process by holding the potential at E₊ for some time, before applying a cathodic sweep. This involved first holding the electrode potential at some chosen value within the rising portion of peak A' for controlled periods of time (e.g. 30 secs) followed by a cathodic potential sweep at

varying sweep rates. Somewhat surprisingly, it was found that a significant portion of the oxidation product formed at constant E_+ could be reduced. The resulting cathodic scans typically revealed (Type I behaviour) either two or four cathodic peaks, depending primarily on the value of the positive potential limit (E_+). When E_+ was less than or equal to 285 mV, two cathodic peaks (C_a and C_b) were seen. When E_+ was extended to more positive values than 285 mV, the subsequent cathodic scan after potential holding usually revealed four cathodic peaks. It should also be noted that there occasionally appeared to be a second type of response of Pb in these solutions (Type II behaviour), where only two cathodic peaks were seen at all E_+ values. This will be discussed further in Section (7.1) below.

Fig. 5.7a and b show the observed effect (Type I) of holding the electrode potential at two different anodic limits within the region of A', where $s_c = 300$ mV/sec in each case. Fig. 5.7a shows the cathodic response after 30 secs ($t_+ = 30$ sec) of potential holding at $E_+ = 300$ mV, i.e. the four cathodic peaks are clearly seen (C_a , C_b , C_c and C_d). Fig. 5.7b represents the case of $E_+ = 250$ mV and $t_+ = 30$ sec, in which only two cathodic peaks (C_a and C_b) are seen during the cathodic sweep.

The fact that four cathodic peaks are seen only when $E_+ > 285$ mV implies that a new phase is formed which is either

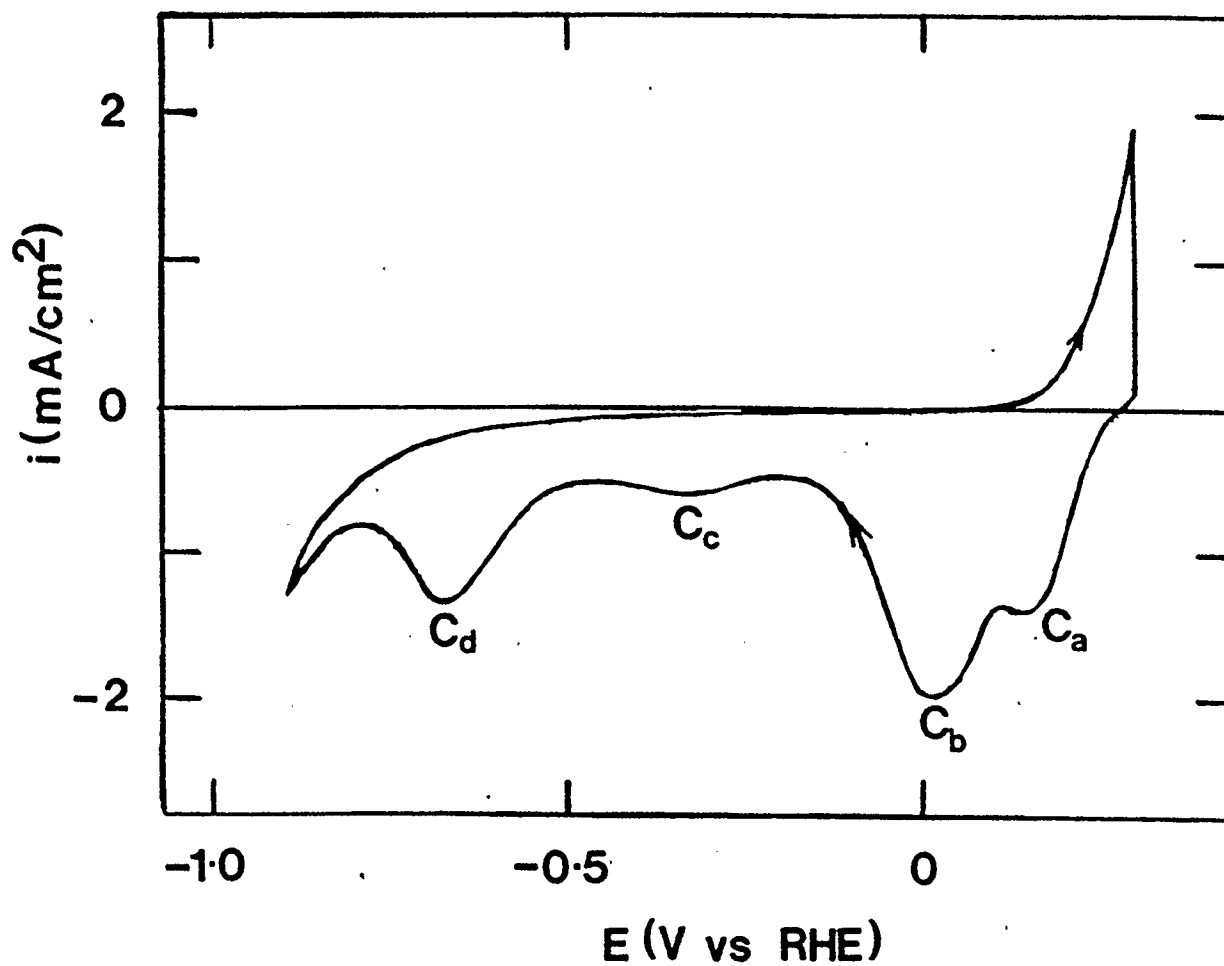


Fig. 5.7(a) Cyclic voltammetric response for Pb chip electrode in 0.05 M NaHCO₃ with potential holding for 30 secs at $E_+ = 300 \text{ mV}$.
 $s = 300 \text{ mV/s}$

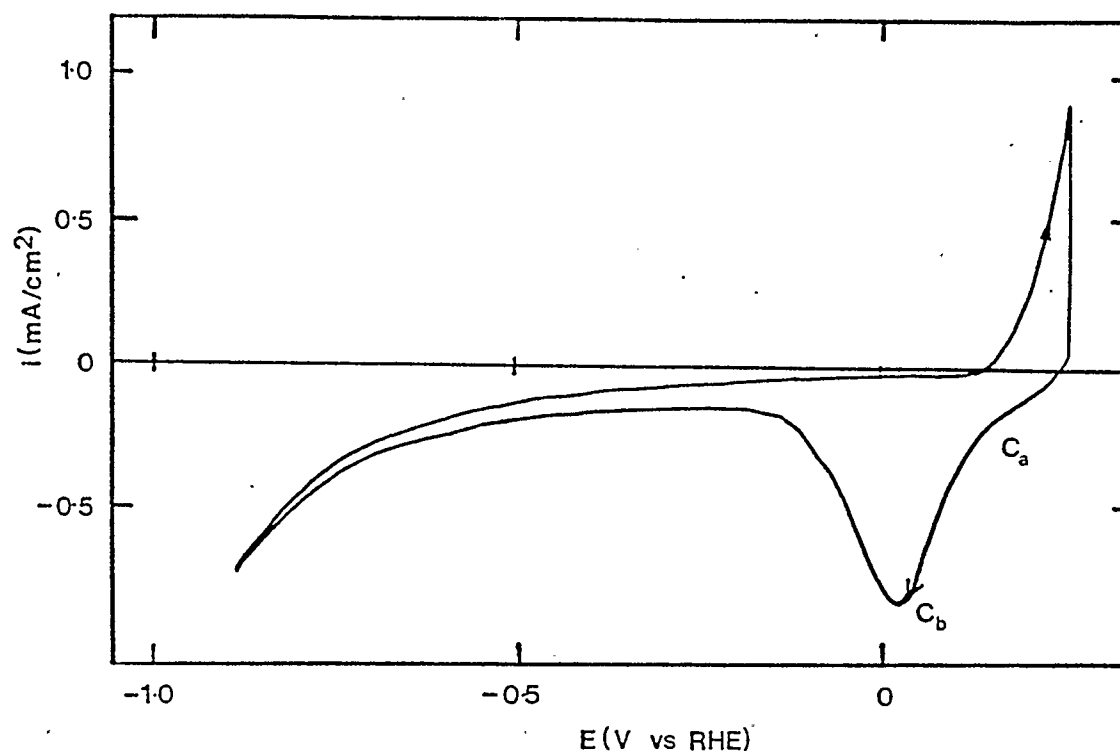


Fig. 5.7(b) Cyclic voltammetric response for Pb chip electrode in 0.05 M NaHCO_3 with potential holding for 30 secs at $E_+ = 250$ mV.
 $s = 100$ mV/s.

structurally or compositionally different from that formed at $E_+ < 285$ mV, when only two cathodic peaks can be seen. This material must also be different from that formed during a normal CV experiment to various E_+ values, as very little cathodic reduction occurs, i.e. none of peaks C_a to C_d can be readily seen. For $E_+ < 285$ mV, peaks C_a and C_b may be related primarily to $Pb(OH)_2$ formation during the oxidation process. During the holding period, it is likely that CO_3^{2-} becomes incorporated into $Pb(OH)_2$ pores such that peak C_a might correspond to the reduction of $Pb(OH)_2$ having few CO_3^- ions while C_b relates to more CO_3^{2-} ions present in $Pb(OH)_2$ pores. On the other hand, when the potential is held in the region of potential where PbO is likely to form (e.g. $E_+ = 300$ mV) additional peaks C_c and C_d are obtained. These latter peaks are therefore more likely related to PbO reduction, perhaps with varying carbonate content.

Similar observations have also been reported by Shoesmith et al (31) in 1 M K_2CO_3 (pH 12) solutions. During a series of potentiostatic oxidations performed for various times (1 to 16 hours) at different potentials, they observed three reduction peaks during a cathodic sweep. Their appearance was also found to be potential dependent. When the potential excursion was only extended to an E_+ of ca. 250 mV, which is in the region of shoulder A', only two cathodic peaks were seen at similar potentials to those that were observed in this work. The anodic oxidation product

formed in the potential range of A' (a shoulder at pH 12) has been identified as plumbonacrite by XRD analysis. When the potential was now held at E₊ (289 mV vs. RHE), i.e. in the region of the main anodic peak (A₁), a third cathodic peak was seen during a cathodic sweep in addition to the two peaks observed at less positive potentials. The third peak was however observed at more positive potentials than the previously seen two cathodic peaks. This peak has been suggested to be related to the reduction of hydrocerrusite, formed during the oxidation process.

With analogy to the present work, the cathodic peaks observed here appear in a reverse order to that shown by Shoesmith et al (31). While up to four peaks are observed in this work, depending on the E₊, the more negative cathodic peaks are only observed if E₊ is extended into the foot of A₁, i.e. E > 285 mV. The fact that they are the last to appear would seem to suggest that the initially formed plumbonacrite is transformed into a more stable hydrocerrusite phase. These results will be discussed in more detail in terms of a model of Pb oxidation in carbonate solutions given in Chapter 7.

The charge passed in the cathodic peaks (Fig. 5.7a) was found to depend on the time of holding at E₊. Fig. 5.8 shows a plot of the total cathodic charge observed, Q_c, vs t^{1/2} when E₊ = 300 mV. A linear relationship is observed,

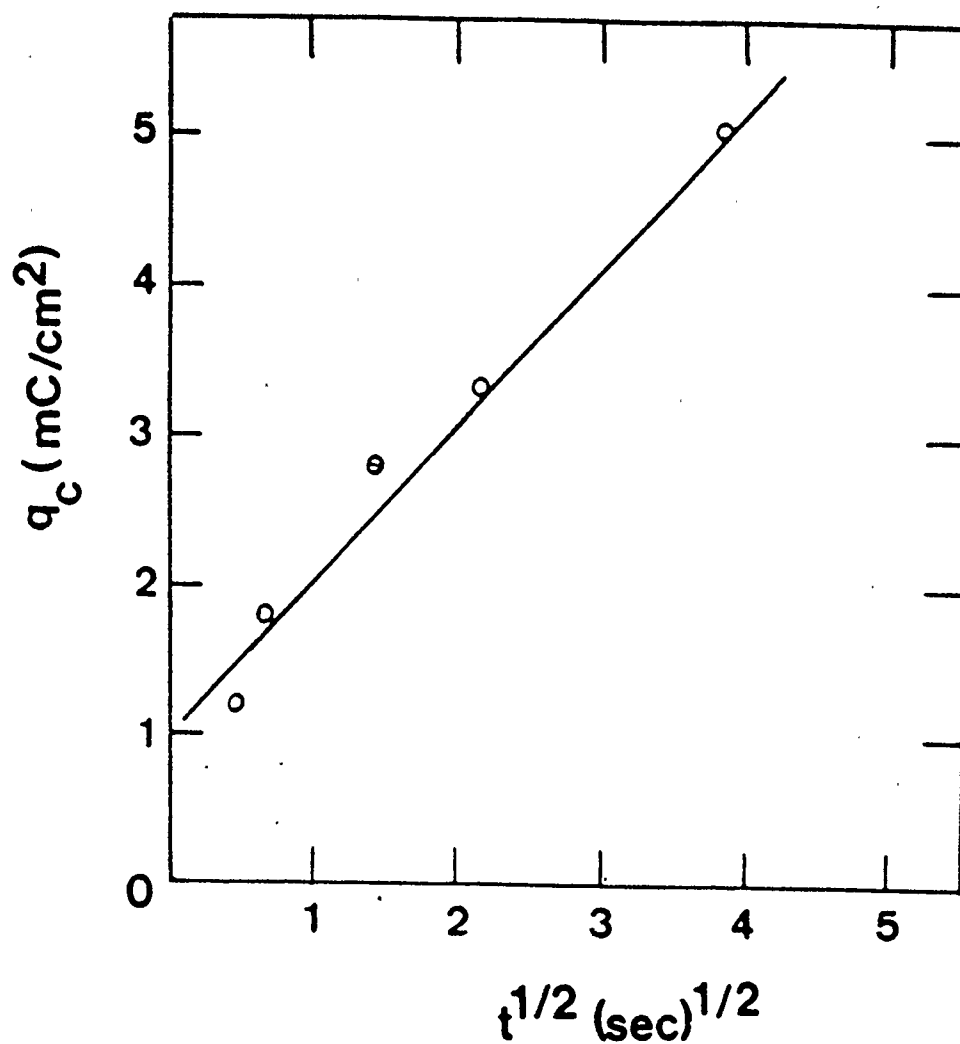


Fig. 5.8 Plot of total cathodic charge, Q_c vs. $t^{1/2}$ for Pb electrode obtained in 0.05 M NaHCO₃ with potential holding at $E_{+} = 300$ mV.

perhaps indicative of a diffusion controlled formation of surface material during potential holding at E_+ (61).

In an effort to further understand peaks C_a to C_d another set of experiments was performed in which the direction of the potential scan was reversed to the anodic direction at various potentials during the cathodic sweep after holding at E_+ (see inset in Fig. 5.9). Fig. 5.9 shows the typical Type I cathodic sweep response obtained after potential holding at $E_+ = 300$ mV for 30 secs, in which all four cathodic peaks are observed. If the potential is reversed to the positive going direction after peak C_a , scanned to E_+ , and then scanned cathodically again, no evidence of peaks C_a and C_b is obtained, and only a much reduced peak C_d is observed.

When the potential is reversed from cathodic to anodic going at an even more negative potential, e.g. after peak C_b , peak C_d is further reduced in magnitude in the subsequent cathodic sweep. If the cathodic scan after holding is extended to E_- (-0.9 V), i.e. beyond peak C_d , then on the next cathodic scan, no cathodic peaks are seen. These observations seem to indicate that the film formed on the electrode during the holding of the electrode potential at E_+ behaves in a 'normal' manner i.e. that by partially reducing it, the remainder is reducible in the next cathodic sweep. It also implies that the unreduced surface material

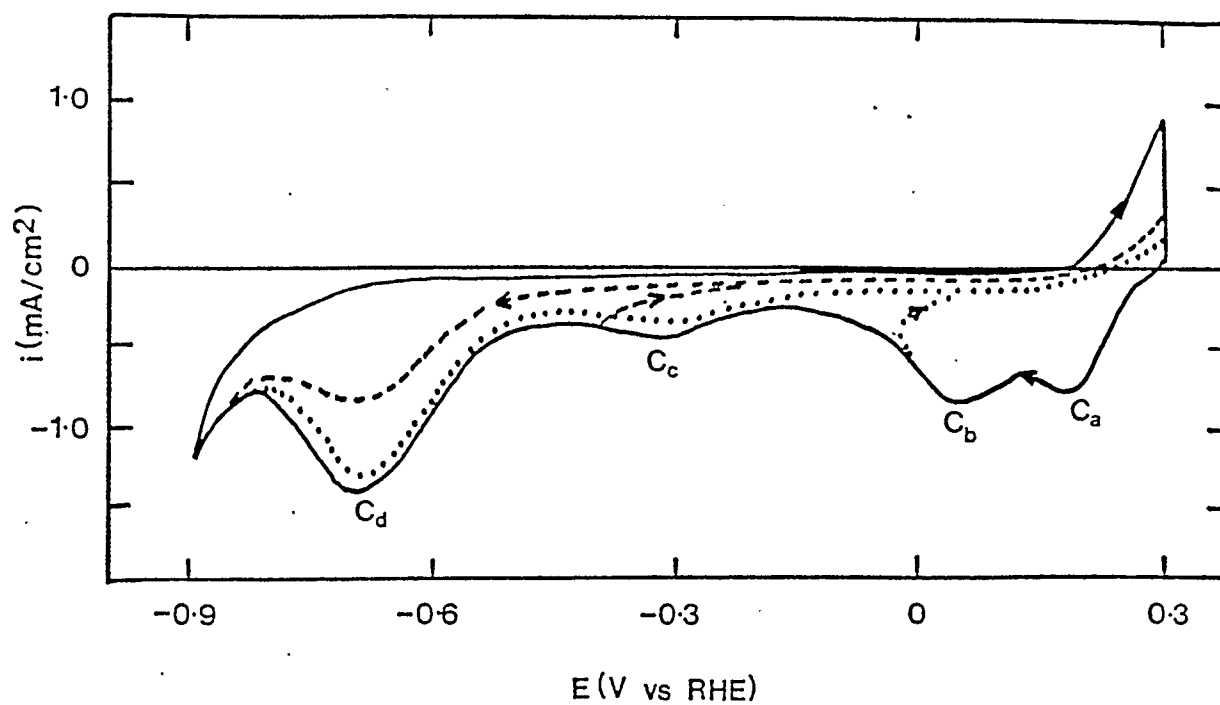


Fig. 5.9 Cyclic voltammetric response for Pb in 0.05 M NaHCO₃ obtained with the perturbation programme depicted in the figure. The potential scan direction is reversed at different E . At C_b (.....); C_c (-----); C_d (—).

does not rearrange during the anodic sweep. Finally, Fig. 5.9 also shows that the unreduced material hinders the oxidation reaction in A', as the current in A' is smaller than when the potential was extended to $E_- = -0.9$ V and the material formed during potential holding (C_a to C_d) was completely reduced.

5.2.2.1 Potentiostatic transients at the Pb electrode in carbonate solutions.

The current-time transients were recorded at potentials in the region of A', where $Pb(OH)_2$ was assumed to be forming. It was hoped that the shape of the i/t transient and its dependence of E_+ and E_- would yield some information regarding the mechanism of the formation of the film material reduced in peaks C_a to C_d .

In these experiments, the potential of the working electrode was stepped from -0.9 V (vs. RHE) to a potential in the region of A' (e.g. 0.35 V) and held there for various times, e.g. 5 to 60 secs. Fig. 5.10 shows a typical i/t response when the potential was stepped to $E_+ = 0.35$ V. It was observed that the current initially decreases very rapidly and then gradually decreases further with time. The large current observed at very short times is due to the charging of the double layer.

Potentiostatic transients have frequently been used to

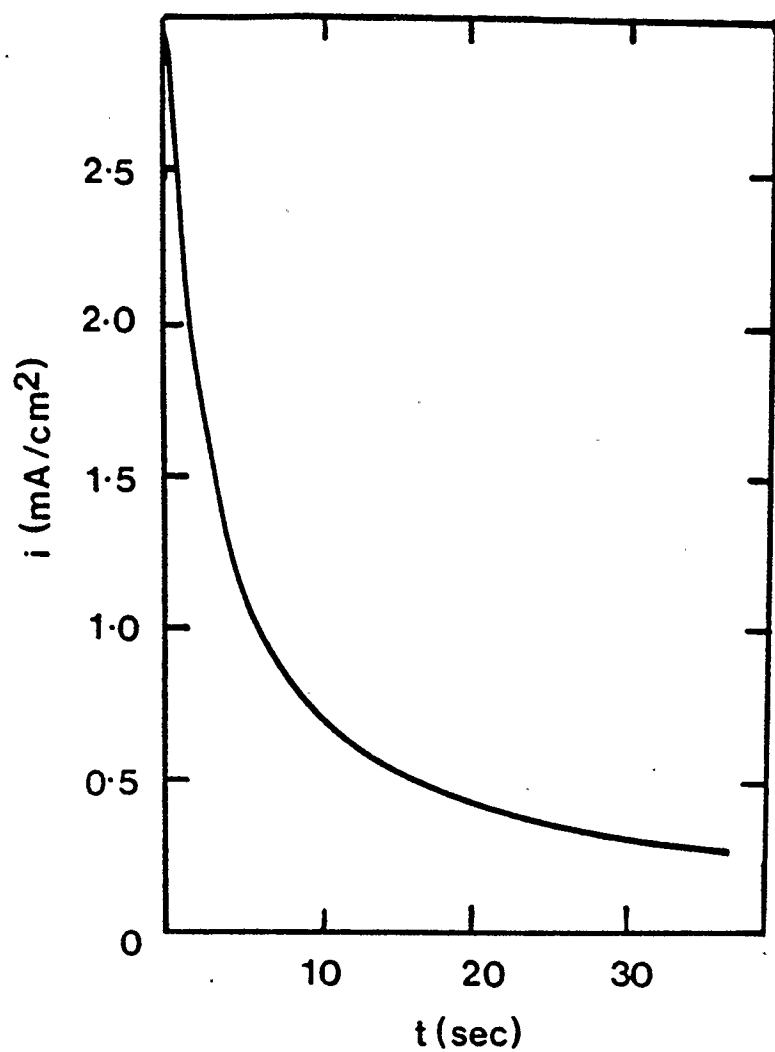


Fig. 5.10 Current-time transient in 0.05 M NaHCO_3 recorded at $E_+ = 350$ mV.

investigate electrode processes which are diffusion controlled. In this case, the Cottrell equation (61), can be utilized, which relates the observed current, i , to time as follows:

$$i = nFAD^{1/2}C_0/\pi^{1/2}t^{1/2} \quad [5.2]$$

where n = number of electrons, F = Faraday constant, D is the diffusion coefficient of the diffusing species, e.g. OH^- , and C_0 is the bulk concentration of the electroactive species.

Since a linear i_p vs. $s^{1/2}$ relationship was observed in the continuous sweep experiments, it might also have been expected that a i vs. $t^{-1/2}$ plot should be linear. However, in the present work, this relationship was not usually obtained. The lack of good fit of the experimental results with the theoretical diffusion controlled prediction [eq. 5.2] suggests that a different rate determining process is involved when the potential is held constant than during continuous scanning experiments. The difference in these two types of experiments is confirmed by the differences in their reduction behaviour. In the continuous sweep experiments, only a very small cathodic charge is passed as compared to that observed in the anodic scan. However, holding the potential in the region of A' , now the film material formed is reducible in peaks C_a to C_d . In

addition, as will be shown in Section 5.2.3, these four peaks show a range of sweep rate dependence, so that the time dependence of the anodic current would not be expected to be related simply to diffusion control.

Another possible mechanism of film reactions is two- or three-dimensional nucleation process (62). A process which would involve a nucleation step in the film formation reaction should show a peak in the i/t response. The absence of such a peak in the i/t transient in Fig. 5.10 makes a nucleation mechanism unlikely for the formation of the film material reduced in peaks C_a to C_d .

Also, as the charges in C_a to C_d are significantly more than one monolayer ($> 250 \mu\text{C}/\text{cm}^2$), the random deposition of a monolayer of film would not apply here. This mechanism of film formation has been reported for the deposition of a monolayer (or less) of film material on electrode surfaces and would be characterized by an exponential decay of current (49).

The effects of solution agitation were also investigated in these i/t transients. Fig. 5.11 shows the effect of increasing solution agitation causes the anodic currents to decrease. This observation is also inconsistent with normal diffusion controlled processes, for solution stirring would be expected to increase the reaction rate. It is therefore suggested that at constant anodic potentials, the

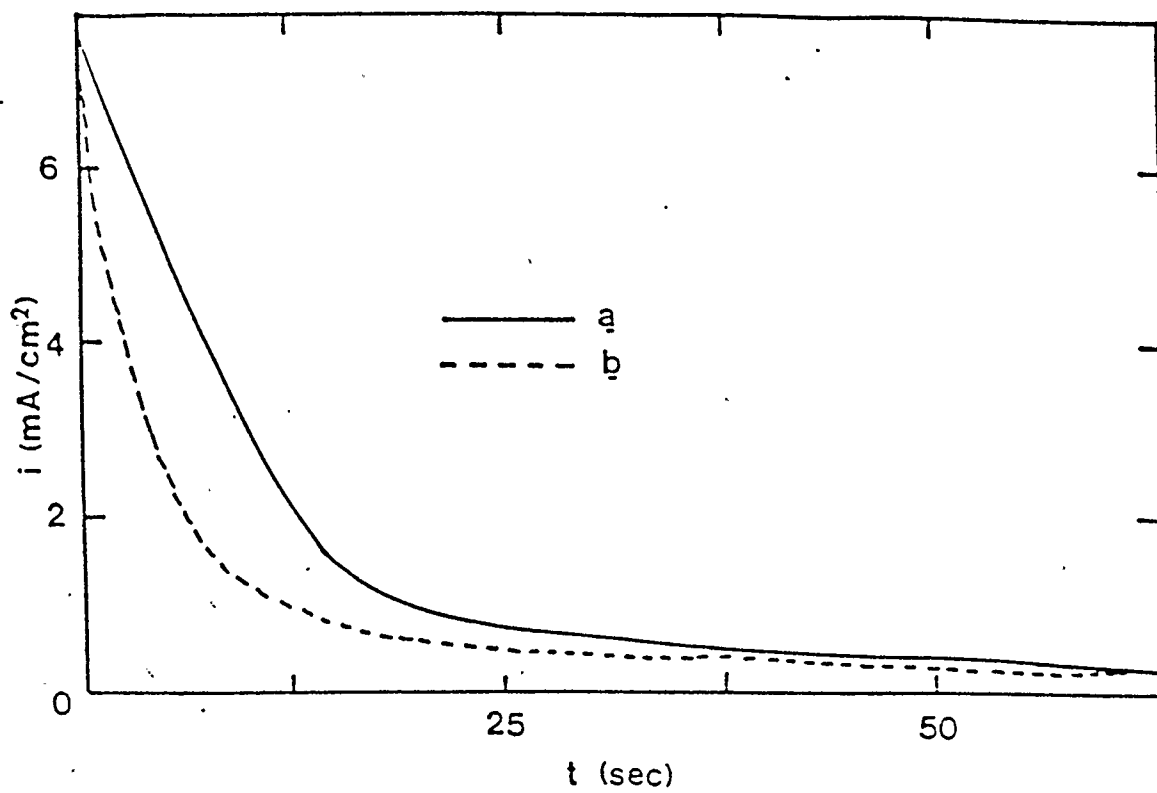


Fig. 5.11 i/t response to potential step from -900 mV to 350 mV in 0.05 M NaHCO₃ with and without stirring. a- without stirring
b - with stirring

composition of the solution in the reaction zone (perhaps at the metal/porous film interface) becomes different from the bulk solution, e.g. the local pH decreases. This could result in different electrochemistry (e.g. film rupture) then when the solution is stirred, which results in partial re-establishment of bulk solution properties within the pores of the film.

Overall, it appears that the mechanism of formation of the film material, reduced in peaks C_a to C_d after potential holding at E_+ , is rather complex, probably involving changing solution conditions inside the film with time. This seems to be quite different from the case of continuous potential cycling as is also seen by the very different reduction behaviour seen in these two types of experiments.

5.2.3 Effect of cathodic sweep rate on C_a to C_d

A number of experiments were carried out over a range of sweep rates from ca. 50 mV/sec to 1 V/sec to establish the relationship between the peak currents of peaks C_a to C_d and s . It was observed that when the potential was held at $E_+ = 300$ mV for 30 secs, and both the anodic (s_a) and cathodic (s_c) scan rates varied in the same way, the peak currents increase with an increase in s .

As it was considered possible that a variable s_a could influence these results, another series of experiments was carried out in which s_a was maintained constant (e.g. 300

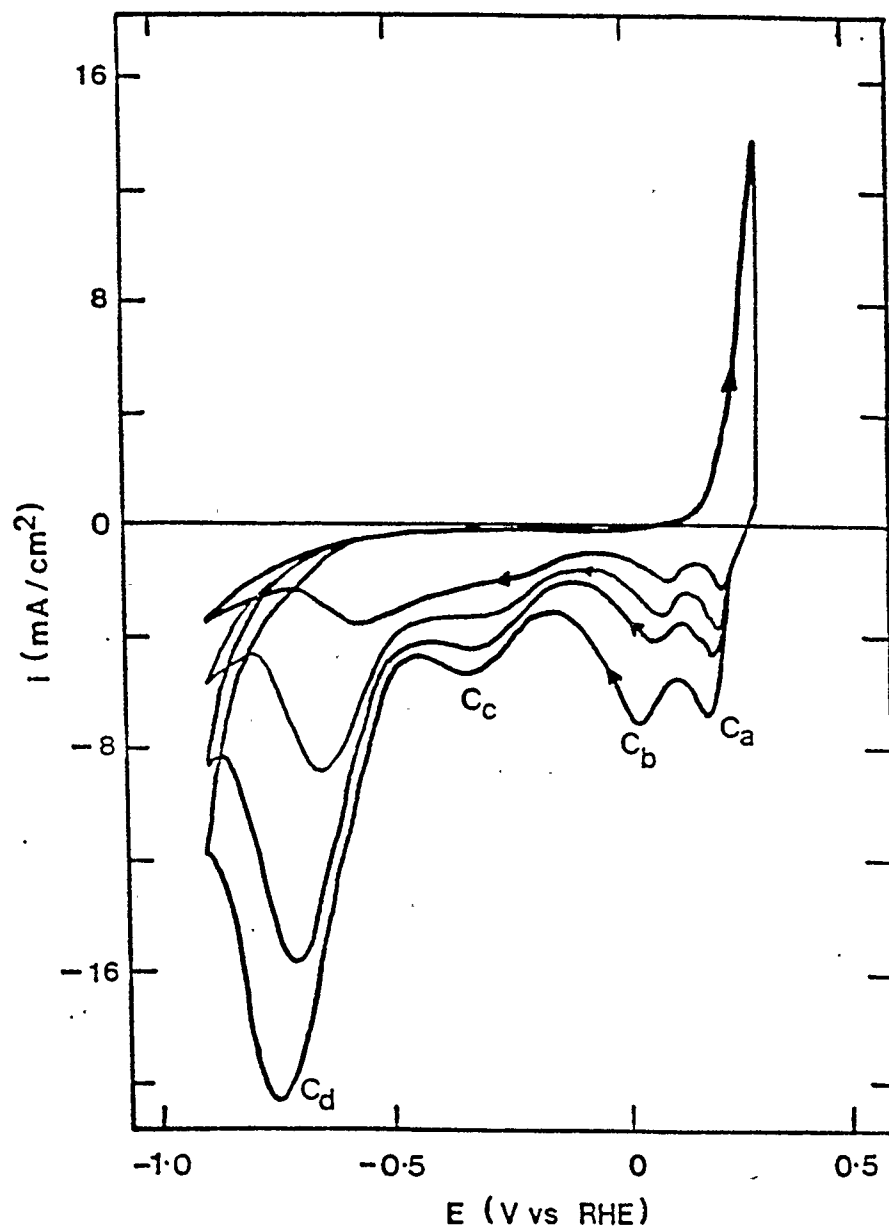


Fig. 5.12 Cyclic voltammetric response for Pb electrode in 0.05 M NaHCO₃ after potential holding at E_+ for 30 secs; various cathodic sweep rates. $s_c = 50, 100, 200$ and 300 mV/s.

mV/sec) while s_c was varied (Fig. 5.12). After 30 sec at E_+ , the four cathodic peaks were usually seen in the cathodic sweep. As was noted above, peaks C_c and C_d were not observed reproducibly from experiment to experiment, apparently due to a dependence of the electrochemical response on the electrode surface preparation. Also, at slow sweep rates (e.g. < 50 mV/sec), C_c and C_d were sometimes hardly visible. However, at high s , all four peaks were usually seen and could therefore be studied.

The relationship of the peak currents, i_p and s can be used to determine the rate determining step of the processes that take place during the sweep experiments. For a diffusion controlled process, the peak current, i_p , is given by the following equation [5.3] (63):

$$i_p = (2.69 \times 10^5) n^{3/2} A D^{1/2} s^{1/2} C_o \quad [5.3]$$

where A is the electrode surface area, C_o is the concentration of the diffusing species and D is the diffusion coefficient, i.e. a linear i_p vs. $s^{1/2}$ relationship is expected. For the reduction of a thin surface film, when diffusion is not the rate determining step, i_p can be given by the following equation [5.4] (64,65)

$$i_p = (kF/4RT)s \quad [5.4]$$

where k is the charge required to form a monolayer of film material on the electrode surface and the other parameters have their usual meaning.

Using these relationships, i_p for each cathodic peak was plotted as a function of both s (to test for the occurrence of a surface-like reaction) and of $s^{1/2}$ (to test for a process in which diffusion is the rate determining step). Fig. 5.13a and b shows that a linear relationship was observed between i_p and s for peak C_d , while for peaks C_a , C_b and C_c , a linear relationship was obtained between i_p and $s^{1/2}$. This implies that the formation and/or reduction of the surface film material attributed to peaks C_a , C_b and C_c may be diffusion controlled. For peak C_d , a different mechanism such as a surface process, seems to be the rate determining step during reduction. If C_d is indeed related to a surface reaction, its appearance would depend on the nature of the electrode surface. This is consistent with the irreproducibility of C_d from experiment to experiment. This result, in which the cathodic peak currents of peaks C_a to C_d show different dependencies on s , would lend support to the non-linearity observed in the i vs. $t^{-1/2}$ plots (seen Section 5.2.2.1).

The peak potentials (E_p) of all of the four peaks also depend on s . As s was increased, all the peak potentials

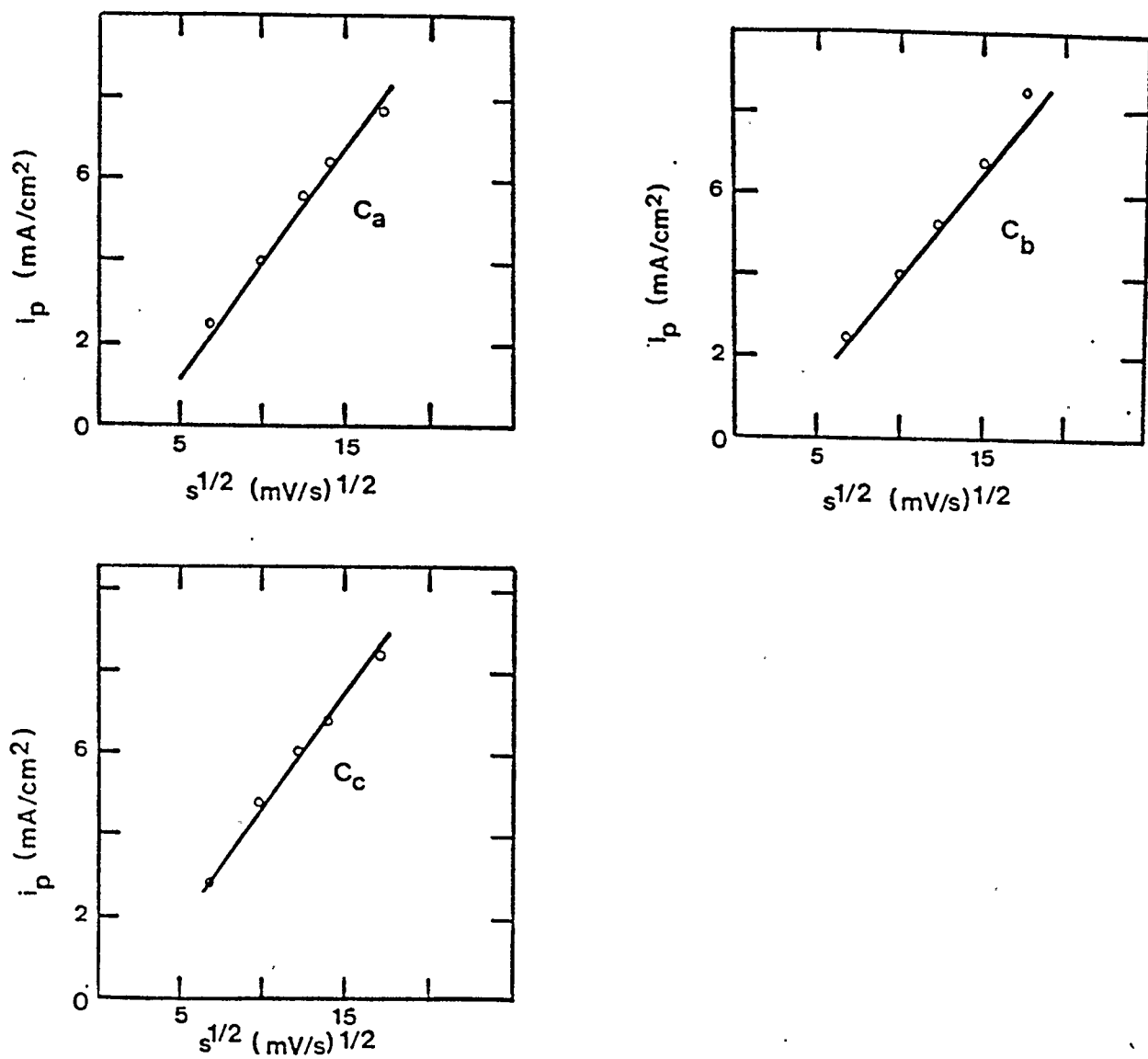


Fig. 5.13(a) Dependence of i_p on $s^{1/2}$ for peaks C_a, C_b and C_c in 0.05 M NaHCO₃.

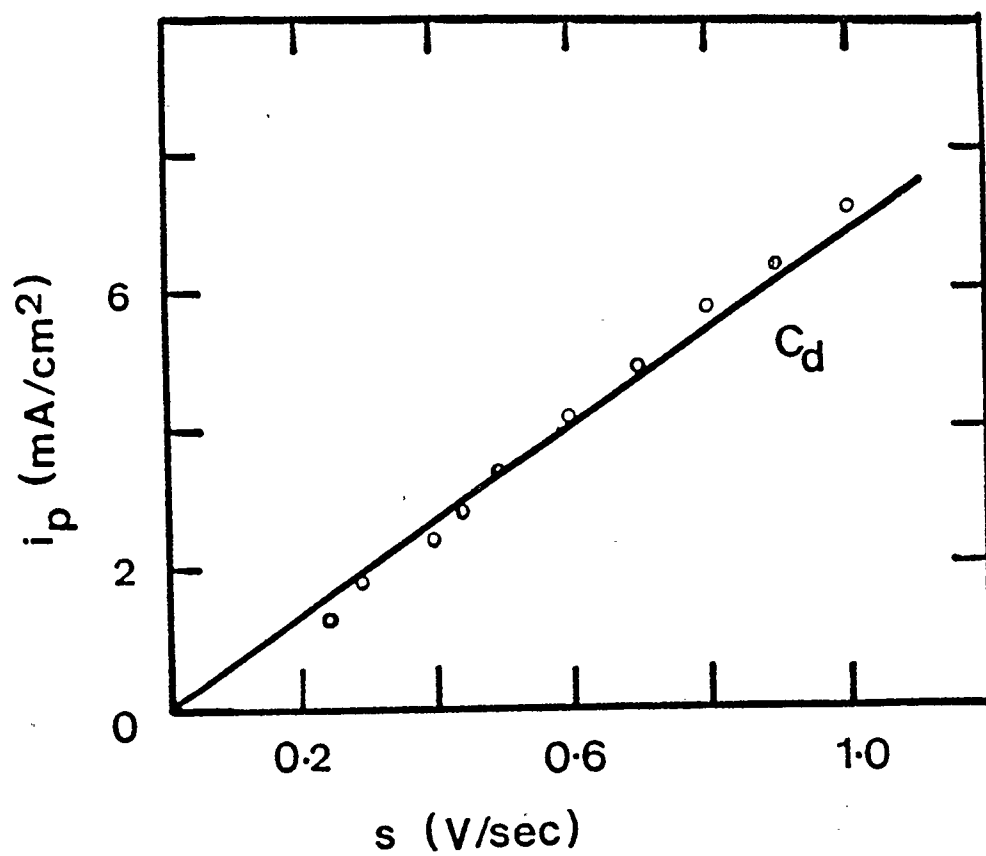


Fig. 5.13(b) Dependence of i_p on s for peak C_d in 0.05 M NaHCO₃.

shifted to more cathodic potentials. This is a further indication of the irreversible electrochemical behaviour of Pb in these solutions.

5.2.4 Effect of negative potential limit

A series of experiments were carried out to investigate the effect of E_- on the initial stages of Pb oxidation (e.g. Peak A') in carbonate solutions. When E_- was made more negative than -0.9 V (e.g. -1.2 V) and the potential was then scanned to ca. 300 mV and held there for ca. 30 secs, the resultant cathodic voltammogram displayed only one cathodic peak, i.e. C_b (Fig. 5.14). The other previously observed peaks (C_a , C_c and C_d) are now absent. This is equivalent to the conversion of Type I to Type II behaviour. However, it was also observed that the single peak seen after holding at E_+ but when E_- is -1.2 V gradually decreased with time of cycling and potential holding (E_+) when E_- was brought back to -0.9 V. Peaks C_a , C_b , C_c and C_d appear again with holding at E_+ , as is seen in Fig. 5.7(a). This kind of behaviour may imply that some re-structuring of the product or compositional changes takes place to some new material that can be reduced at C_c and C_d .

When E_- was extended more negatively, e.g. to potentials less than ca. -2.0, copious hydrogen evolution occurs, and in the subsequent sweep to A' , it is now seen that even

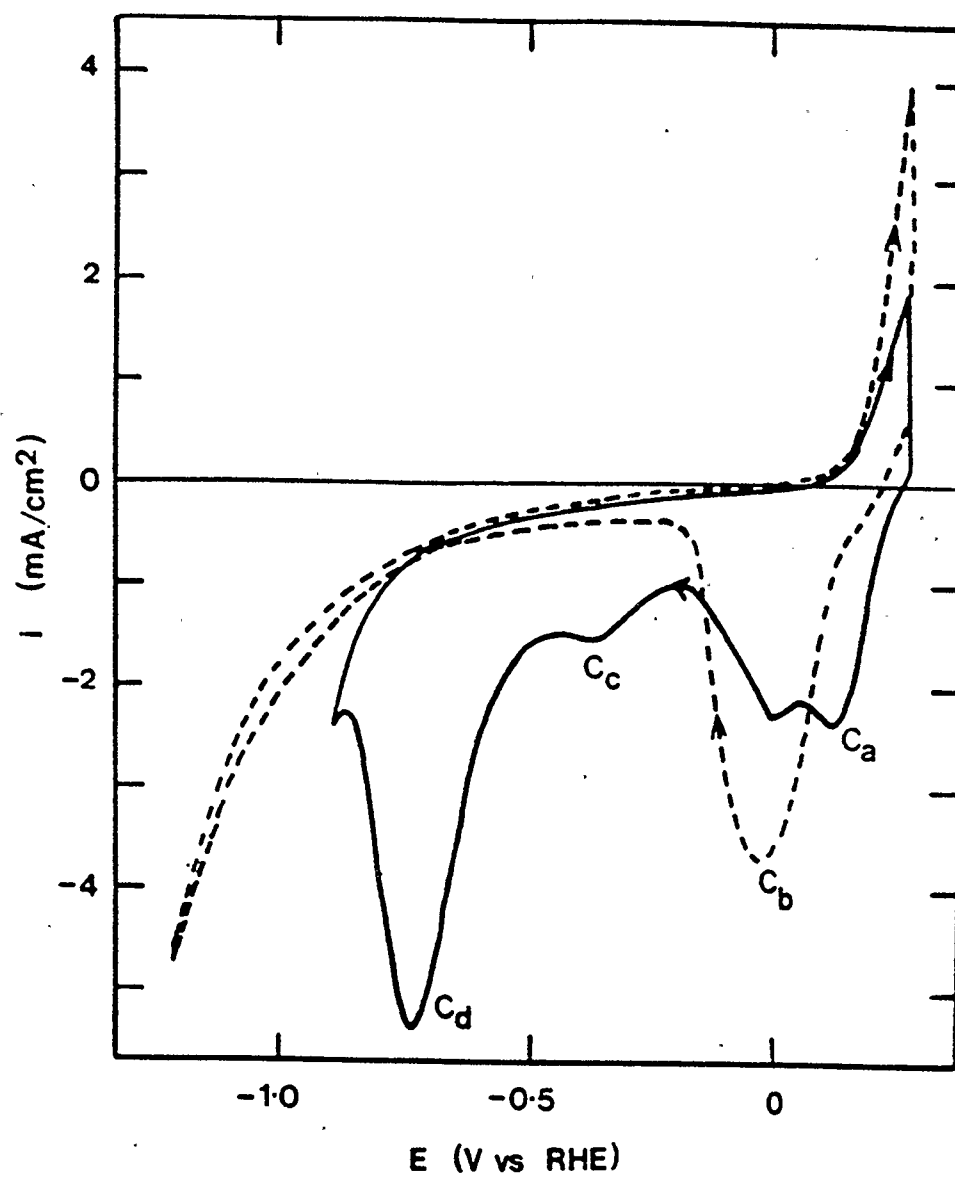


Fig. 5.14 The effect of negative potential limit on CV response of Pb in 0.05 M NaHCO_3 solution. $E_- = -0.9$ V (—), -1.2 V (---), $s = 300$ mV/s

without potential holding, but in a normal continuous sweep experiment, the anodic product can now be reduced fully i.e. $Q_a = Q_c$ (Fig. 5.15). This observation is a very important one and of major significance in aiding in the understanding of the electrochemical behaviour of Pb in carbonate solutions. It is possible that during hydrogen evolution at these very negative potentials, the local pH increases significantly, resulting in an electrochemical behaviour less influenced by the presence of carbonate species. It is reasonable to suggest that likely the OH^- build-up in the solution near the electrode surface during hydrogen evolution now dominates the electrode surface, thus competing successfully with carbonate species for adsorption sites on the electrode surface. This might then minimize the reaction of carbonate species with surface Pb oxides, hence preventing the formation of the difficult-to-reduce Pb/oxy/carbonate surface films.

Another possibility is that these very negative potentials bring about the removal/reduction of film material from the electrode surface. It is possible that carbonate and bicarbonate ions may become trapped in the pores of a Pb oxide film during its formation in Peaks A' and A₁, hence making it difficult to reduce the oxide in the normal potential range and at reasonable rates. Therefore, very negative potentials are required to remove these

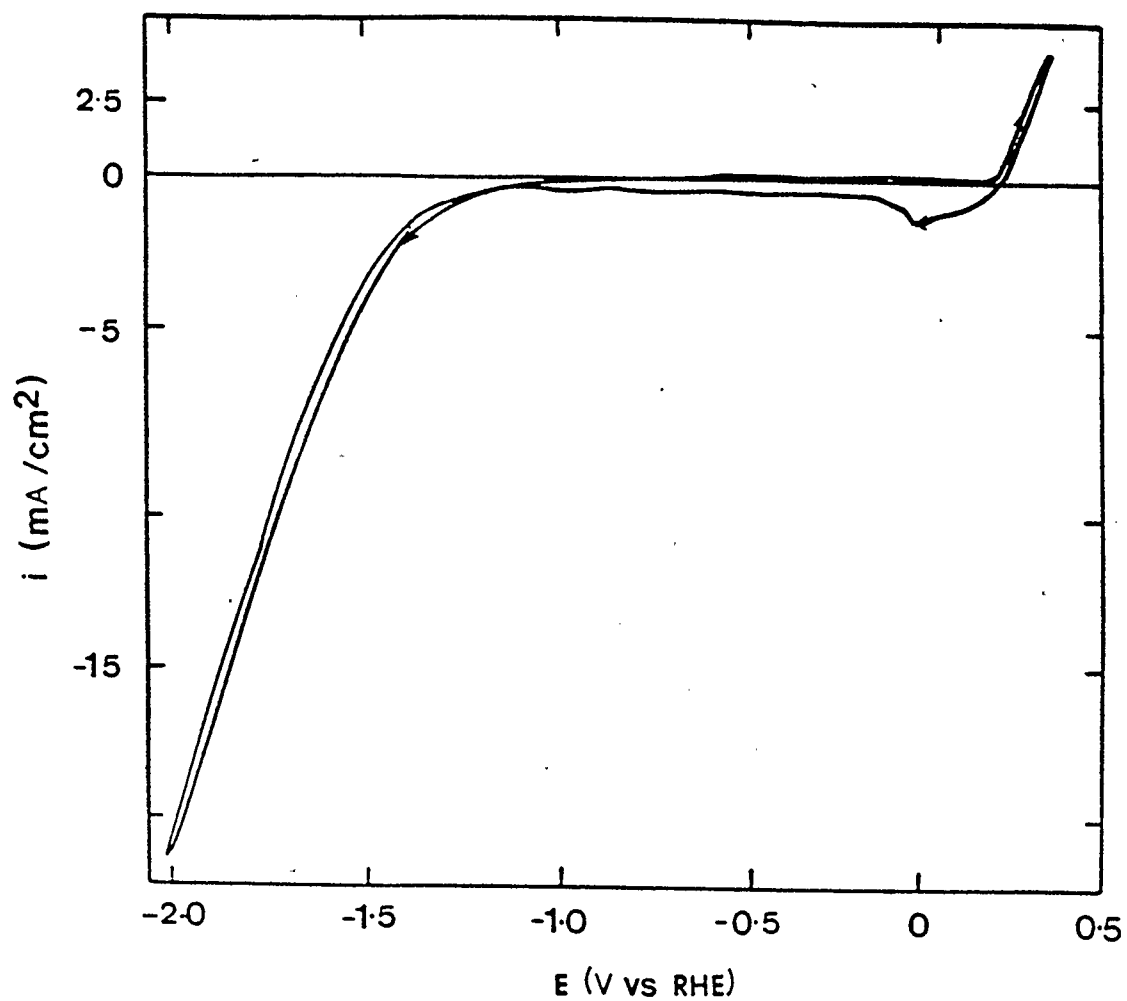


Fig. 5.15 Cyclic voltammogram of Pb electrode
obtained in 0.05 M NaHCO₃ when the
negative potential limit was extended to
-2.0 V. $s = 50 \text{ mV/s}$.

surface films.

This idea is consistent with the results of Shoesmith et al (31). In their work, the cathodic peaks observed even during potential cycling are attributed to the reduction of some hydroxycarbonate phases which are formed during the oxidation process. During the sweep experiments in the present work, by not extending the potential more negatively than ca. -0.9 V, the hydroxycarbonate phase is not fully reducible, resulting in an inhibition of the oxidation process during the subsequent anodic scan and the gradual build-up of more material on the electrode surface. The overall observed decrease of the Pb electrode reactivity (i.e. the diminished electrochemical response in peak currents with continuous cycling in carbonate solutions has also been reported for Cd and Zn electrodes (57,66). For example Cd electrodes used as negative electrodes in Ni-Cd battery systems have been known to have less power output due to carbonate contamination of the electrolyte (66). This has been explained in terms of carbonate ions being locked in the pores of an oxide film on the surface of the Cd electrode resulting in a product which is very difficult to reduce electrochemically.

CHAPTER 6

SURFACE ANALYSIS OF Pb ELECTRODE AFTER ELECTROCHEMICAL EXPERIMENTATION

6.1 SEM results

A study of the morphology and structure of a sheared electrode surface after electrochemical experimentation was carried out. This approach was utilized in order to determine the potential at which film material could form and be removed, to estimate the amount of film material present and to compare the nature of the film material formed at different potentials and pHs (to compare with pH 14).

An initial experiment involved the polishing of a freshly sheared Pb electrode with tissue paper to produce a smooth and reproducible surface. The electrode was then immersed in a pH 9.6 solution of 0.05 M NaHCO_3 and the potential was scanned between the potential limits of -0.9 and 0.35 V for 10 minutes.

This procedure has been suggested (Section 5.2.1) to result in the build-up of some film material on the electrode with time of cycling. After this electrochemical oxidation, the electrode was withdrawn from the solution at E_+ (= 350 mV) and then thoroughly rinsed with distilled water. The electrode was then partially re-immersed into

the solution. The potential was then scanned from 0.35 V to -2.0 V and then held at -2.0 V for about 5 minutes. The electrode was then removed from the solution, rinsed well with distilled water and then carefully dried. The washing and drying procedure of the electrode is extremely important in order to remove any traces of electrolyte from the surface, which could obscure important structural features of the electrode surface.

It is important to note that the differences of the two regions of the electrode surface were visible to the naked eye. The region ('a') that had been exposed to continuous potential cycling between -0.9 and 0.35 V appeared relatively dark in colour. The region ('b') of the electrode which had been subjected to -2.0 V for 5 minutes, resulting in copious evolution of hydrogen, appeared relatively bright and shiny. Fig. 6.1 shows the SEM view of the interfacial region between the light and the dark parts of the surface. It can be clearly seen that structural differences are present between these two regions of the electrode surface. In the darker region, a filament-like material is randomly distributed on the electrode surface. In the region when E- was extended to -2.0 V, a much finer structure is observed. It is apparent from this study that a surface film is deposited and not removed from the electrode surface with continuous cycling in the region of

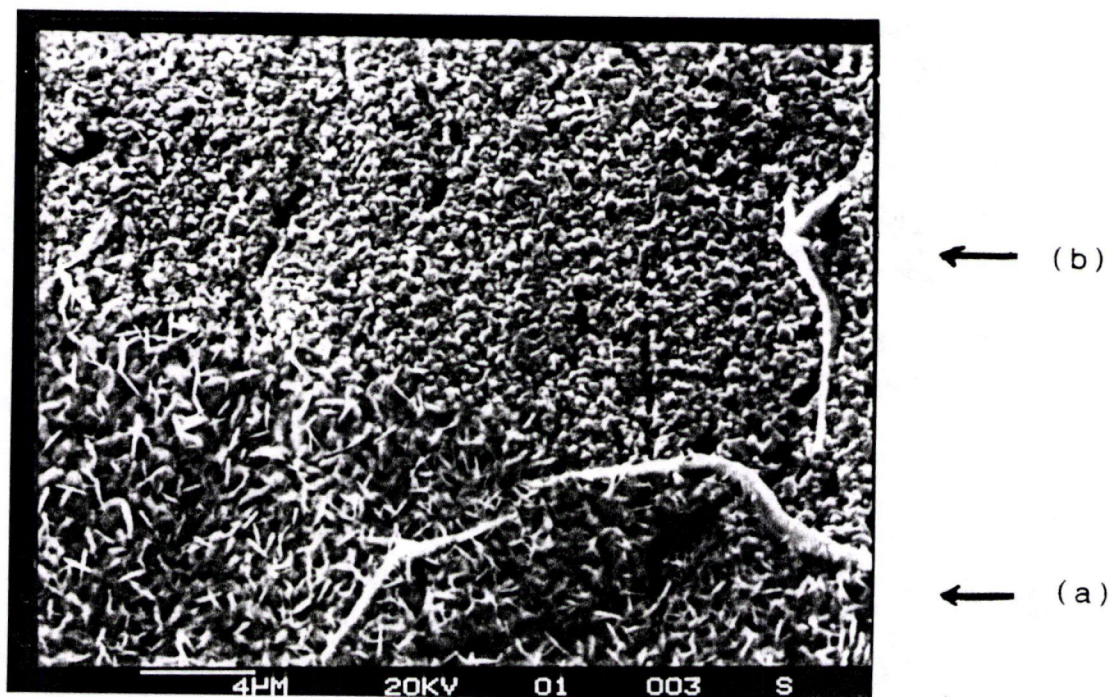


Fig. 6.1 SEM view of electrode surface following
(a) continuous potential cycling between
-0.9 V and 0.3 V in 0.05 M NaHCO_3 ;
(b) as in (a), but followed by holding at
-2.0 V for 5 min.

-0.9 to 0.35 V. This supports the AAS results, which showed that although the CV results may have indicated Pb dissolution at low potentials (Section 5.2.1), this is not the case. Rather, the deposition of film material which is difficult (slow) to remove electrochemically occurs.

It is also very clear that at -2.0 V, a substantial amount of the oxidation product is removed from the electrode surface. This is consistent with the lowered electrode activity with continuous cycling between -0.9 and 0.35 V (Fig. 5.5), and the increase in activity after potential excursion to -2.0 V (Fig. 5.15).

Fig. 6.2 shows a higher magnification view of region 'a' (Fig. 6.1) which was subjected to repetitive voltammetric scans at 50 mV/sec between the potential limits of -0.9 to 0.35 V. The electrode surface is fully covered with small platelets which are randomly distributed on the surface. The complete surface coverage by this deposit supports the observation that it becomes difficult to reduce this material electrochemically during a cathodic scan. Even so, this surface deposit must be porous enough to allow continued oxidation of the underlying Pb surface, as is seen by the further oxidation of Pb in each anodic cycle, although with diminishing currents with continuous cycling.

Another SEM investigation involved the examination of the electrode surface after one anodic scan over the

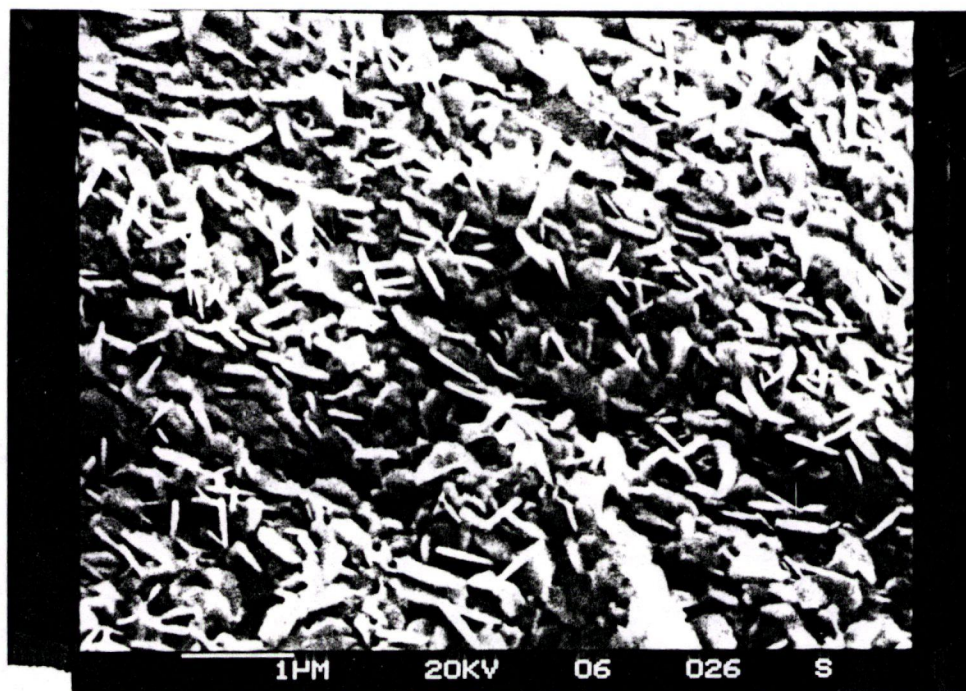


Fig. 6.2 A high magnification SEM view of Fig. 6.1, region "a".

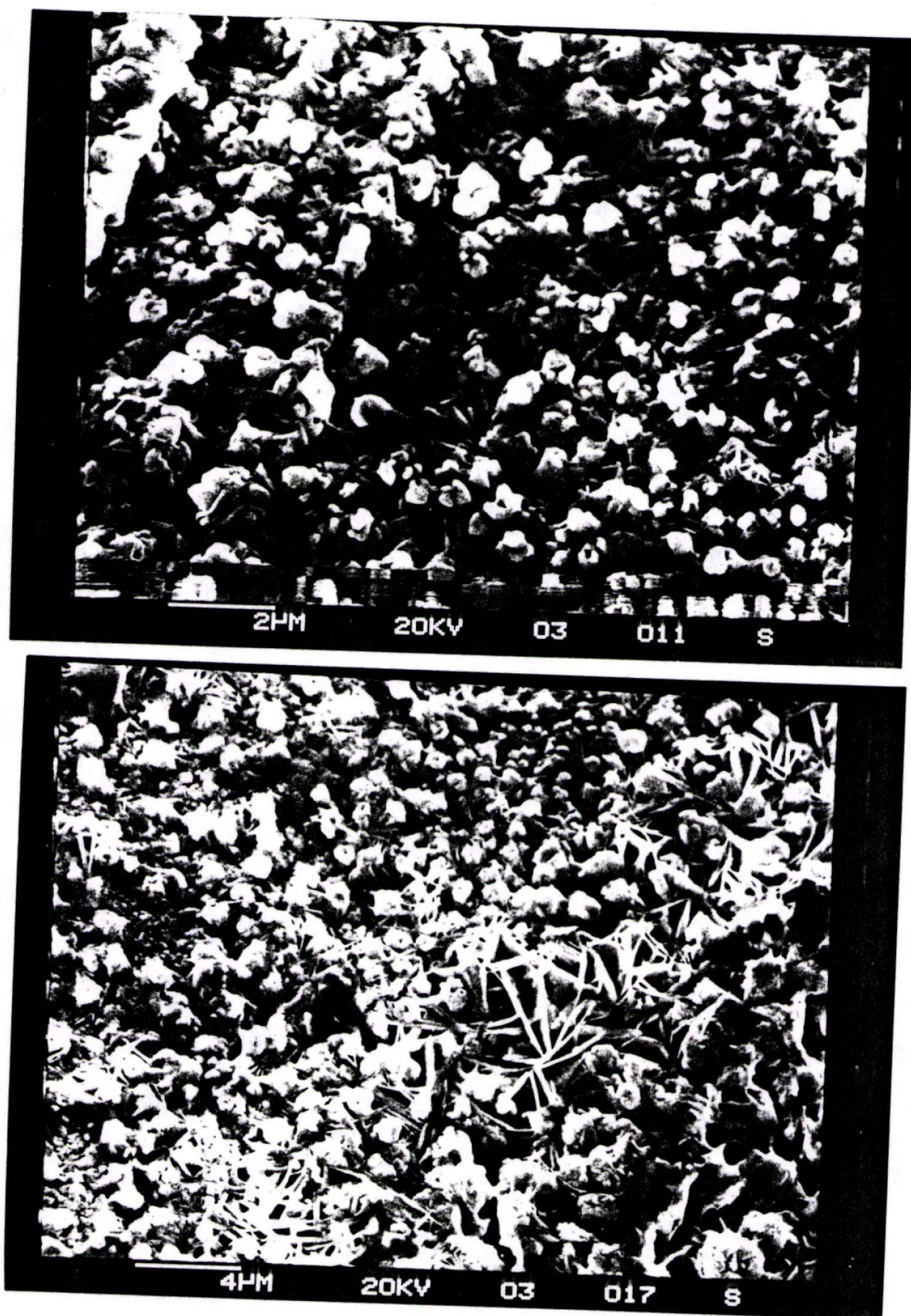


Fig. 6.3 SEM view of a sheared Pb electrode surface polished with tissue, after anodic scan to potential positive of peak A_1 , in carbonate solutions (pH 9.6).

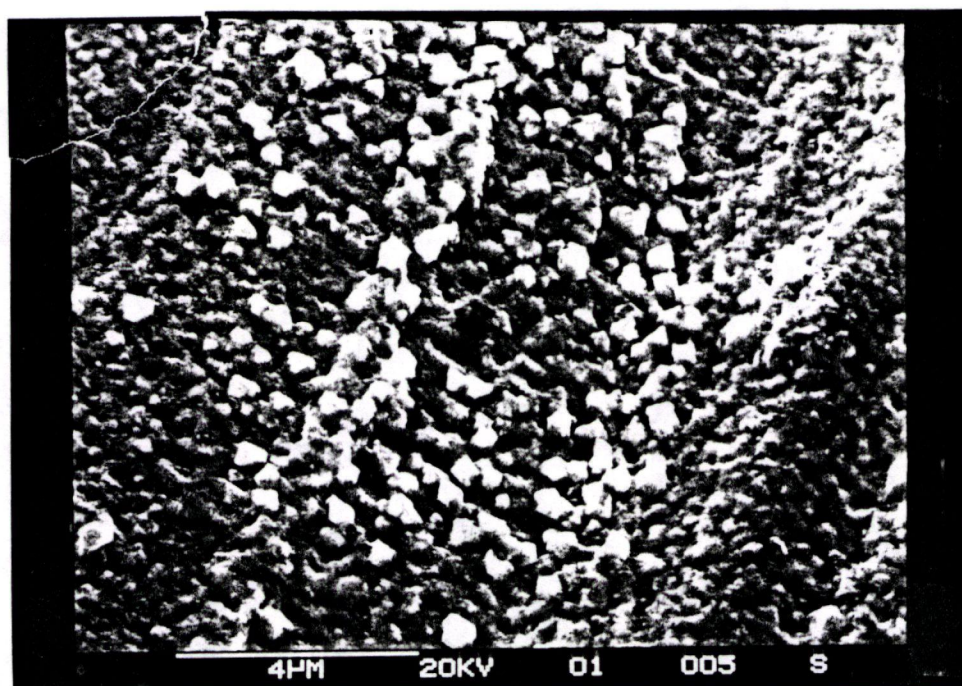


Fig. 6.4 SEM view of Pb electrode surface after one anodic scan beyond peak A₁ in 1 M NaOH.

principal anodic peak, A_1 , (Fig. 6.3). Comparison with Fig. 6.2 shows the presence of many small rounded crystallites (ca. 2 μm) at these higher potentials. These nodular deposits may depict the formation of PbO at this potential. The oxidation of Pb in 1 M NaOH beyond peak A_1 , also yields similar nodular deposits (Fig. 6.4). Peak A_1 is related to the nucleation of PbO on the electrode surface. The general similarity in the appearance of the surface deposits formed in A_1 in bicarbonate solutions (Fig. 6.3) and in 1 M NaOH (Fig. 6.4) may support the suggestion that PbO is also the principal species forming in peak A_1 (i.e. at ca. 1.0 V) in the carbonate solutions. It is also possible that the similarity in the appearance of these deposits in pH 9.6 (carbonate) and 14 solutions is due to a similar mechanism of film formation, e.g. nucleation and growth.

6.2 Scanning Auger Microscopy Results

Scanning auger microscopy was also utilized to study the composition of the electrode surface after it had been exposed to various voltammetric experiments. This was necessary to augment the results as seen by SEM. The the samples submitted for analysis were subjected to three different voltammetric programmes.

(1) A freshly prepared lead electrode was continuously cycled between the potential limits of -0.9 V to 0.35 V for about 10 minutes.

(2) A second lead electrode was exposed to one potential scan from -0.9 V to 0.35 V and held at E_+ for 1 min.

(3) A third electrode was also subjected to one anodic scan from -2.0 V to 0.35 V and then the sample was immediately withdrawn from the solution.

All the samples were thoroughly rinsed with distilled water and well dried before transferring to the SAM instrument.

Fig. 6.5 shows the photomicrograph of electrode (1), showing thin platelets distributed randomly on the surface. These platelets were found to consist of a lead oxide, most probably PbO .

Fig. 6.6 shows the result of a potentiostatic experiment in which the potential had been scanned from -0.9 V to 0.35 V and maintained at the higher potential for 1 min. The surface was found to be non-uniformly covered with flakes. This non-uniform distribution would be a clue to the mechanism of crystal growth on the electrode surface. It is most probable that the mechanism is a progressive one rather than an instantaneous process.

Fig. 6.7 shows that the electrode surface is covered with small flakes after an oxidative sweep from -2.0 V to 0.35 V. The flakes were analyzed and were also found to consist of lead oxide. The random manner in which these flakes are arranged on the surface leads to a porous structure.



Fig. 6.5 SEM view of Pb electrode surface after continuous cycling between -0.9 V and 0.35 V in 0.05 M NaHCO₃ solutions.



Fig. 6.6 SEM view of Pb electrode surface after potential holding in the region of peak A' in 0.05 M NaHCO₃

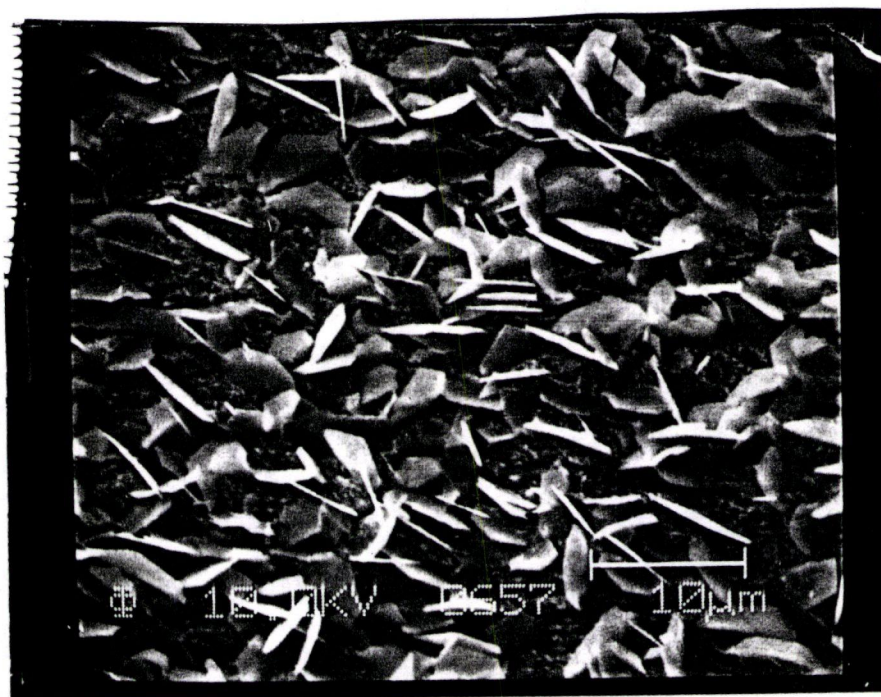


Fig. 6.7 SEM view of Pb electrode surface after potential scan is extended to -2.0 V in 0.05 M NaHCO_3

It was also observed that the surface of all of the samples was covered with carbon, which was quickly removed by ion etching. There was, however, no evidence of carbonate incorporation in the lead oxide structure from this data.

An XRD analysis of the outer surface of samples (2) and (3) was also obtained, and this suggested the presence of PbO (orthorhombic) and hydrocerrusite ($\text{Pb}_3(\text{CO}_3)_2(\text{OH})_2$), as well as Pb metal. The intensity of the X-ray lines were, however, very weak.

CHAPTER 7

MODEL FOR THE EARLY STAGES OF THE ANODIC OXIDATION OF Pb IN CARBONATE/BICARBONATE SOLUTIONS

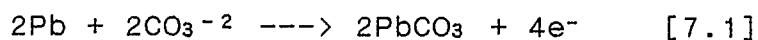
The electrochemistry of Pb in alkaline solutions has been studied with the use of linear and cyclic voltammetry as well as potential step methodologies. The behaviour of Pb in buffered carbonate solutions (e.g. 0.05 M carbonate, pH 9.6) has been compared with that in borate buffered alkaline solutions as well as in pH 14 (NaOH) solutions. It was found that the results obtained in the carbonate solutions were rather unusual and somewhat irreproducible, unlike the more satisfactory results obtained in pH 14 or in the borate buffered (pH 9.6) solutions. Shoesmith et al (31) have carried out studies of the electrochemical behaviour of lead in 1M K_2CO_3 (pH 9-14) solutions, in which a high degree of irreproducibility of the electrochemistry was also reported.

As another example of the peculiar behaviour of lead in carbonate solutions, it was seen in typical CV experiments (e.g. Fig. 5.1) that the anodic charge densities are generally much greater than the cathodic ones, i.e. $q_a \gg q_c$, while for pH 14 and for pH 9.6 borate solutions, $q_a = q_c$. These high charge ratios, found to be unrelated to Pb dissolution, as well as the magnitude of the charge

densities, have also been found to be critically dependent on the negative potential limit, contrary to the case in the other solutions studied. The electrode surface preparation methods may also be of importance to the behaviour of Pb in these bicarbonate solutions.

Other interesting observations about the electrochemical behaviour of Pb in these alkaline carbonate-containing solutions include the ability to reduce the surface film formed at constant potentials, as compared to the reduction of only very small amounts of film formed with continuous potential cycling. Also, two distinct types of behaviour during the cathodic sweeps after potential holding were observed. All of the results referred to above have led to the proposal of a model of Pb oxidation in aqueous bicarbonate/carbonate solutions.

It is suggested that when a Pb electrode initially comes into contact with an alkaline carbonate solution (pH 9.6) under open circuit conditions, carbonate ions rapidly adsorb on the electrode surface, perhaps forming a small quantity of PbCO_3 or a mixed Pb carbonate/oxide phase on the electrode surface by an open circuit (OC) corrosion process (Fig. 7.1 (1)). This is supported by the grey discoloration of the Pb electrode surface after a short time at these conditions, e.g.



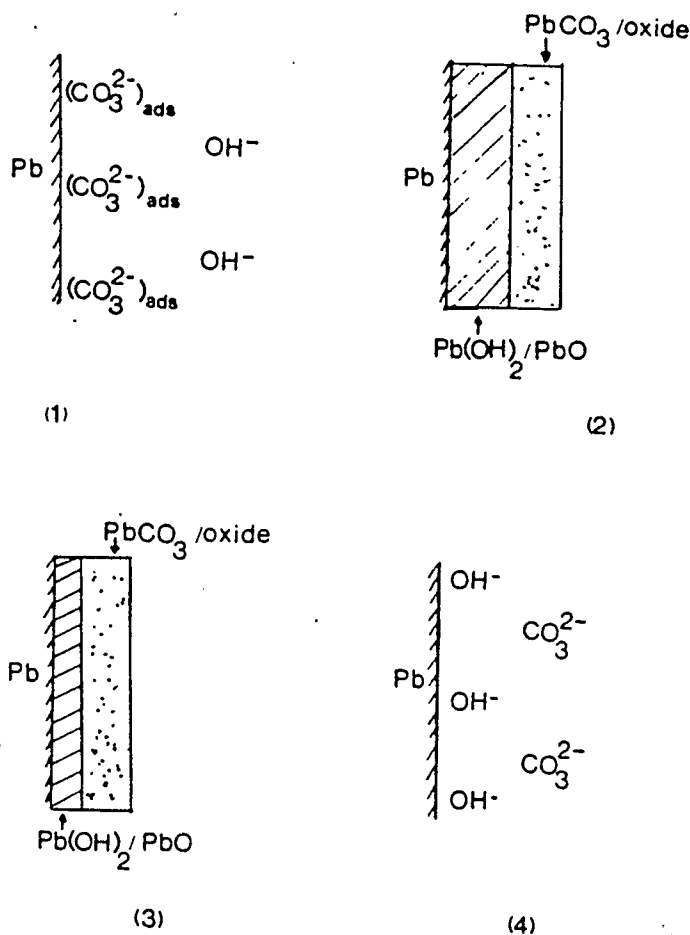
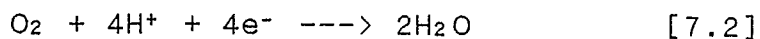


Fig. 7.1 Schematic representation of Pb electrode surface in carbonate solutions during potential sweep experiments.

- (1) Pb in carbonate solutions (pH 9.6) at open circuit conditions
- (2) after potential cycle from -0.9 V to ca. 0.35 V vs. RHE
- (3) partial reduction of underlying oxide in potential scan to ca. -1.0 V vs. RHE;
- (4) all surface film removed at $E = -2.0$ V vs. RHE.



When a potential scan from, e.g. -0.9 to ca. +0.3 V vs. RHE is applied to the Pb electrode (Fig. 7.2), it is seen that although anodic current flows at a potential positive of ca. 0.15 V, very little cathodic current is observed in the negative sweep. This is the typical behaviour of a fresh Pb electrode in these solutions under these electrochemical conditions. The explanation of the absence of significant cathodic current cannot involve Pb dissolution during the anodic sweep, as has been discussed in detail in Section (5.2.1). Instead, it is suggested that the surface bound PbCO_3 /oxide compound formed at OC and/or during the scan of the potential from -0.9 to 0.15 V is porous enough to allow further Pb oxidation to occur at potentials positive of 0.15 V, probably initially forming $\text{Pb}(\text{OH})_2$ (as the potential at the foot of A' matches the calculated potential for $\text{Pb}(\text{OH})_2$ formation) and perhaps some PbO (Fig. 7.1 (2)). It appears that this $\text{Pb}(\text{OH})_2/\text{PbO}$ film is not readily removable electrochemically, although the small cathodic current seen in Fig. 7.2 may depict the partial reduction of the surface film (Fig. 7.1 (3)). It is noteworthy that with continuous potential cycling within the range of potential of peak A', the current gradually decreases (Fig. 5.5), indicative of the gradual blockage of the electrode surface due to the incomplete removal of a

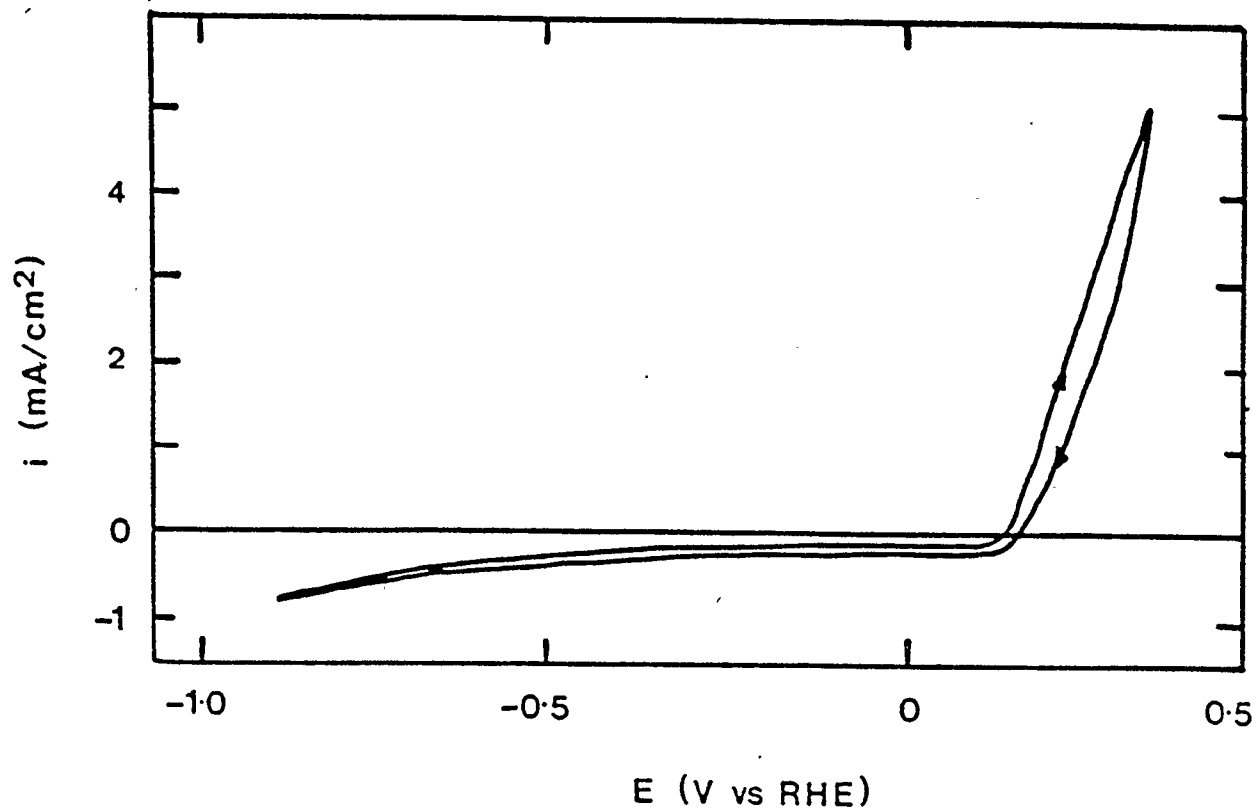


Fig. 7.2 Cyclic voltammetric response of a fresh Pb electrode in 0.05 M NaHCO₃ when the positive potential limit is only +300 mV.
 $s = 50$ mV/s.

surface film. This suggestion is supported by the AES results, which showed that a Pb hydroxide or oxide film is present beneath a thin layer of carbonate-containing film at the Pb electrode.

A very important result which confirms the hypothesis that the presence of carbonate ions results in the formation of a very tenacious surface film was obtained from a series of experiments in which E_- was extended more negatively than -0.9 V. Fig. 5.15 shows the result when E_- is extended to ca. -2.0 V, i.e. when hydrogen evolution occurs at a significant rate, and when the potential is then swept positively to ca. 0.35 V and reversed again. Now a single cathodic peak can be seen in the region of C_a and C_b even during continuous scanning of potential, so that $q_a = q_c$. It is believed that potential excursions to ca. -2.0 V result in the reduction or removal of all surface films (Fig. 7.1 (4)). Also it is expected that adsorbed carbonate ions would be expelled from the surface at these negative potentials as a result of the increased local basicity caused by extensive hydrogen evolution. It is logical that as the ratio of hydroxide to carbonate increases at the surface, hydroxide ions will more successfully compete for the electrode surface, thus preventing the adsorption of carbonate and allowing normal surface film formation and removal processes to occur.

It is important to note that the extension of the

potential to these very negative values causes the Pb electrochemistry to become significantly less complex, i.e. very much like that in borate solutions (Fig. 5.2). Peak A' (Pb(OH)_2) formation is now matched by a single cathodic peak (C') and $q_a = q_c$, even in continuous potential cycling experiments with E_- values more positive than -2.0 V. This result also confirms that the observed excess of q_a vs. q_c in carbonate-buffered solutions was not related to Pb dissolution, but was simply the result of the inability to fully remove the Pb hydroxide/oxide/carbonate films from the electrode surface when E_- was positive of -0.9 V.

An interesting observation which has aided in the development of the present model was described in Fig. 5.7a (Section 5.2.2), i.e. that when the potential was held for short times at E_+ in the range of 250 to 350 mV, and then a cathodic sweep was applied, the reduction of the film material formed during potential holding occurred readily. When E_+ is held at values < 285 mV only peaks C_a and C_b are seen, while after holding at E_+ greater than 285 mV either C_a and C_b simply increase, or peaks C_c and C_d are also seen with time. It is suggested here that after the forward sweep to E_+ (Fig. 7.3 (1) and (2)), with time of holding at E_+ between 250 and 285 mV, further Pb(OH)_2 and PbO continues to form underneath the carbonate-containing surface film. Thickening of the underlying $\text{Pb(OH)}_2/\text{PbO}$ film causes the

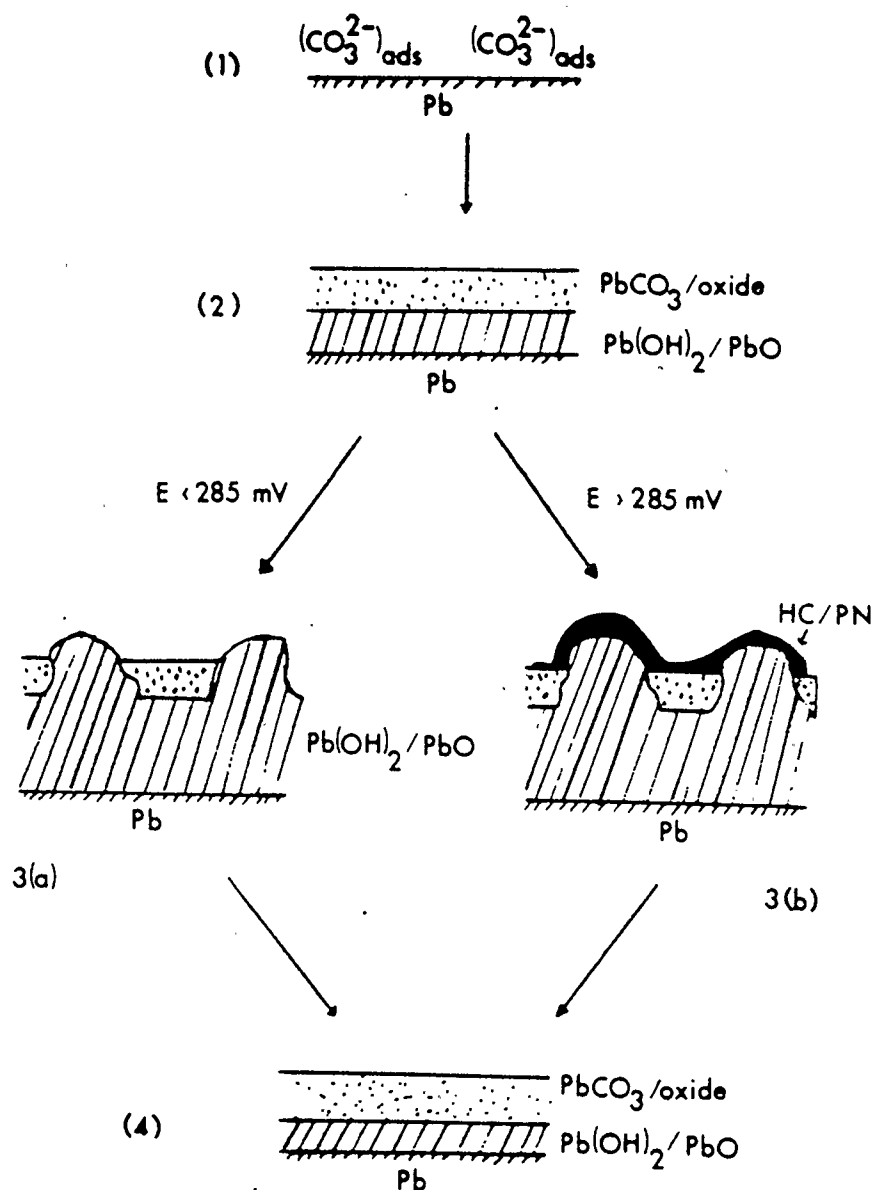


Fig. 7.3 Schematic representation of surface processes at lead electrode in carbonate solutions during potential holding experiments.

- (1) Adsorption of CO_3^{2-} at open circuit conditions;
- (2) After potential scan to A' ;
- (3) Rupture of $\text{PbCO}_3/\text{oxide}$ film due to thickening of underlying Pb oxides;
 - (a) $E < 285 \text{ mV}$, only $\text{Pb(OH)}_2/\text{PbO}$ form
 - (b) $E > 285 \text{ mV}$, HC or PN form at outer surface
- (4) Reduction of HC/PN and part of the underlying Pb oxide

rupture of the thin carbonate-containing surface film and further oxide growth (Fig. 7.3 (3a)). Now, the Pb oxide film is in direct contact with the solution and therefore can be reduced in the cathodic sweep (peaks C_a and/or C_b). Because the cathodic charge passed is less than or equal to the anodic charge passed during potential holding, it is believed that not all the surface film is removed in the cathodic sweep to -0.9 V. Also, the surface of the electrode remains grey, indicative of the continuing presence of a surface film. Also, as the electrochemical response in the subsequent sweep is identical to that observed before the potential holding experiment the final state of the surface (Fig. 7.3 (4)) is considered to be similar to that in Fig. 7.1 (3).

That these peaks (C_a and C_b) are associated with $Pb(OH)_2$ and PbO reduction is supported by the results in borate buffered solutions, where anodic peak A' , associated with $Pb(OH)_2$ formation (by the match of its onset potential with the theoretical potential for $Pb(OH)_2$ formation and the similarity of this value (vs. RHE) to that in pH 14 solutions), is related to C' (Fig. 5.2), and C' appears at a very similar potential to C_a and C_b in carbonate solutions. Also, the reduction of PbO in borate-buffered solutions (peak C_1) also occurs in the potential range of C_a and C_b .

When E_+ is extended to ca. 0.35 V in carbonate solutions and held there for some time, two kinds of behaviour can

then be observed. The first type of behaviour (Type I) is that, in the subsequent cathodic sweep, four cathodic peaks (C_a , C_b , C_c and C_d) are seen (Fig. 5.7a). C_c and C_d are observed at significantly more negative potentials than C_a and C_b and have the general appearance suggested by Shoesmith et al (31) of the peaks for the reduction of the HC phase.

It should be noted that the dependence of the peak current density of C_d on s is linear (Fig. 5.13b), indicative of the reduction of a single layer of film. Therefore, it is suggested that when Type I behaviour is seen, a thin layer of HC is formed at the outer surface of the $Pb(OH)_2/PbO$ deposit (Fig. 7.3 3(b)). In the cathodic sweep, the $Pb(OH)_2/PbO$ phases reduce as usual in peaks C_a and C_b , while the thin layer of HC is subsequently reduced in C_c and C_d . For the reasons outlined above, it is considered that a thin, adherent film remains on the electrode surface, (Fig. 7.3 (4)) after a cathodic sweep.

In the second case (Type II), peaks C_a and C_b increase and broaden significantly with time of holding at E_+ . Shoesmith et al (31) have claimed that PN reduces in the range of peak C_b . As Type II behaviour is characterized by unusually broad C_a and C_b peaks, it is possible that this depicts the transformation of the outer surface of the now exposed $Pb(OH)_2/PbO$ film to PN (Fig. 7.3 (3b)). Again, most

of the $\text{Pb}(\text{OH})_2/\text{PbO}$ and PN are reduced in the range of C_a and C_b during the cathodic scan, (Fig. 7.3 (4)).

The occurrence of these two types of behaviour (Types I and II) with holding of the potential at $E_+ > 285 \text{ mV}$ appeared to be related to two distinct states of the electrode surface brought about by different surface preparation methods. An electrode polished with emery paper and alumina paste tended to yield Type I behaviour, i.e. four cathodic peaks after holding at E_+ (HC formation). A sheared Pb surface (much smoother, no possibility of embedding of polishing compound into the Pb surface) tended to promote Type II behaviour (PN formation). The fact that HC and PN reduction could be seen only when $E_+ > 285 \text{ mV}$ may imply that the surfaces of PbO nuclei (thermodynamically predicted to form only at $E > \text{ca. } 260 \text{ mV}$) are more susceptible to reaction with carbonate ions than are $\text{Pb}(\text{OH})_2$ nuclei (predicted to form at $E > \text{ca. } 115 \text{ mV}$). It is also possible that the potential for the formation of HC and/or PN is close to 285 mV and are therefore are not thermodynamically stable at potentials more negative than this.

CHAPTER 8

CONCLUSIONS

The oxidation and reduction processes which take place at Pb electrodes in carbonate-containing solutions have been investigated using cyclic voltammetry and potential step techniques. This behaviour has been compared with that in borate-buffered and in simple NaOH alkaline solutions. SEM was used to investigate the morphological properties of the electrode surface before and after the electrochemical experiments, while Auger electron spectroscopy was used to determine the elemental composition of the surface film as a function of depth.

8.1 Initial stages of lead oxidation in alkaline solutions

A study of the electrochemistry of lead in three alkaline solutions of varying pH and ion content revealed a strong similarity in the initial stages of lead oxidation. This is seen from cyclic voltammetry experiments, where an anodic shoulder (A') in pH 14 solutions occurs at the same potential (vs. RHE) as the small peak (A') in borate and carbonate solutions of lower pH. The potential at the onset of the shoulder (or peak) is ca. 140 ± 10 mV vs. RHE in all of these solutions. As the shoulder in pH 14 solutions has been identified previously (26-28) as being due to Pb(OH)_2

formation, it is proposed that the same product forms in all of these solutions.

In pH 14 alkaline solutions, it has been shown in this work that at $s < 200$ mV/sec, the shoulder A' has no corresponding cathodic peak. This is caused by Pb(OH)_2 dissolution to form a soluble Pb(OH)_3^- species. At higher sweep rates, when less time is available for Pb(OH)_2 dissolution, a cathodic peak can be observed due the reduction of Pb(OH)_2 . In pH 9.6 solutions, significantly less dissolution of Pb(OH)_2 is observed than at pH 14. In borate-buffered solutions, the Pb(OH)_2 surface film can be reversibly removed, while in carbonate solutions, the Pb(OH)_2 film is modified, leading to an adherent surface film which is difficult to remove electrochemically.

After numerous hours of experimentation with a Pb electrode in the same 1 M NaOH solution, it was observed that a new process takes place at potentials just negative of A' (peaks A_0/C_0). These peaks may be related to the adsorption of OH^- ions at high energy Pb nuclei formed on the electrode surface by the deposition of Pb from solution (from Pb(OH)_3^-).

The presence of carbonate and borate ions in aqueous solutions showed a very interesting effect on the oxidation and reduction processes that take place at the lead electrodes. It has been shown that the extent of oxidation

of Pb is less in these solutions than in pH 14 solutions. This is evidenced from the high currents observed in the voltammograms during anodic oxidation in pH 14 solutions as compared to pH 9.6 carbonate or borate solutions. The film material formed in carbonate solutions has been shown to be removable only at very negative potentials, when copious hydrogen evolution takes place. It is suggested that extensive hydrogen evolution increases the ratio of $\text{OH}^-:\text{CO}_3^{2-}$ at the Pb surface, thereby diminishing the participation of CO_3^{2-} in the oxidation of lead. This results in the formation of a surface film which is electrochemically reducible.

8.2 Potential holding experiments

Pb electrochemistry in carbonate-containing solutions has also been investigated by holding the electrode potential constant in the region of A' for controlled periods of time, followed by cathodic sweeps at controlled rates (Fig. 5.7). Up to four cathodic peaks were observed depending on E_+ and the electrode surface preparation method used. The fact that the cathodic peaks (C_a to C_d) are readily observed after potential holding in A' shows that the material that forms under normal sweep conditions is structurally or compositionally different from that formed at constant potential. It is suggested that potential

holding causes the rupture of an outer carbonate- containing layer leading to the formation of electrochemically reducible $\text{Pb(OH)}_2/\text{PbO}$, PN and HC phases. Both sweep rate and AES studies suggest that the HC and PN phases form only at the Pb oxide/solution interface and that the major part of the surface film is $\text{Pb(OH)}_2/\text{PbO}$.

8.3 Electrode surface preparation

The effects of different methods of electrode preparation were investigated by scanning electron microscopy during the course of this study. This has revealed major morphological differences of the electrode surface as a function of the preparation method. The nature of the electrode surface also appears to influence the electrochemical response of the Pb electrode, particularly in the carbonate solutions. The mechanically polished electrode tends to exhibit Type I behaviour while the sheared electrode shows Type II behaviour.

Studies with the SEM have also elucidated the need for proper electrode surface preparation methods. Mechanical polishing of soft metals such as Pb with emery paper should be avoided since polishing material can be embedded in the metal surface. It was therefore found that shearing of lead with a stainless steel knife exposes a smooth and clean surface. This can then be polished further with a soft

material such as tissue paper. Proper ultrasonic rinsing in acetone and distilled water is necessary to remove any adherents from the electrode surface.

8.4 Future work

The present study has demonstrated the complex nature of the electrochemical processes which take place at a Pb electrode in a range of alkaline solutions. Since Pb has been proposed as an underground storage material for nuclear waste, the need to investigate the influence of other ions present in typical alkaline ground waters (e.g. Cl^- , SO_4^{2-} , etc.) on Pb reactivity is necessary.

Further work on the electrochemistry of Pb in carbonate solutions is also needed to clarify the precise identity of the film material reducing in Ca to Cd . This requires the use of surface analytical techniques such as ESCA, AES, etc. to verify whether peaks Ca and Cb are indeed related to plumbonacrite reduction, and peaks Cc and Cd are due to hydrocerrusite reduction. The question of why adsorbed carbonate or a thin, outer, carbonate ion-containing film inhibits underlying Pb oxide reduction also needs further consideration.

The use of a rotating ring disk electrode could aid in determining the role of any dissolution processes in pH 9.6 solutions. Also, the electroformation of higher oxides

(e.g. Pb_3O_4 , PbO_2) in these carbonate solutions should also be investigated.

REFERENCES

1. Lead for corrosion resistant applications
Lead Industries Association, Inc., New York
2. R.L. Boeckx, J. Anal. Chem. 58, 275A (1986).
3. W. Hoffman, "Lead and lead alloys", 2nd ed.,
Springer-Verlag New York (1970).
4. P. Jones, R. Lind and W.F.K. Wynne-Jones, Trans. Faraday
Soc. 50, 972 (1954).
5. L.M. Baugh and K.L. Bladen, J. Electroanal. Chem. 145,
325, 339, 355 (1983).
6. S.R. Ellis, N.A. Hampson, M.C. Ball and F. Wilkison,
J. Appl. Electrochem. 16, 159 (1986).
7. J.J. Lander, J. Electrochem. Soc. 98, 213 (1951).
8. J. Burbank, *ibid.*, 103, 87 (1956).
9. Hans Bode, "Lead-acid batteries", J. Wiley and Sons, New
York (1977).
10. A.T. Kuhn, "The electrochemistry of lead", Academic Press,
London (1979).
11. A.A. Abdul Azim, Corros. Sci. 10, 421 (1970).
12. J.P. Carr, N.A. Hampson and Taylor, J. Electroanal. Chem.
33, 109 (1971).
13. V. Danel and V. Plichon, Electrochim. Acta. 28, 781
(1983).
14. N. Hampson and J.B. Lakeman, J. electroanal. Chem. 119, 3
(1981).
15. G. Archdale and J.A. Harrison, *ibid.*, 47, 93 (1973)
16. N.A. Hampson, P.C. Jones and R.F. Phillips, Can. J. Chem.
45, 2039 (1967).
17. K.R. Bullock and D.H. McClelland, J. Electrochem. Soc. 124,
1478 (1977.)
18. M. Pourbaix, "Atlas of Electrochemical Equilibria in Aqueous
Solutions", 2nd Ed., N.A.C.E., Houston, TX. (1974).

19. G. Vinal, "Storage batteries", J. Wiley and sons, New York (1955)
20. K. Elbs and J. Forsell, Zeit. Elektrochem. 8, 760 (1902)
21. S. Glasstone, J. Chem. Soc. 121, 2091 (1922).
22. P. Jones, H.R. Thirsk and W.F.K. Wynn-Jones, Trans. Faraday Soc. 52, 1003 (1956).
23. S.S. Popova and A.V. Fortunatov, Sov. Electrochem. 2,413 (1966).
24. A.A. Abdul Azim and K.M. El-Sobki, Corros. Sci. 12, 207 (1972).
25. M.V. Ptitsyn, G.S. Zenin and K.I. Tikhonov, Sov. Electrochem. 13, 1144 (1977).
26. V.I. Birss and M.T. Shevalier, J. Electrochem. Soc. 134, 802 (1987).
27. V.I. Birss and M.T. Shevalier, ibid, 134, 1594 (1987).
28. M.T. Shevalier, M.Sc. Thesis, University of Calgary, Calgary, Canada (1985).
29. A.A. Abdul Azim and M.M.Anwar, Corros. Sci. 9, 245 (1969).
30. J.S. Buchanan, N.P. Freestone and L.M. Peter, J.Electroanal. Chem. 182, 383 (1985).
31. D.W. Shoesmith, Pers. Comm. (1987).
32. L.M. Peter, J. Electroanal. Chem. 144, 315 (1983).
33. E.M. Khairy, A.A. Abdul Azim and K.M. El-Sobki, ibid., 11, 282 (1966).
34. A.M Beccaria, E.D. Mor, G. Bruno and G.Poggi, Br. Corros. J. 17, 87 (1982).
35. E.W. Abel, " In comprehensive inorganic chemistry. vol.2. Edited by J.C. Bailar, H.J. Emeleus, R.Nyholm and A.F. Trotman Dickinson, Pergamon Press. (1973), pp 119-123.
36. P. Dehalay, M. Pourbaix and P.V, Rysselberghe, J. Electrochem. Soc. 98, 59 (1951).
37. J.K. Obly, J. Inorg. Nucl. Chem. 28, 2507 (1966).

38. P. Taylor and V.J. Lopata, Can. J.Chem. 62, 395 (1984).
39. D.F. Haacke and P.A. Williams, J.Inorg. Nucl. Chem. 43, 406 (1981).
40. P. Ruetchi and B.D. Cahan, J. Electrochem. Soc. 104, 406 (1957).
41. R.R. Stasko and G.V. Vivian, Proc. of Int. Conf. on Radioactive Waste Management, Canadian Nuclear Society, Winnipeg, Sept. 1982.
42. J. Boulton, Atomic Energy of Canada Ltd., Report AECL-6314 (1978).
43. D.L. Sawyer and J.L. Roberts, "Experimental electrochemistry for Chemists", John Wiley and Sons, New York (1974). p.259
44. R.G. Barradas and S.Fletcher, Electrochim. Acta. 22, 237 (1977).
45. R.C. Weast ed., "Handbook of Chemistry and Physics", 66th ed., CRC Press, Inc., Boca Raton, Florida (1986)
46. P. Delahay, " New Instrumental Methods in Electrochemistry", Interscience Publishers, New York, 1954. p.349.
47. V.F. Ivanov and Z.N. Ushakova, Soviet Electrochem. 9, 753 (1973).
48. D. Britz, J. Electroanal. Chem. 88, 307 (1978).
49. H. Angerstein-Kozlowska, B.E. Conway and J.Klinger, ibid, 87, 821 (1978).
50. V.I. Birss and L.E. Kee, J.Electrochem. Soc. 133, 2097 (1986).
51. L.M. Peter, Electrochim. Acta 23, 165 (1978).
52. J.W. Schultze and F.D. Koppitz, ibid., 21, 327 (1976).
53. V.I. Birss and C.K. Smith, ibid, 32, 259 (1987).
54. M. Sluyters-Rehbach and J.H. Sluyters in "Electroanalytical Chemistry, vol.4. (edited by A.J. Bard) Marcel Dekker, New York (1970), p.64.
55. S. Fletcher and D.B. Matthews, J. appl.Electrochem. 11, 11 (1981).
56. P.V. Shigolev, "Electrolytic and Chemical Polishing of

- Metals", Freund Publishing House, Israel (1974).
57. D.C.W. Kannangara and B.E. Conway, J. Electrochem. Soc. 134, 894 (1987).
 58. C. R. Valentini, C.A. Moina, J.R. Vilche and A.J. Arvia, Corros. Sci. 25, 985 (1985).
 59. E.B. Castro, C.R. Valentini, C.A. Moina, J.R. Vilche and A.J. Arvia, *ibid.*, 26, 781 (1986).
 60. V.I. Birss and G.A. Wright, Electrochim. Acta. 27, 1429 (1982).
 61. A.J. Bard and L.F. Faulkner, "Electrochemical Methods: Fundamentals and Applications", John Wiley and Sons, Toronto (1980).
 62. B. Scharifker and G. Hills, Electrochim. Acta. 28, 879 (1983).
 63. R.S. Nicholson and I. Shain, Anal. Chem. 36, 706 (1964).
 64. S. Srinivasan and E. Gileadi, Electrochim. Acta. 11, 321 (1966).
 65. D.D. Macdonald, "Transient Techniques in Electrochemistry", Plenum Press, New York, (1981). pp 273-307.
 66. E.J. Casey, A.R. Dubois, P.G. Lake and W.J. Moroz, J. Electrochem. Soc. 112, 371 (1965).